### Title

Search for heavy right-handed Majorana neutrinos in the decay of top quarks produced in proton-proton collisions at s=13 TeV with the ATLAS detector




### Journal

Physical Review D, 110(11)

### ISSN

2470-0010



### Authors

Aad, G

Aakvaag, E

Abbott, B

et al.



### Publication Date

2024-12-01

### DOI

10.1103/physrevd.110.112004

# Search for heavy right-handed Majorana neutrinos in the decay of top quarks produced in proton-proton collisions at $\sqrt{s} = 13$ TeV with the ATLAS detector

G. Aad *et al.*[*]
(ATLAS Collaboration)

(Received 12 August 2024; accepted 18 September 2024; published 2 December 2024)

A search for heavy right-handed Majorana neutrinos is performed with the ATLAS detector at the CERN Large Hadron Collider, using the 140 fb$^{-1}$ of proton–proton collision data at $\sqrt{s} = 13$ TeV collected during Run 2. This search targets $t\bar{t}$ production, in which both top quarks decay into a bottom quark and a $W$ boson, where one of the $W$ bosons decays hadronically and the other decays into an electron or muon and a heavy neutral lepton. The heavy neutral lepton is identified through a decay into an electron or muon and another $W$ boson, resulting in a pair of same-charge same-flavor leptons in the final state. This paper presents the first search for heavy neutral leptons in the mass range of 15–75 GeV using $t\bar{t}$ events. No significant excess is observed over the background expectation, and upper limits are placed on the signal cross sections. Assuming a benchmark scenario of the phenomenological type-I seesaw model, these cross section limits are then translated into upper limits on the mixing parameters of the heavy Majorana neutrino with Standard Model neutrinos.

DOI: 10.1103/PhysRevD.110.112004

## I. INTRODUCTION

The observation of flavor oscillations in neutrinos produced in the sun, the earth atmosphere, reactors and accelerators implies that neutrinos have nonzero masses [1–4]. Over the past decades, there were several important developments at the theoretical and experimental frontiers addressing the question of neutrino-mass generation, the simplest among them being the type-I seesaw mechanism [5] that defines three heavy neutral lepton (HNL) candidates, which are heavy right-handed Majorana neutrinos. These heavy neutrinos are their own antiparticles, and processes involving such a particle can violate lepton number ($L$) conservation with $|\Delta L| = 2$.

Before the Large Hadron Collider (LHC) [6], the best direct constraints in the HNL mass range 2–75 GeV came from an analysis of the data collected by the DELPHI Collaboration at the LEP collider using $3.3 \times 10^6$ hadronic $Z$ boson decays [7]. At the LHC, the most stringent limits on the HNL production cross section come from searches for an HNL in $W$ boson decays. The CMS Collaboration explored the mass range 50 GeV–25 TeV using 138 fb$^{-1}$ of $\sqrt{s} = 13$ TeV proton–proton ($pp$) collision data in the same-charge dimuon final state, which provides the most stringent upper limits for the mass range above 650 GeV [8]. The CMS Collaboration also searched for the decay products of long-lived HNLs as hadronic and electromagnetic showers detected in the muon chambers of the CMS detector [9], a distinctive signature to probe for HNLs with masses lower than 4 GeV and proper decay lengths of a few meters. This signature is sensitive to HNL couplings to all three generations of leptons, and the analysis set the most stringent limits to date on the strength of HNL mixing with electron (muon) neutrinos in the mass range of 2.1–3.0 (1.9–3.3) GeV. In another analysis, the CMS Collaboration searched for both, Dirac and Majorana HNLs in the mass range of 10 GeV–1.5 TeV using three lepton final states [10]. This produced more stringent upper limits than the previously achieved experimental constraints for a wide range of HNL masses, and set limits on the strength of HNL mixing with $\tau$-neutrinos above the $W$ boson mass for the first time.

A previous result from the ATLAS Collaboration using 36.1 fb$^{-1}$ of $\sqrt{s} = 13$ TeV $pp$ collision data constrained the HNL mixing to muon and electron neutrinos in the mass range of 4.5–50 GeV [11]. The ATLAS Collaboration recently searched for HNLs in $W$ boson decays using a dilepton displaced vertex, in the mass range of 3–15 GeV [12]. The latest ATLAS analyses searched for Majorana neutrinos in same-charge $WW$ scattering events through their coupling with electrons and muons in the HNL mass range 50 GeV–20 TeV [13,14].

[*]Full author list given at the end of the article.



 

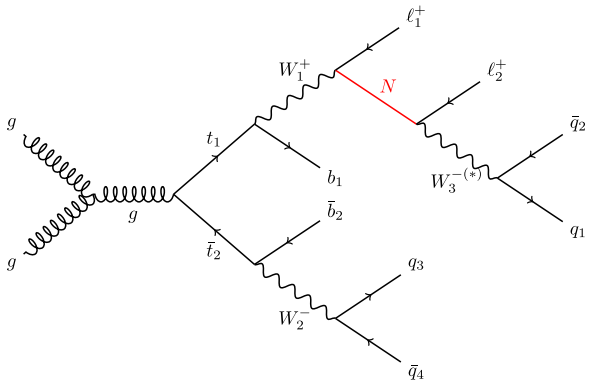


FIG. 1. Example Feynman diagram of the signal process. The heavy neutral lepton is denoted by the symbol $N$. The charge-conjugate of this diagram is also a valid signal process. The off shell $W$ boson is marked with an asterisk.

This is the first search for HNLs using $t\bar{t}$ events [15], where one top quark decays into a bottom quark and a $W$ boson, with the $W$ boson further decaying into an electron or muon and a heavy neutral lepton. The heavy neutral lepton decays promptly into another charged lepton and a $W$ boson, yielding a final state characterized by a pair of same-charge same-flavor leptons. The other top quark decays hadronically according to the Standard Model (SM), as illustrated in Fig. 1. A detailed description of the signal model considered is provided in Sec. III A.

Compared with the previous efforts in which HNLs are searched for in the decay of $W$ bosons originating directly from the proton–proton collisions, the advantage of using a $W$ boson from a $t\bar{t}$ event is the possibility of identifying one of the top quarks through its decay according to the SM, while utilizing the decay of the other top quark to search for HNLs. Although the same signal model is expected to lead to fewer events in this channel, the background is also expected to be much smaller because of the state-of-the-art $b$-tagging algorithms. Because of the very different final states, this analysis provides complementary sensitivity to the previous searches.

Final states that have two same-charge electrons ($ee$ channel) or muons ($\mu\mu$ channel) are targeted. A multivariate analysis is performed in combination with a statistical inference to extract the signal. No significant excess is observed over the background expectation, and upper limits on the strength of the HNL mixing with electron and muon neutrinos are set in the mass range of 15 GeV $< m_{\mathrm{HNL}} <$ 75 GeV, using 140 fb$^{-1}$ of $pp$ collision data collected by the ATLAS detector at $\sqrt{s} = 13$ TeV. The $ee$ and $\mu\mu$ channels are also used to constrain the strength of HNL mixing with $\tau$-neutrinos, considering purely leptonic decays of $\tau$-leptons. While calculating the upper limits on one mixing parameter, the other two are assumed to be zero.

The paper is structured as follows. Section II provides a brief overview of the ATLAS detector used to collect the data. Section III describes the signal model, the background processes, the detector simulation, and the theoretical predictions considered. The objects used for the analysis, the event selection, and the event reconstruction are described in Sec. IV. The signal and control regions are defined in Sec. V, which also describes the multivariate analysis used for the signal extraction. Systematic uncertainties are described in Sec. VI. Finally, Sec. VII describes the statistical method used to analyze the experimental data, and presents the final results, while Sec. VIII presents the conclusion.

## II. ATLAS DETECTOR

The ATLAS detector [16] at the LHC covers nearly the entire solid angle around the collision point.[1] It consists of an inner tracking detector surrounded by a thin superconducting solenoid, electromagnetic and hadronic calorimeters, and a muon spectrometer incorporating three large superconducting air-core toroidal magnets.

The inner-detector system (ID) is immersed in a 2 T axial magnetic field and provides charged-particle tracking in the range $|\eta| < 2.5$. The high-granularity silicon pixel detector covers the vertex region and typically provides four measurements per track, the first hit generally being in the insertable B-layer (IBL) installed before Run 2 [17,18]. It is followed by the semiconductor tracker (SCT), which usually provides eight measurements per track. These silicon detectors are complemented by the transition radiation tracker (TRT), which enables radially extended track reconstruction up to $|\eta| = 2.0$. The TRT also provides electron identification information based on the fraction of hits (typically 30 in total) above a higher energy-deposit threshold corresponding to transition radiation.

The calorimeter system covers the pseudorapidity range $|\eta| < 4.9$. Within the region $|\eta| < 3.2$, electromagnetic calorimetry is provided by barrel and endcap high-granularity lead/liquid-argon (LAr) calorimeters, with an additional thin LAr presampler covering $|\eta| < 1.8$ to correct for energy loss in material upstream of the calorimeters. Hadronic calorimetry is provided by the steel/scintillator-tile calorimeter, segmented into three-barrel structures within $|\eta| = 1.7$, and two copper/LAr hadronic endcap calorimeters. The solid angle coverage is completed with forward copper/LAr and tungsten/LAr calorimeter modules

[1]ATLAS uses a right-handed coordinate system with its origin at the nominal interaction point (IP) in the center of the detector and the $z$-axis along the beam pipe. The $x$-axis points from the IP to the center of the LHC ring, and the $y$-axis points upwards. Polar coordinates $(r, \phi)$ are used in the transverse plane, $\phi$ being the azimuthal angle around the $z$-axis. The pseudorapidity is defined in terms of the polar angle $\theta$ as $\eta = -\ln\tan(\theta/2)$ and is equal to the rapidity $y = \frac{1}{2}\ln(\frac{E+p_z c}{E-p_z c})$ in the relativistic limit. Angular distance is measured in units of $\Delta R \equiv \sqrt{(\Delta y)^2 + (\Delta\phi)^2}$.

optimized for electromagnetic and hadronic energy measurements, respectively.

The muon spectrometer (MS) has separate trigger and high-precision tracking chambers measuring the deflection of muons in a magnetic field generated by the superconducting air-core toroidal magnets. The field integral of the toroids ranges between 2.0 Tm and 6.0 Tm across most of the detector. Three layers of precision chambers, each consisting of layers of monitored drift tubes, cover the region $|\eta| < 2.7$, complemented by cathode-strip chambers in the forward region, where the background is highest. The muon trigger system covers the range $|\eta| < 2.4$ with resistive-plate chambers in the barrel, and thin-gap chambers in the endcap regions.

The luminosity is measured mainly by the LUCID–2 [19] detector that records Cherenkov light produced in the quartz windows of photomultipliers located close to the beam pipe.

Events are selected by the first-level trigger system implemented in custom hardware, followed by selections made by algorithms implemented in software in the high-level trigger [20]. The first-level trigger accepts events from the 40 MHz bunch crossings at a rate below 100 kHz, which the high-level trigger further reduces to record complete events to disk at about 1 kHz.

A software suite [21] is used in data simulation, in the reconstruction and analysis of real and simulated data, in detector operations, and in the trigger and data acquisition systems of the experiment.

## III. DATA AND SIMULATED EVENT SAMPLES

The search uses LHC $pp$ collision data at $\sqrt{s} = 13$ TeV collected with the ATLAS detector. Data quality requirements are applied to ensure that all detector components are fully operational [22]. The resulting data sample corresponds to an integrated luminosity of 140 fb$^{-1}$, obtained using the LUCID-2 detector [19] for the primary luminosity measurements, complemented by measurements using the inner detector and calorimeters [23].

Simulated Monte Carlo (MC) events are used to model the signal and the SM backgrounds. The effects of the detector are incorporated using a simulation of the ATLAS detector [24] obtained with the GEANT4 program [25] or with a faster approach employing parametrized showers in the calorimeter. The effects of the additional $pp$ collisions in the same or a nearby bunch crossing (pileup) are modeled by overlaying minimum bias events simulated using PYTHIA8.1 [26] with the A3 set of tuned parameters (tune) on events from hard-scatter processes [27]. The MC events are weighted to reproduce the distribution of the average number of interactions per bunch crossing observed in the data. All samples simulated with POWHEG BOX [28–31], and MADGRAPH5_AMC@NLO [32] are interfaced to PYTHIA8 to simulate the parton shower, fragmentation, and underlying event with the A14 tune [33] and the NNPDF2.3LO [34] parton distribution function (PDF) set. Samples using PYTHIA8 and HERWIG7 [35,36] have heavy-flavor hadron decays modeled by EVTGEN [37]. The masses of the top quark, $m_t$, and of the Higgs boson, $m_H$, are set to 172.5 GeV and 125 GeV, respectively. The data and simulated events are processed with the same reconstruction and analysis algorithms.

### A. Signal modeling

Fig. 1 shows an example Feynman diagram of the signal process, with the final state used in this search. The signal is a beyond the Standard Model (BSM) process, and it is simulated using an extension to the minimal Standard Model, called $\nu$MSM [38], which is implemented as a universal FeynRules output (UFO) model called HEAVYN [39].

A simplified benchmark model is assumed that proposes a single HNL candidate $N$, which couples with either electrons, muons, or $\tau$-leptons through a mixing with the corresponding neutrinos. In this model, the mass $m_N$ and couplings $V_{\ell,N}$ of this new particle are free parameters. These couplings can be expressed through a mixing matrix,

$$V_{\ell,N} = \begin{pmatrix} V_{e,N} & 0 & 0 \\ 0 & V_{\mu,N} & 0 \\ 0 & 0 & V_{\tau,N} \end{pmatrix}, \tag{1}$$

where only one of the three diagonal terms can be nonzero at a time.

The width of the HNL is automatically computed by the MADGRAPH5_AMC@NLO [32] generator, which provides matrix elements at next-to-leading-order (NLO) in QCD using the NNPDF3.0NLO [40] PDF set, and uses the five-flavor scheme. The QCD factorization ($\mu_{\mathrm{F}}$) and renormalization ($\mu_{\mathrm{R}}$) scales are set to be equal [41], given by the dynamical expression $\frac{1}{4}\sum_i \sqrt{m_i^2 + p_{\mathrm{T},i}^2}$, where the sum runs over all the particles generated in the matrix element calculation, and the mass and transverse momentum of each particle are denoted by $m_i$ and $p_{\mathrm{T},i}$, respectively. The decay of the top quarks is simulated using the MADSPIN [42,43] module, allowing three-body off shell decays. The parton shower, the hadronization, and the decay of the $\tau$-leptons are simulated using PYTHIA8 with the A14 set of tuned parameters.

Signal samples are generated for ten values of $m_N$: 15, 25, 35, 40, 45, 50, 55, 60, 70 and 75 GeV. The HNL decays promptly in this mass range. For each mass point, six separate samples are produced for the two possible choices in the sign of the same-charge leptons ($\ell^+\ell^+$ or $\ell^-\ell^-$) and three possible choices in their flavor ($\ell = e, \mu$ or $\tau$-lepton).

### B. Background processes with prompt leptons

Leptons that originate from the primary hard-scattering event and satisfy all selection requirements, described in

Sec. IV B, are referred to as prompt leptons. Conversely, leptons that enter the final states by any background process other than $W$, $Z$ or Higgs boson decays are called nonprompt leptons. Samples of simulated events are produced to model the different background processes, along with additional samples to estimate the modeling uncertainties for each process.

The production of $t\bar{t}$ events is modeled using the POWHEG BOXv2 generator that provides matrix elements at NLO precision with the NNPDF3.0NLO PDF set and the $h_{\text{damp}}$ parameter[2] set to 1.5 $m_{\text{t}}$ [44]. The functional form of the renormalization and factorization scale is set to the default scale $\sqrt{m_{\text{t}}^2 + p_{\text{T}}^2}$. The parton shower and hadronization are modeled with the PYTHIA8.2 generator. The uncertainty in matching the NLO matrix elements to the parton shower when generating $t\bar{t}$ events is evaluated by comparing the nominal samples of simulated events to samples with an alternative setting of the $p_{\text{T}}^{\text{hard}}$ parameter in the matching code, using $p_{\text{T}}^{\text{hard}} = 1$ instead of the default setting of $p_{\text{T}}^{\text{hard}} = 0$ [45]. This parameter regulates the definition of the vetoed region of the parton shower and is important in avoiding overlap in the phase space filled by POWHEG and PYTHIA. The uncertainty in the choice of the $h_{\text{damp}}$ parameter for the $t\bar{t}$ event generation is estimated using an additional $t\bar{t}$ sample produced as the nominal sample, but with the $h_{\text{damp}}$ parameter set to $3m_t$ [46]. The uncertainty in the parton-shower and hadronization model for the $t\bar{t}$ events is evaluated by comparing the nominal generator setup with a sample produced with the POWHEG BOXv2 generator and the HERWIG7.2.1 parton-shower and hadronization model. In this alternative sample, the HERWIG7 default set of tuned parameters [36,47] and the MMHT2014LO PDF set [48] are used. All $t\bar{t}$ samples are normalized to the cross section prediction at next-to-next-to-leading-order (nnlo) in QCD, including the resummation of next-to-next-to-leading logarithmic (NNLL) soft-gluon terms calculated using the TOP++2.0 program [49–55]. This cross section corresponds to $\sigma(t\bar{t})_{\text{NNLO+NNLL}} = 832 \pm 51\text{fb}$.

The events for the $t\bar{t}H$ process are simulated at NLO with POWHEG BOXv2 using the NNPDF3.0NLO PDF set, while the Higgs-boson decay, hadronization, parton shower, and the underlying event are simulated with PYTHIA8.2. The resulting sample is normalized to a cross section of $507^{+35}_{-50}$ fb, which is calculated at NLO for both QCD and electroweak (EW) using MADGRAPH5_AMC@NLO as reported in Ref. [56]. An additional $t\bar{t}H$ sample is simulated with $p_{\text{T}}^{\text{hard}} = 1$. The uncertainty in the parton-shower and hadronization model is evaluated with the help of an alternative sample produced with POWHEG BOXv2+HERWIG7.2.1, using the same prescription as the $t\bar{t}$ process.

For the $t\bar{t}W$ process, the SHERPA2.2.10 [57] generator and its default parton shower are used at NLO accuracy in QCD, with multileg merging of up to one additional parton at NLO and up to two additional partons at leading-order (MEPS@NLO [58–61] set up with a merging scale of 30 GeV). Additionally, a leading-order (LO) EW sample also simulated with SHERPA2.2.10, but for the $t\bar{t}W + 1$ jet final state, is used to simulate the EW corrections to the $t\bar{t}W$ production. Following the recommendations of the LHC Top and the LHC Higgs boson working groups, the cross sections of these QCD and EW $t\bar{t}W$ samples are scaled separately to 674.7 fb and 47.7 fb, respectively [62]. The impact of the systematic uncertainty in the choice of generator is evaluated using an alternative $t\bar{t}W$ sample simulated with up to one additional parton in the final state at NLO accuracy in QCD using MADGRAPH5_AMC@NLO. In this sample, the different jet multiplicities are merged using the FxFx NLO matrix-element and parton-shower merging prescription [62] with a merging scale of 30 GeV. The events are interfaced with PYTHIA8.2.

The $t\bar{t}Z$ production, with the $Z$ boson decaying leptonically, is simulated with MADGRAPH5_AMC@NLO, interfaced with PYTHIA8.2. Three samples corresponding to the three leptonic decay modes of the $Z$ boson are produced, and they are normalized to the total $t\bar{t}Z$ production cross section of $0.84^{+0.09}_{-0.10}$ pb [56]. The impact of the systematic uncertainty in the choice of generator is assessed through alternative $t\bar{t}Z$ samples. The alternative sample addresses the uncertainty in the parton-shower and hadronization model by comparing the nominal generator setup with a sample produced using the POWHEG BOXv2 generator and the HERWIG7 parton-shower and hadronization model.

The $t\bar{t}\gamma$ process is simulated with MADGRAPH5_AMC@NLO and the parton shower is simulated using PYTHIA8.2. An overlap removal with the $t\bar{t}$ sample is implemented based on the procedure used by the charge asymmetry analysis of the $t\bar{t}\gamma$ process [63]. This sample corresponds to a total cross section of 5.36 pb, as calculated by the MC generator at NLO.

The $tW$ production is modeled using the POWHEG BOXv2 generator at NLO in QCD using the five-flavor scheme and the NNPDF3.0NLO set of PDFs. The PYTHIA8.2 generator is used to model the parton shower and hadronization using the A14 tune and the NNPDF2.3LO PDF set.

Single-top-quark $t$-channel production is modeled using the POWHEG BOXv2 generator at NLO in QCD using the four-flavor scheme and the corresponding NNPDF3.0NLO PDF set. Single-top-quark $s$-channel production is modeled using the POWHEG BOXv2 generator at NLO in QCD in the five-flavor scheme with the NNPDF3.0NLO PDF set. Both the samples are interfaced with PYTHIA8.2 to model parton-showering and hadronization.

In addition, the electroweak background ($V$ EW, where $V = W, Z$), composed of the $V$ + jets, diboson ($VV$) and

[2]The $h_{\text{damp}}$ parameter controls the matching between the matrix elements in POWHEG and parton shower in PYTHIA. It effectively regulates the high-$p_{\text{T}}$ radiation against which the $t\bar{t}$ system recoils.

triboson ($VVV$) processes, is considered. The production of $V+$jets is simulated with the SHERPA[2.2.1] generator using NLO-accurate matrix elements for up to two jets, and LO-accurate matrix elements for up to four jets calculated with the COMIX [64] and OPENLOOPS [65,66] libraries. They are matched with the SHERPA parton shower [67] using the MEPS@NLO prescription that uses the set of tuned parameters developed by the SHERPA authors. The NNPDF3.0NNLO [40] PDF set is used, and the samples are normalized to the NNLO prediction [68].

Samples of diboson events are simulated with the SHERPA2.2.1 or SHERPA2.2.2 generator, depending on the process. Fully leptonic final states and semileptonic final states, where one boson decays leptonically and the other hadronically, are simulated using matrix elements at NLO accuracy in QCD for up to one additional parton and at LO accuracy for up to three additional parton emissions. Samples for the loop-induced processes $gg \to VV$ are generated using LO-accurate matrix elements for up to one additional parton emission for both the fully leptonic and semileptonic final states. The matrix element calculations are matched and merged with the SHERPA parton shower based on Catani–Seymour dipole factorization using the MEPS@NLO prescription. The virtual QCD corrections are provided by the OPENLOOPS library. The NNPDF3.0NNLO PDF set is used, along with a dedicated set of tuned parton-shower parameters developed by the SHERPA authors.

The production of triboson events is simulated with the SHERPA2.2.2 generator using factorized gauge boson decays. Matrix elements, calculated at NLO for the inclusive process and at LO for up to two additional parton emissions, are matched and merged with the SHERPA parton shower using the same prescription as the diboson sample. The virtual QCD correction for matrix elements is also performed similarly.

The $t\bar{t}ZZ$, $t\bar{t}WZ$, $t\bar{t}HH$, and $t\bar{t}WH$ processes are simulated using MADGRAPH with the NNPDF2.3LO PDF set, whereas the $t\bar{t}t$, $t\bar{t}t\bar{t}$, $tHW$, $t\bar{t}WZ$, $t\bar{t}WW$, $tHq$, $tWZ$, and $tZq$ samples are simulated using MADGRAPH5_AMC@NLO with the NNPDF3.0NLO PDF set. The $VH$ sample is simulated using PYTHIA8.2. All these rare processes are normalized using their NLO theoretical cross sections and are combined into the 'Top other' category.

### C. Background processes with nonprompt leptons

Besides prompt leptons, nonprompt leptons are also produced in many of the background processes, predominantly in $t\bar{t}$ decays. Based on the information provided by the record of the simulated particles in the produced MC samples, each lepton is sorted into one of several lepton-origin categories. These categories distinguish between prompt leptons, electrons from prompt muon decay, electrons from photon conversion and leptons from the decay of a hadron. While selecting a simulated event, two same-charge same-flavor leptons ($ee$ or $\mu\mu$) are required in the final state, at least one of which is a prompt lepton. The following nonprompt categories are defined based on the origin of the second lepton.

The label '$t\bar{t}\gamma$-conv' refers to events from the $t\bar{t}\gamma$ and $t\bar{t}$ samples in which the second lepton originates from photon conversion. Events from these two samples are merged after removing the $t\bar{t}\gamma$ events from the inclusive $t\bar{t}$ sample. The label '$t\bar{t}$ Q-flip' refers to events from the $t\bar{t}$ sample in which the second same-charge lepton has a misidentified charge, known as 'charge-flip'. The labels '$t\bar{t}$ dec $e$' and '$t\bar{t}$ dec $\mu$' indicate the background processes in which the second lepton originates from either a heavier lepton decay or a hadron decay. Finally, if a simulated $t\bar{t}$ event has a second lepton which does not correspond to any of the processes discussed above, it is included in the 'Top other' category, mentioned in the previous section.

## IV. OBJECT RECONSTRUCTION AND EVENT SELECTION

The signal process involves $t\bar{t}$ events, in which one of the top quarks decays hadronically according to the SM, and the decay chain of the other top quark contains an HNL. The targeted final state consists of two same-charge light leptons (electrons or muons), two bottom quarks and four light quarks ($u$, $c$, $d$ or $s$-quark).

### A. Object reconstruction

The primary vertex of an event is defined as the three-dimensional point inside the beampipe that maximizes the $\sum p_{\mathrm{T}}^2$ of the contributing tracks.

Electron candidates are reconstructed from energy deposits in the electromagnetic calorimeter matched to reconstructed tracks in the inner detector. The selected candidates are required to have transverse momenta $p_{\mathrm{T}} > 10$ GeV and pseudorapidity $|\eta| < 2.47$. Candidates in the transition region between the barrel and endcap calorimeters, $1.37 \leq |\eta| \leq 1.52$, have poorer energy resolution and are excluded. To reduce the background from nonprompt sources, electron candidates are also required to satisfy $|d_0|/\sigma(d_0) < 5$ and $|z_0 \sin\theta| < 0.5$ mm, where $d_0$ is the transverse impact parameter, with uncertainty $\sigma(d_0)$, and $z_0$ is the longitudinal impact parameter relative to the primary vertex. The electron candidates are identified using a likelihood-based method and are required to satisfy the 'TightLH' working point [69]. Leptons from heavy-flavor hadron decays, misidentified jets, or photon conversions are further suppressed using a boosted decision tree (BDT) based discriminant [70], which provides several isolation working points. The electrons are required to satisfy the loose isolation working point to ensure enough separation from nearby particles. For some of the analysis regions discussed in Sec. V, a tighter isolation working point is used for better rejection of nonprompt leptons.

The sign of the charge of an electron candidate is determined from the curvature of its track under the effect of the magnetic field present in the inner detector. For a highly energetic electron, this curvature can be very small, making it difficult to determine the direction in which the track bends, and consequently its electric charge. Charge misidentification can occur if the electron emits a hard bremsstrahlung and subsequently produces an electron–positron pair through photon conversion, with one of these leptons having a high $p_{\mathrm{T}}$. Typically, these conversions would be reconstructed as such, but in some asymmetric conversions only one of the tracks is reconstructed, and the charge of the corresponding electron candidate can be opposite of the charge of the original lepton that radiated the photon. To deal with this challenge, a BDT-based tool [69] is employed, which combines several properties of an electron candidate, such as its charge, impact parameters, energy, and inner detector track, into a single discriminant. For some of the analysis regions, the electrons are additionally required to satisfy this BDT based selection criterion for an improved rejection of electrons with a misidentified charge. This is referred to as the 'electron charge identity selector' (ECIDS) tool.

A likelihood-based multivariate discriminant is constructed to enhance the selection of prompt electrons, while suppressing contributions from photon conversions and hadrons misidentified as electrons. It evaluates several properties of the electron candidates simultaneously, which include the shower shapes in the electromagnetic calorimeter, the quality of the track, and the detection of transition radiation in the TRT [69]. This is referred to as the '$e/\gamma$ ambiguity removal'.

The reconstruction of muon candidates combines charged particle tracks in the inner detector with those found in the muon spectrometer [71]. These tracks must be consistent with originating from the primary vertex. Muon candidates must satisfy the 'Medium' [71] identification and the loose isolation criteria [70]. Similar to the electrons, a tighter isolation criterion is also employed in the definition of some of the analysis regions, as discussed in Sec. V. In addition, the muons must have impact parameters satisfying $|d_0/\sigma(d_0)| < 3$ and $|z_0 \sin\theta| < 0.5$ mm. Muon candidates are required to have $p_{\mathrm{T}} > 10$ GeV and $|\eta| < 2.5$.

One of the possible semileptonic decays of a top quark is into a $\tau$-lepton. Only leptonically decaying $\tau$-leptons are considered via their decays into electrons or muons, which are reconstructed according to the criteria described above. Hadronically decaying $\tau$-leptons are reconstructed as jets, and treated as light jets during the event selection.

Jets are reconstructed using a particle flow algorithm [72] by combining information from both the inner detector and the calorimeters. The anti-$k_t$ algorithm [73,74] with a radius parameter of $R = 0.4$ is used. Jets are required to have $p_{\mathrm{T}} > 20$ GeV and $|\eta| < 4.5$ and are calibrated as described in Ref. [75]. To reduce the effect of pile up, the jet-vertex tagger (JVT) [76], which identifies jets originating from the primary vertex, is applied to the jets with $p_{\mathrm{T}} < 60$ GeV and $|\eta| < 2.4$, using the tight working point. Additionally, 'forward jets' with $2.5 < |\eta| < 4.5$ and $p_{\mathrm{T}} < 120$ GeV are required to satisfy a dedicated forward-JVT WP of fJVT $< 0.4$, in addition to a timing requirement [77]. The inclusion of forward jets enhances the analysis sensitivity by increasing the signal (and background) yields by about 20%.

Jets originating from the hadronization of bottom quarks are identified ($b$-tagged) via the DL1r algorithm [78]. This algorithm uses deep neural networks exploiting the distinct features of $B$-hadrons in terms of track impact parameters and displaced vertices reconstructed in the inner detector. The inputs to the DL1r network include discriminating variables constructed by a recurrent neural network, which exploits the spatial and kinematic correlations between tracks originating from the same $B$-hadron. A jet is considered $b$-tagged if it satisfies the operating point corresponding to an 85% average efficiency for $b$-quark jets in simulated $t\bar{t}$ events.

The missing transverse momentum, whose magnitude is denoted in the following by $E_{\mathrm{T}}^{\mathrm{miss}}$, is defined as the negative vector sum of the $p_{\mathrm{T}}$ of the reconstructed and calibrated objects in the event [79]. This sum also includes the momenta of the inner detector tracks with $p_{\mathrm{T}} > 0.5$ GeV that are matched to the primary vertex but are not matched to any other reconstructed objects.

An overlap removal procedure is applied to reduce any double counting of objects that are independently reconstructed. An electron candidate is rejected if it shares a track with a muon candidate or if it has a track overlapping with another electron candidate. If there are jets within $\Delta R(j, e) = 0.2$ of an electron candidate, the closest one fulfilling this criterion is removed. If there are other jets within $\Delta R(j, e) = 0.4$ of the electron candidate, the electron candidate is removed. Jets that are within $\Delta R(j, \mu) = 0.2$ of a muon candidate or share a track with that muon candidate are removed if they contain fewer than three tracks. After that, any muon candidate that is within $\Delta R(j, \mu) = 0.4$ of the remaining jets is removed.

### B. Event selection and reconstruction

Each selected event is required to have exactly two light leptons ($e$ or $\mu$) of the same charge and flavor. The events are selected using single-lepton triggers [80,81], where the leading lepton is required to satisfy the trigger selection criteria. The leading lepton is also required to have $p_{\mathrm{T}} > 27$ GeV, where the trigger efficiency is 99%. Jets in the central region ($|\eta| < 2.5$) are required to have $p_{\mathrm{T}} > 20$ GeV, whereas jets in the forward region are required to have $p_{\mathrm{T}} > 35$ GeV. The $b$-tagged jets are required to have $p_{\mathrm{T}} > 25$ GeV. Events are required to have at least two $b$-tagged jets and at least four jets without a $b$-tag. Finally, the lepton pair is required to have an

invariant mass $m_{\ell\ell} > 12$ GeV to suppress the background from the Drell-Yan process.

As illustrated in Fig. 1, the specific signal process[3] considered is: $t_1 \to W_1^+ b_1, W_1^+ \to \ell_1^+ N, N \to W_3^- \ell_2^+$ and $\bar{t}_2 \to W_2^- \bar{b}_2, W_2^- \to q_3 \bar{q}_4$. The off shell $W_3^-$ decays hadronically. This provides four constraints on the invariant masses of the following reconstructed particles: $t_1$, $\bar{t}_2$, $W_1^+$ and $W_2^-$. All possible combinations of the available objects are considered, and the decay chain is reconstructed using the one which minimizes

$$\chi^2 = \frac{(m(t_1) - m_t)^2}{\sigma_t^2} + \frac{(m(W_1^+) - m_W)^2}{\sigma_W^2} + \frac{(m(\bar{t}_2) - m_t)^2}{\sigma_t^2} + \frac{(m(W_2^-) - m_W)^2}{\sigma_W^2},$$

where $m_t = 172.76$ GeV and $m_W = 80.379$ GeV are the top and $W$ masses, respectively [82]. The parameters $\sigma_t = 32$ GeV and $\sigma_W = 27$ GeV are the widths of the reconstructed top quark and $W$ boson mass distributions, obtained by averaging over all the signal samples the individual results of a Gaussian distribution fit to these masses.

The invariant mass of the $W_1$ boson, decaying into the heavy neutral lepton, offers a good separation between signal and background. For the signal process, the distribution of this variable peaks near the $W$ boson mass, as shown in Fig. 2(c). For background processes passing the signal selection criteria, the invariant mass calculated from the two same-charge leptons and two light jets coming from different parents is expected to follow a broad nonresonant distribution. This is used as one of the input variables for the multivariate analysis training, as discussed in Sec. V C.

## V. SIGNAL EXTRACTION

Although all three flavors of HNLs are considered in this search, only the processes with $ee$ or $\mu\mu$ as the same-charge leptons in their final states are used for signal extraction. This implies that, while searching for the signal process with $\tau$-leptons, only the processes where both the $\tau$-leptons decay into same-flavor lighter leptons are considered.

Several analysis regions are defined; one signal region (SR) for each of the $ee$ and $\mu\mu$ channels, four control regions (CR) for the $ee$ channel and two CRs for the $\mu\mu$ channel. While the SRs are enriched in signal events, each CR is enriched in events from a specific background process and have less than 1% signal contamination. A multivariate analysis is performed on the events belonging to each SR to achieve further separation between signal and background.

[3]The charge conjugate is also considered and implied throughout the paper.

The selection criteria for the different signal and control regions are described in the following and summarized in Table I.

### A. Signal regions

The signal regions for both the $ee$ and $\mu\mu$ channels are defined by applying the tighter isolation criteria described in Sec. IV A on the same-charge leptons, and requiring $m_{\ell\ell} < 80$ GeV to minimize the $Z \to ee$ background. Additionally, in the $ee$ channel, both electrons are required to satisfy the criteria of the ECIDS tool and the $e/\gamma$ ambiguity removal, which are applied to suppress the charge flip and photon conversion contamination, respectively.

### B. Control regions

Various background processes, with similar final states as the signal processes, can mimic their signature and enter the SRs. In both the $ee$ and $\mu\mu$ channels, the $t\bar{t}W$ process is an important background. In the $ee$ channel, the SM $t\bar{t}$ process also produces the same-charge electron pair in the final state through heavy-flavor decay, photon-conversion, or charge-flip. In the $\mu\mu$ channel, the $t\bar{t}$ process produces the same-charge muon pair mostly through heavy-flavor decay, as the occurrence of charge-flip in the $\mu\mu$ channel is found to be negligible. To understand the impact of the background contributions, dedicated CRs are defined.

To define a CR for the $t\bar{t}W$ background, events with $m_{\ell\ell} > 100$ GeV (in the $ee$ channel) or $m_{\ell\ell} > 80$ GeV (in the $\mu\mu$ channel) are selected, while keeping all other criteria of the SR unchanged. The tighter selection in the $ee$ channel reduces the contribution from the $Z \to e^+e^-$ process, which can produce a same-charge electron pair in the final state through charge-flip. A single $t\bar{t}W$ CR is defined by merging events from both channels.

'Fake leptons' are reconstructed lepton candidates that originate either from real leptons, produced in nonprompt decays or photon conversion, or from jets with an electromagnetic signature that mimics that of electrons. Fake leptons are often created when a hadron, containing a $b$- or $c$-quark, decays into a lighter hadron and a lepton. A CR for such heavy flavor fake leptons is defined by selecting events in which at least one of the leptons does not satisfy the tighter isolation criteria described in Sec. IV A, along with a requirement of $m_{\ell\ell} > 70$ GeV (for the $ee$ channel) or $m_{\ell\ell} > 75$ GeV (for the $\mu\mu$ channel) to minimize the signal contamination.

A CR with an enhanced contribution of the electron charge-flip background is defined by requiring at least one of the electrons to satisfy the reversed ECIDS criterion. In this CR, the contribution from the $Z \to ee$ process is mitigated by rejecting the events with $m_{\ell\ell}$ in a 10 GeV window around the $Z$ boson mass ($Z$ veto). A requirement of $m_{\ell\ell} > 60$ GeV is also imposed to reduce the signal contamination.

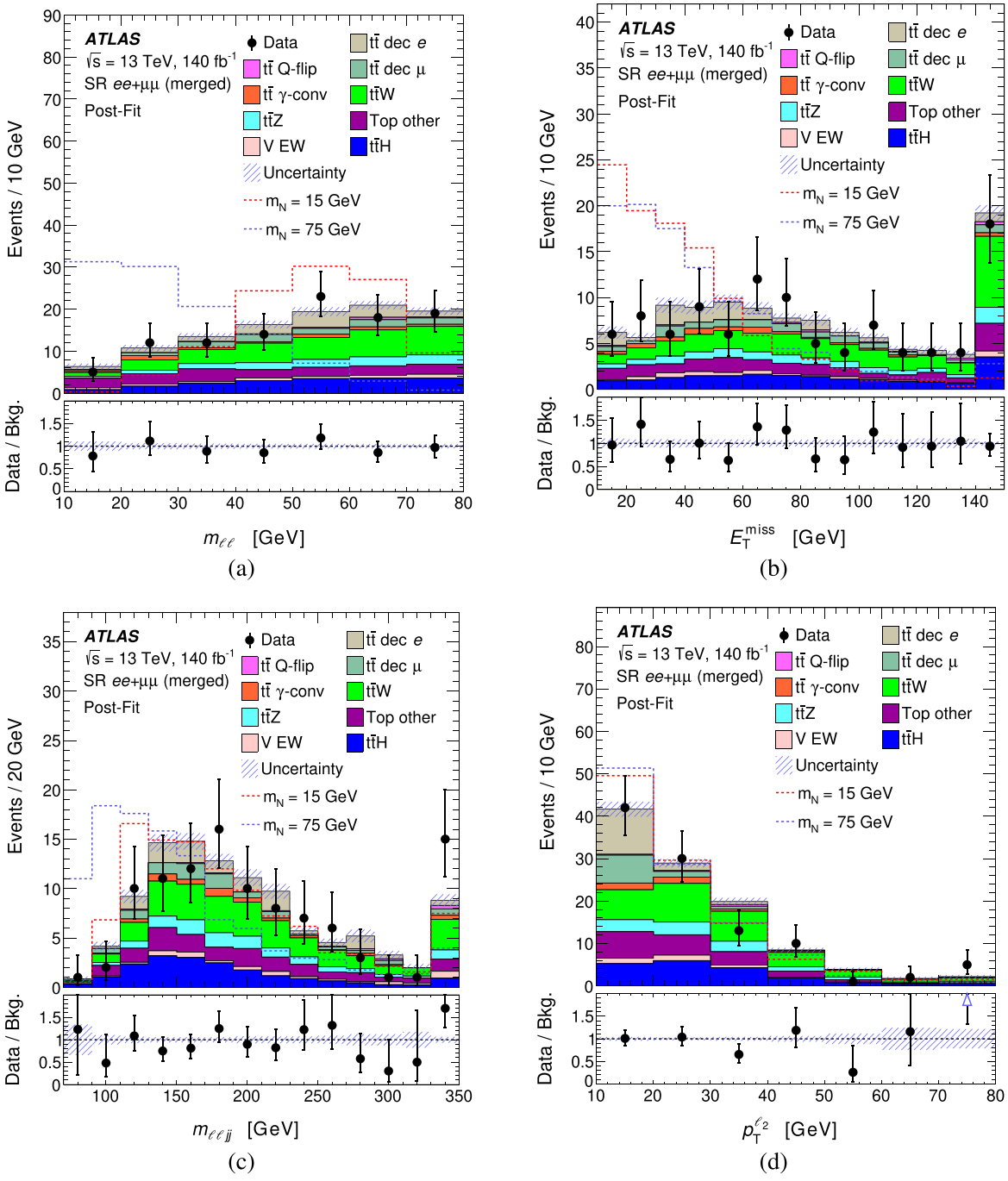


FIG. 2. Distributions of the BDT input variables for two signal mass points and all background processes: (a) invariant mass of the two same-charge leptons, (b) missing transverse momentum, (c) invariant mass of the $W_1$ candidate, and (d) transverse momentum of the subleading lepton. The normalizations of the background processes are obtained from a background-only fit to data across all the CRs in both channels. The signal distributions are normalized to the same number of events as the sum of all background processes. The vertical error bars represent the statistical uncertainty in the data, shown as black dots, and the hatched band includes the MC statistical uncertainty and all the other systematic uncertainties added in quadrature. The first and last bins include the events below and above the histogram range, respectively.

Finally, another CR is defined for the electrons originating from the interaction of photons with the detector material, known as photon conversion, by inverting the $e/\gamma$ ambiguity removal criterion to enhance the contribution from this targeted process. Additionally, in this CR, a lower bound of $m_{\ell\ell} > 75$ GeV and the $Z$ veto are applied to reduce the signal contamination and the background events originating from the $Z \to ee$ process.

TABLE I. Definitions of different signal and control regions. The control regions are enriched in events from the following processes: $t\bar{t}W$, heavy-flavor (HF) fake, photon-conversion (PC), and charge-flip (CF). The 'Z veto' is defined as $m_{ee} \notin [m_Z - 10\ \text{GeV}, m_Z + 10\ \text{GeV}]$.

| Analysis regions for the $ee$ channel | | | | |
|---|---|---|---|---|
| Region | Tight isolation | $e/\gamma$ ambiguity removal | ECIDS criteria | $m_{ee}$ requirement |
| SR | Both $e$ | Both $e$ | Both $e$ | <80 GeV |
| $t\bar{t}W$ CR | Both $e$ | Both $e$ | Both $e$ | >100 GeV |
| HF CR | At most one $e$ | Both $e$ | Both $e$ | >70 GeV |
| PC CR | | At most one $e$ | Both $e$ | >75 GeV and $Z$ veto |
| CF CR | | Both $e$ | At most one $e$ | >60 GeV and $Z$ veto |

| Analysis regions for the $\mu\mu$ channel | | |
|---|---|---|
| Region | Isolation criteria | $m_{\mu\mu}$ requirement |
| SR | Both $\mu$ | <80 GeV |
| $t\bar{t}W$ CR | Both $\mu$ | >80 GeV |
| HF CR | At most one $\mu$ | >75 GeV |

### C. Multivariate analysis

A multivariate analysis is performed in the SRs to achieve further separation between signal and background. The `GradientBoostingClassifier` model from the `scikit-learn` [83] package is used to train boosted decision trees, using binary cross-entropy as the loss function.

Two separate BDTs are trained in different mass regions to maximize the separation power across the whole mass range: one for the low-mass region using the four signal MC samples generated with $m_N$ between 15 GeV and 40 GeV, and another for the high mass region using the six samples with $m_N$ between 45 GeV and 75 GeV. The same BDTs are used for the $ee$ and $\mu\mu$ channels, and trained

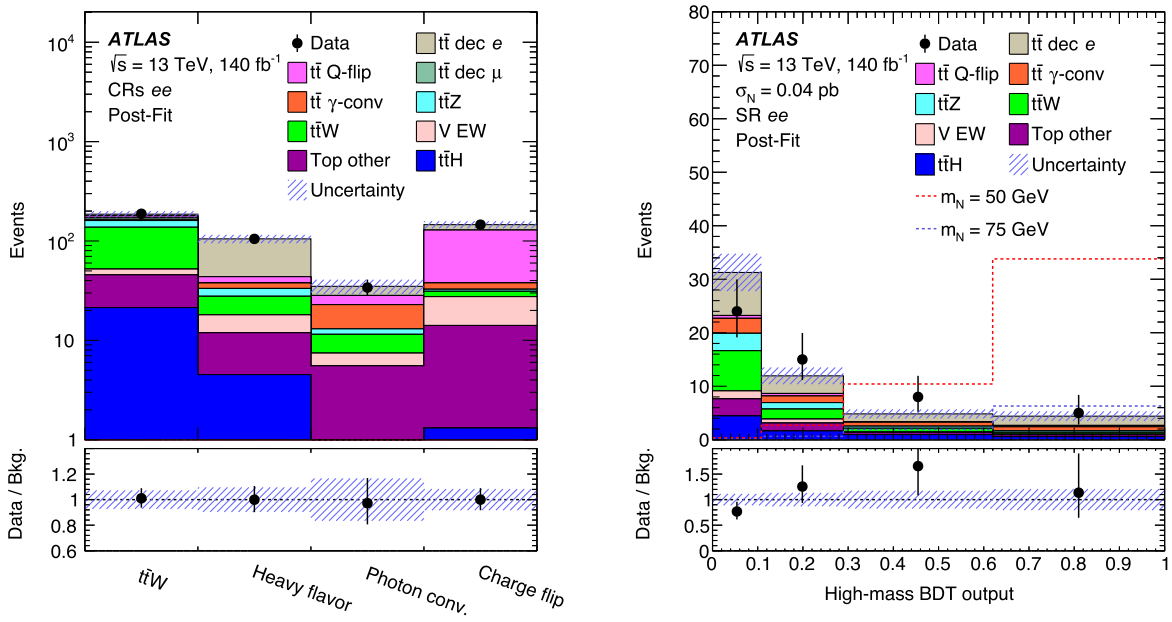


FIG. 3. Data (dots) and MC (histograms) distributions, as obtained from the background-only fit in the $ee$ channel for (a) the event yields from different background processes in the respective control regions, and (b) the distributions of the high-mass BDT output in the signal region for two signal mass points and all background processes. The distributions for the signal processes correspond to the HNL mixing with electron neutrinos, and are overlaid on the stacked background distributions. Each of the signal distributions is normalized to a cross section of 0.04 pb. The vertical error bars represent the statistical uncertainty in the data, and the hatched band includes the MC statistical uncertainty and all the other systematic uncertainties added in quadrature.

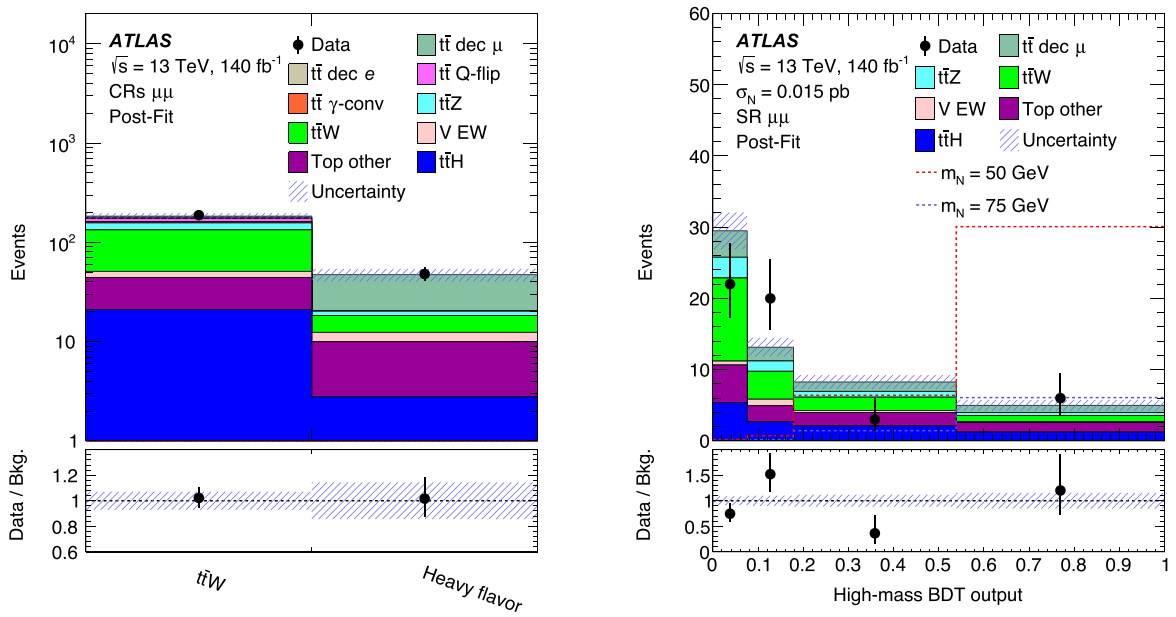


(a) (b)

FIG. 4. Data (dots) and MC (histograms) distributions, as obtained from the background-only fit in the $\mu\mu$ channel for (a) the event yields from different background processes in the respective control regions, and (b) the distributions of the high-mass BDT output in the signal region for two signal mass points and all background processes. The distributions for the signal processes correspond to the HNL mixing with muon neutrinos, and are overlaid on the stacked background distributions. Each of the signal distributions is normalized to a cross section of 0.015 pb. The vertical error bars represent the statistical uncertainty in the data, and the hatched band includes the MC statistical uncertainty and all the other systematic uncertainties added in quadrature.

using a mixture of signal samples of the first two HNL generations, along with all the nominal background samples described in Sec. III B. The mixture of signal samples used for the BDT training is prepared by aggregating equal numbers of events from the simulated samples belonging to the mass range corresponding to that BDT. The search for the third generation of HNL utilizes the same BDTs as the ones used in the searches for the first two generations.

Each simulated MC event has an associated event weight, which is the product of the generator-level weight and various scale factors applied for the calibration of different reconstructed objects present in that event. While training the model, absolute values of these event weights are used to preserve the convexity of the loss function. Different background components are normalized to the same luminosity according to their SM cross sections while preparing the background sample. The signal and background samples are normalized to the same number of weighted events. A twofold cross-validation was performed by splitting the whole dataset based on odd and even event numbers to check for overtraining. Although there was no sign of overtraining, the events with odd event number are nevertheless evaluated using the model trained on events with even event number, and vice versa.

Based on optimization studies, the following input variables were found to be the most important (in decreasing order of importance), and are used to build the BDT models:

(i) Invariant mass of the two same-charge leptons ($m_{\ell\ell}$);
(ii) Missing transverse momentum of the event ($E_{\mathrm{T}}^{\mathrm{miss}}$);
(iii) Invariant mass of the $W$ boson decaying into an HNL and a lepton ($m_{\ell\ell jj}$);
(iv) Transverse momentum of the subleading lepton ($p_{\mathrm{T}}^{\ell_2}$).

The reconstruction of the second-last variable is discussed in Sec. IV B. The distributions of the input variables for the two BDTs are shown in Fig. 2 for signal and background events separately. The signal distributions are normalized to the same number of events as the sum of all background processes to highlight the difference between their shapes. A satisfactory data-MC agreement is observed for all four input variables.

The separations obtained for two example mass points are illustrated in Fig. 3(b) (for the $ee$ channel) and Fig. 4(b) (for the $\mu\mu$ channel). The BDTs offer a better discrimination between signal and background than any of the input variables alone for all HNL mass points considered.

## VI. SYSTEMATIC UNCERTAINTIES

The predictions of the signal and background processes are affected by theoretical uncertainties, and the data are affected by various sources of experimental uncertainties. The uncertainties are classified into three different categories; uncertainties arising from the reconstruction and

calibration of the jet and lepton candidates, the uncertainty in the background normalizations, and the uncertainty arising from the modeling of the signal and background processes. They are detailed in the following subsections.

### A. Experimental uncertainties

One of the primary sources of experimental uncertainty is the lepton efficiency, which is the efficiency of selecting an event containing the required number of leptons. This includes the reconstruction and identification efficiencies, the isolation efficiency, and the trigger efficiency. These efficiencies are different for data and simulated events, primarily because of the imperfect detector simulation. For simulated events, this is corrected by applying scale factors, calculated as the ratio of the efficiencies measured in the data to those measured in the simulation using the tag-and-probe method in $Z \to \ell\ell$ events. These scale factors, which depend on $p_{\mathrm{T}}$ and $\eta$, are varied up and down by one standard deviation to study the impact of the lepton efficiency uncertainties in the analysis result [71,84]. The uncertainty in the lepton trigger efficiency is calculated by propagating the uncertainties in individual trigger scale factors, which are derived in the same way as the identification and isolation scale factors for electrons and muons.

The lepton energy (momentum) measurements and correction factors are derived from a comprehensive study of dileptonic decays of the $Z$ boson, involving both the data and simulation. They are applied to correct possible mismodeling of the detector during the calibration. These correction factors are varied up and down by one standard deviation to study the lepton energy (momentum) scale uncertainty. The energy of the electrons is calibrated at the electromagnetic scale. For muons, the momentum scale and resolution corrections are applied to the MC simulations. Additional uncertainties are considered to account for the charge-dependent scale correction applied to data [85].

An uncertainty in the measurement of $E_{\mathrm{T}}^{\mathrm{miss}}$ is assigned due to a possible miscalibration of its soft-track component, which are tracks that cannot be matched to any of the reconstructed and calibrated physics objects, i.e. hard components. They are derived from the level of agreement between data and simulation of the $p_{\mathrm{T}}$ balance between the hard and soft $E_{\mathrm{T}}^{\mathrm{miss}}$ components [79]. The scale and resolution uncertainties in the soft $E_{\mathrm{T}}^{\mathrm{miss}}$ component are treated as separate contributions.

The overall uncertainty in the jet energy scale (JES) consists of individual components derived from *in situ* measurements, pileup effects, flavor dependence, and additional effects like calorimeter responses and out-of-cone radiation. To determine the JES and its uncertainty, information from test-beam data, LHC collision data and simulation are used [75].

Precise knowledge of the jet energy resolution (JER) is important for the correct modeling of jet production. Thirteen orthogonal components account for jet $p_{\mathrm{T}}$- and $\eta$-dependent differences between simulation and data, which are determined using dijet events and noise measurements [75].

The uncertainties in JVT and fJVT are calculated by studying track-to-vertex matching [76]. The $b$-tagging performance, characterized by the probability of correctly tagging a $b$-jet and the probability of mis-tagging a $c$-jet or a light flavor jet as a $b$-jet, are also taken into account [86–88].

To account for the differences in the pileup distribution between data and simulation, the pileup profile in the simulation is corrected to match the one in data by applying several correction factors. The uncertainties in these correction factors are also taken into account.

Finally, the uncertainty in the measurement of the combined Run-2 integrated luminosity is estimated to be 0.83% [23].

### B. Background normalization uncertainties

Uncertainties of 12% and 10% are included for the $t\bar{t}Z$ and $t\bar{t}H$ production cross-sections, respectively [56]. The $VEW$ background consists of $Z+$jets events, with a 20% uncertainty [89], and $VV/VVV$ events, with a 50%–60% uncertainty [90] in their cross sections. Hence, an overall 30% normalization uncertainty is considered for the $VEW$ background as a weighted average. For the $tW$, single-top-quark ($t$-channel and $s$-channel), and the minor backgrounds included in the 'Top other' category, a 50% normalization uncertainty is assigned. The normalizations of the $t\bar{t}W$ events, and of the $t\bar{t}$ events with nonprompt leptons in their final states, are kept unconstrained and are determined by the fit, which is described in Sec. VII.

### C. Modeling uncertainties

The systematic uncertainties in MC modeling are estimated by comparing different generators or by varying the parameters used for the event simulation.

For the HNL signal samples, the following modeling systematic uncertainties are considered. The uncertainty in the parton distribution functions is propagated using the PDF4LHC15 prescription [91]. The uncertainty due to missing higher-order corrections in the matrix element calculation is estimated by independently varying $\mu_{\mathrm{R}}$ and $\mu_{\mathrm{F}}$ up and down by a factor of two.

The dominant background is from the $t\bar{t}$ events, in which at least one of the top quarks decays leptonically. To estimate the uncertainty related to the choice of parton shower and hadronization model, the POWHEG+PYTHIA8 sample is compared with the POWHEG+HERWIG7.2.1 sample. Independent variations of the renormalization and factorization scales are considered to account for missing higher-order corrections in the matrix element calculation. The uncertainty in $t\bar{t}$ modeling due to the initial-state-radiation is estimated by varying the renormalization and factorization scales by factors of two around their original values,

whereas the uncertainty in the modeling of final-state-radiation is evaluated by varying the renormalization scale for QCD emissions in the final-state shower by a factor of two around its original value. The uncertainties in the cross section due to the choice of PDF and the value of the strong coupling $\alpha_s$ are calculated using the PDF4LHC prescription [91] with the MSTW2008 68% confidence level (CL) NNLO [92,93], CT10 NNLO [94,95] and NNPDF2.3LO PDF sets. The uncertainty in matching the NLO matrix elements to the parton shower when simulating $t\bar{t}$ events is evaluated by comparing nominal samples of simulated events with samples generated with an alternative setting of the $p_{\mathrm{T}}^{\mathrm{hard}}$ parameter in the matching code, as discussed in Sec. III B. The uncertainty related to the choice of the $h_{\mathrm{damp}}$ parameter for the $t\bar{t}$ event simulation is estimated by using an additional $t\bar{t}$ sample produced with this parameter set to $3m_t$, while keeping all other generator settings unchanged.

The nominal sample for the $t\bar{t}H$ background is produced with the same generator as for the $t\bar{t}$ background. Therefore, the uncertainties related to the parton shower, hadronization, renormalization and factorization scales, and the choice of $p_{\mathrm{T}}^{\mathrm{hard}}$ parameter are estimated following the $t\bar{t}$ recipe, except for the $h_{\mathrm{damp}}$ parameter, which is set to $3/4(m_t + m_{\bar{t}} + m_H) = 352.5$ GeV, and is not varied.

For the $t\bar{t}W$ background, the uncertainty related to the choice of parton shower and hadronization model is estimated by comparing the POWHEG+PYTHIA8 sample with the POWHEG+HERWIG7 sample. To estimate the uncertainty related to the choice of generator, the nominal SHERPA2.2.10 sample is compared with the sample generated using MADGRAPH5_AMC@NLO+PYTHIA8 with the FxFx merging scheme. The uncertainties in scale variations are estimated from the independent variations of the renormalization and factorization scales by factors of two. The uncertainty in the parton distribution functions is propagated using the PDF4LHC15 prescription.

To estimate the uncertainty in the $t\bar{t}Z$ background related to the choice of parton shower and hadronization model, the nominal sample is compared with the sample simulated using MADGRAPH5_AMC@NLO+HERWIG7. The uncertainties in scale variations are estimated from the independent variations of the renormalization and factorization scales by factors of two. The uncertainties arising from initial-state-radiation and missing higher-order terms in matrix element calculation are also accounted for.

## VII. STATISTICAL ANALYSIS AND RESULTS

The signal strength $\mu$ is obtained from a simultaneous binned profile-likelihood fit [96] across the signal and control regions, with systematic uncertainties included as nuisance parameters. The histograms used for constructing the likelihood with `HistFactory` [97] are the distributions of BDT output in the SRs, and are single-bin histograms with the event yields in the CRs. During the simultaneous fit, these single-bin histograms help to determine the normalizations of the particular background processes corresponding to the CRs.

The likelihood is constructed as a product of individual Poisson likelihoods over all considered bins. The fitted event yields in the bins depend on nuisance parameters $\theta$, which include the effects of systematic uncertainties. Each nuisance parameter, except those representing the MC statistical uncertainties, is constrained by a Gaussian distribution term in the likelihood function. Some systematically varied discriminant distributions are smoothed and nuisance parameters of systematic uncertainties with negligible impact are removed entirely to reduce spurious effects in minimization, improve convergence of the fit, and reduce the computing time. The effects of normalization and shape of a source of systematic uncertainty are treated separately in this removal process.

The test statistic $q_\mu$ is defined as the profile likelihood ratio,

$$q_\mu = -2\ln\frac{\mathcal{L}(\mu,\hat{\hat{\theta}})}{\mathcal{L}(\hat{\mu},\hat{\theta})},$$

where $\hat{\mu}$ and $\hat{\theta}$ are the values of the parameters that maximize the likelihood function and $\hat{\hat{\theta}}$ are the values of the nuisance parameters that maximize the likelihood function for a given value of $\mu$. The test statistic is evaluated with the `RooStats` package [98] and is used in the modified frequentist ($\mathrm{CL}_S$) method [99] to obtain upper limits on the signal strength. For a given signal mass, the range of $\mu$ yielding $\mathrm{CL}_S < 0.05$, where $\mathrm{CL}_S$ is computed using the asymptotic approximation [96], is excluded at 95% confidence level.

While searching for an HNL mixing with a particular generation of SM neutrinos, the mixing with the other two generations is assumed to be zero. This implies, for an HNL mixing with the first two generations, the same-charge leptons in the final states of the signal processes directly couple to the HNLs and do not originate from $\tau$-lepton decays. Simultaneous fits across the signal and control regions are performed separately for the $ee$ and $\mu\mu$ channels to extract the signal strengths $\sigma_{e,N}$ and $\sigma_{\mu,N}$, respectively. In the search for an HNL mixing with electron neutrinos, one SR and four CRs are included in the simultaneous fit. The CRs used in the $ee$ channel are enriched in events from these background processes; $t\bar{t}W$, fake electrons from heavy flavor hadron decays, charge flip and photon conversion. In the search for an HNL mixing with muon neutrinos, one SR and two CRs are included in the simultaneous fit, where the CRs are enriched in either $t\bar{t}W$ or fake muons from heavy flavor hadron decays.

The background-only fit distributions in the high mass region for the $ee$ and $\mu\mu$ channels are shown in Figs. 3 and 4, respectively. The normalizations of the background

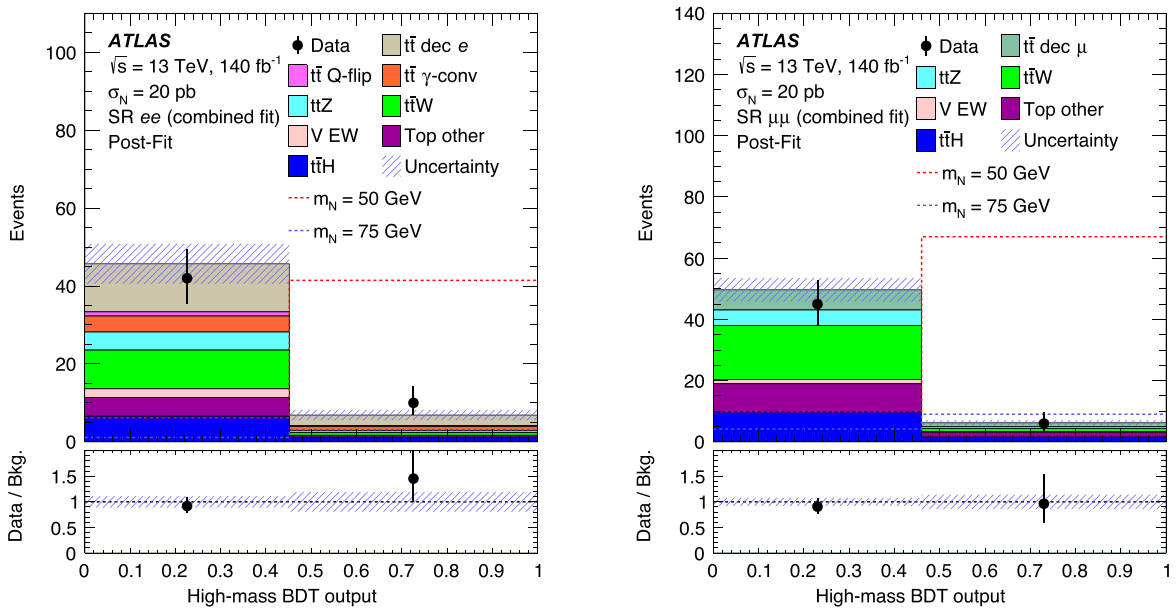


FIG. 5. Data (dots) and MC (histograms) distributions of the high-mass BDT output, as obtained from the combined background-only fit, in the signal regions of the (a) $ee$ and (b) $\mu\mu$ channels, used to search for HNL mixing with $\tau$-neutrinos. Distributions are shown for two signal mass points and all background processes. The distributions for the signal processes correspond to the HNL mixing with $\tau$-neutrinos, and are overlaid on the stacked background distributions. Each of the signal distributions is normalized to a cross section of 20 pb. The vertical error bars represent the statistical uncertainty in the data, and the hatched band includes the MC statistical uncertainty and all the other systematic uncertainties added in quadrature.

components in the $ee$ channel, obtained from this fit, are $0.55 \pm 0.42$ for photon conversion, $1.52 \pm 0.69$ for heavy-flavor fake, $0.80 \pm 0.39$ for charge-flip, and $1.09 \pm 0.39$ for $t\bar{t}W$. In the $\mu\mu$ channel, the background normalizations are $0.75 \pm 0.32$ for heavy-flavor fake, and $1.05 \pm 0.41$ for $t\bar{t}W$. The net acceptance times efficiency for the signal processes in their corresponding SRs ranges from 0.26% to 1.3% depending on the HNL mass.

Similarly, while searching for an HNL mixing with the third generation, the same-charge electrons or muons in the final state of the signal process come from the $\tau$-lepton decays only. In this case, a simultaneous fit is performed across both the $ee$ and $\mu\mu$ channels. The distributions from the background-only fit in the CRs are very similar to the ones obtained for the other two searches. Because of the lower number of expected signal events, a coarser binning

TABLE II. Postfit event yields for the different background processes in the signal regions, as obtained from the background-only fit in the high-mass region.

| | Separate fits | | Combined fit | |
|---|---|---|---|---|
| | SR $ee$ | SR $\mu\mu$ | SR $ee$ | SR $\mu\mu$ |
| $t\bar{t}$ decay $e$ | $15 \pm 6$ | | $15 \pm 7$ | |
| $t\bar{t}$ Q-flip | $1.4 \pm 0.9$ | | $1.3 \pm 0.8$ | |
| $t\bar{t}$ $\gamma$-conv | $6 \pm 4$ | | $5 \pm 4$ | |
| $t\bar{t}$ decay $\mu$ | | $8.0 \pm 3.2$ | | $8.4 \pm 3.0$ |
| $t\bar{t}W$ | $10.4 \pm 2.6$ | $18 \pm 5$ | $10.4 \pm 2.6$ | $19 \pm 4$ |
| $t\bar{t}Z$ | $5.2 \pm 1.1$ | $5.6 \pm 1.1$ | $5.0 \pm 1.1$ | $5.5 \pm 1.1$ |
| $t\bar{t}H$ | $7.6 \pm 1.3$ | $11.4 \pm 1.9$ | $7.5 \pm 1.3$ | $11.2 \pm 1.8$ |
| V EW | $2.4 \pm 0.9$ | $1.9 \pm 1.5$ | $2.3 \pm 0.8$ | $1.5 \pm 1.2$ |
| Top other | $5.4 \pm 2.2$ | $11 \pm 4$ | $5.1 \pm 2.2$ | $11 \pm 4$ |
| Total prediction | $52 \pm 6$ | $56 \pm 4$ | $52 \pm 6$ | $56 \pm 4$ |
| Data | 52 | 51 | 52 | 51 |

TABLE III. Expected (exp.) and observed (obs.) upper limits on the signal cross sections at 95% CL.

| $m_N$ (GeV) | 15 | 25 | 35 | 40 | 45 | 50 | 55 | 60 | 70 | 75 |
|---|---|---|---|---|---|---|---|---|---|---|
| Exp. $\sigma_{e,N}$ (fb) | 21 | 9.8 | 7.3 | 6.9 | 6.9 | 6.7 | 7.2 | 8.5 | 18 | 36 |
| Obs. $\sigma_{e,N}$ (fb) | 26 | 12 | 8.2 | 7.8 | 10 | 9.7 | 10 | 12 | 26 | 52 |
| Exp. $\sigma_{\mu,N}$ (fb) | 9.3 | 5.0 | 3.7 | 3.5 | 3.2 | 3.1 | 3.2 | 4.0 | 8.2 | 15 |
| Obs. $\sigma_{\mu,N}$ (fb) | 7.5 | 3.9 | 2.8 | 2.6 | 3.2 | 3.1 | 3.3 | 4.2 | 8.3 | 15 |
| Exp. $\sigma_{\tau,N}$ (pb) | 8.9 | 2.6 | 2.1 | 1.7 | 1.8 | 1.8 | 2.0 | 3.7 | 7.0 | 19 |
| Obs. $\sigma_{\tau,N}$ (pb) | 13 | 3.6 | 2.7 | 2.3 | 2.5 | 2.2 | 3.2 | 5.5 | 7.3 | 20 |

has been used in the SRs of the $ee$ and $\mu\mu$ channels while searching for HNL mixing with $\tau$-leptons, as shown in Fig. 5.

### A. Upper limit on the signal strength

The data and SM predictions agree within uncertainties, and no significant deviation is observed, as illustrated in Table II. In the absence of any observed signal, upper limits are set on the signal strength at 95% confidence level for different masses. The upper limits on the cross sections of the signal process are listed in Table III. The most stringent limits are observed for $m_{\mathrm{HNL}} = 50$ GeV, for all three flavors of HNL.

The dominant sources of systematic uncertainties are the ones related to the modeling of the $t\bar{t}$ process, normalization of the $t\bar{t}W$ sample, and the JES/JER uncertainties. However, the effect of the systematic uncertainties on the expected and observed upper limits is small, as compared with its statistical counterpart. For $m_N = 50$ GeV, the expected

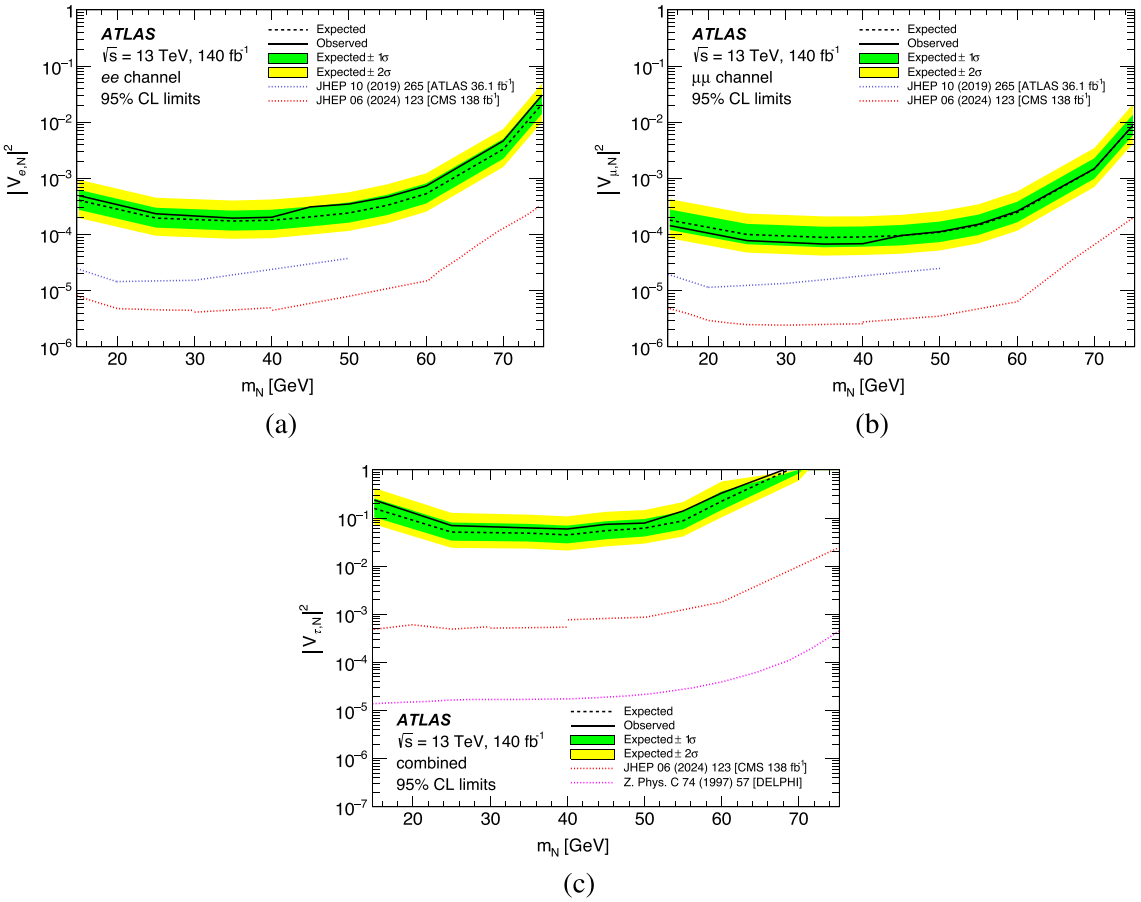


FIG. 6. Expected (dashed black lines) and observed (solid black lines) upper limits on the strength of HNL mixing with (a) electron neutrinos, (b) muon neutrinos and (c) $\tau$-neutrinos at 95% CL, along with the $1\sigma$ (green) and $2\sigma$ (yellow) uncertainty bands. The small discontinuity after 40 GeV reflects the use of a different BDT beyond this mass point. The observed upper limits from some of the previous searches for HNLs in $W$ boson decays are shown as dotted lines [7,10]. The discontinuities seen in the result from the CMS Collaboration originate from the different optimization strategies applied in different mass regions.

upper limits on $\sigma_{e,N}$ and $\sigma_{\mu,N}$ change from 6.7 fb$^{-1}$ to 6.1 fb$^{-1}$ and from 3.1 fb$^{-1}$ to 2.8 fb$^{-1}$, respectively, if the systematic uncertainties are not accounted for during the fit. This change is less than 10% compared with the values obtained from the fits with all the systematic uncertainties included, for all the masses considered. The expected upper limit on $\sigma_{\tau,N}$ for the same mass decreases by 6%.

The upper limits on the signal cross sections are translated into upper limits on the mixing parameters, using the following equation:

$$\sigma_{\ell,N} = 2 \cdot \sigma_{t\bar{t}} \cdot |V_{\ell,N}|^2 \cdot \mathcal{B}(W^+ \to N_{|V_{\ell,N}|=1} \ell^+) \cdot \mathcal{B}(N \to \ell^+ W^-), \tag{2}$$

where $\mathcal{B}(W^+ \to N_{|V_{\ell,N}|=1}\ell^+)$ is the branching ratio of the $W^+ \to N\ell^+$ decay, for $|V_{\ell,N}| = 1$. The value of $\mathcal{B}(N \to \ell^+ W^-)$ does not depend on the mixing parameter $V_{\ell,N}$, and varies from 36% to 39% in the mass range considered.

Fig. 6 shows the upper limits on the three mixing parameters as functions of the HNL mass. The observed upper limits on $|V_{e,N}|^2$ and $|V_{\mu,N}|^2$ are comparable across the whole mass range, $|V_{\mu,N}|^2$ being slightly more stringent. Nevertheless, these limits are weaker compared with some of the previous results that are shown in this figure. The limits on $|V_{\tau,N}|^2$ are three orders of magnitude weaker than the other two, and cross unity for the mass points above 68 GeV. This large difference in sensitivity is primarily because the analysis targets only $ee$ and $\mu\mu$ final states, consequently all the signal events where the same-charge $\tau$-leptons decay into two different flavors of lighter leptons or decay hadronically are not selected by the selection criteria of the SRs.

This study provides complementary information for combinations with other HNL measurements, and may be reinterpreted within the framework of effective field theories (EFT). Dimension-7 (and above) EFT operators, which enable lepton-number violation and complex five-fermion interactions, could produce final states similar to those considered [100].

## VIII. CONCLUSION

A search for heavy neutral leptons produced in $t\bar{t}$ events with dileptonic final states is performed using 140 fb$^{-1}$ of proton–proton collision data collected by the ATLAS detector at the LHC at a center-of-mass energy of 13 TeV. This is the first search for HNLs using $t\bar{t}$ events, and uses the distinct signature of same-charge leptons in the final states.

Observations are consistent with the Standard Model predictions, and the search results are presented as 95% CL upper limits on the mixing parameters $|V_{e,N}|^2$, $|V_{\mu,N}|^2$ and $|V_{\tau,N}|^2$ as functions of the mass of the heavy neutral lepton candidates.

The analysis is optimized to the search for mixing with the first two generations of leptons, and is also used to search for the mixing with the third generation. The best observed upper limits on the mixing parameters in the search region are $|V_{e,N}|^2 < 2.0 \times 10^{-4}$, $|V_{\mu,N}|^2 < 6.8 \times 10^{-5}$ and $|V_{\tau,N}|^2 < 5.9 \times 10^{-2}$. While these upper limits are about one order of magnitude weaker than those obtained in the previous ATLAS search for HNLs in the decays of $W$ bosons [11], this analysis extends the search region for the first two generations beyond $m_N = 50$ GeV, probing HNL masses up to 75 GeV, and broadens the scope of previous ATLAS searches by looking for an HNL mixing with the third generation.

Although the sensitivity of this channel to HNL mixing is about 2–3 orders of magnitude lower than channels with $W$ bosons produced directly in proton–proton collisions, searches for anomalous couplings in top-quark interactions remain a valuable endeavor, as the final states probed here can also be predicted by other theories such as EFT models allowing lepton-number violation and complex five-fermion interactions.

## ACKNOWLEDGMENTS

We thank CERN for the very successful operation of the LHC and its injectors, as well as the support staff at CERN and at our institutions worldwide without whom ATLAS could not be operated efficiently. The crucial computing support from all WLCG partners is acknowledged gratefully, in particular from CERN, the ATLAS Tier-1 facilities at TRIUMF/SFU (Canada), NDGF (Denmark, Norway, Sweden), CC-IN2P3 (France), KIT/GridKA (Germany), INFN-CNAF (Italy), NL-T1 (Netherlands), PIC (Spain), RAL (UK) and BNL (USA), the Tier-2 facilities worldwide and large non-WLCG resource providers. Major contributors of computing resources are listed in Ref. [101]. We gratefully acknowledge the support of ANPCyT, Argentina; YerPhI, Armenia; ARC, Australia; BMWFW and FWF, Austria; ANAS, Azerbaijan; CNPq and FAPESP, Brazil; NSERC, NRC and CFI, Canada; CERN; ANID, Chile; CAS, MOST and NSFC, China; Minciencias, Colombia; MEYS CR, Czech Republic; DNRF and DNSRC, Denmark; IN2P3-CNRS and CEA-DRF/IRFU, France; SRNSFG, Georgia; BMBF, HGF and MPG, Germany; GSRI, Greece; RGC and Hong Kong SAR, China; ISF and Benoziyo Center, Israel; INFN, Italy; MEXT and JSPS, Japan; CNRST, Morocco; NWO, Netherlands; RCN, Norway; MNiSW, Poland; FCT, Portugal; MNE/IFA, Romania; MESTD, Serbia; MSSR, Slovakia; ARIS and MVZI, Slovenia; DSI/NRF, South Africa; MICIU/AEI, Spain; SRC and Wallenberg Foundation, Sweden; SERI, SNSF and Cantons of Bern and Geneva, Switzerland; NSTC, Taipei; TENMAK, Türkiye; STFC/UKRI, United Kingdom; DOE and NSF, United States of America. Individual groups and members have received support from BCKDF, CANARIE, CRC and DRAC, Canada; CERN-CZ, FORTE and PRIMUS, Czech Republic; COST, ERC, ERDF, Horizon 2020,

ICSC-NextGenerationEU and Marie Skłodowska-Curie Actions, European Union; Investissements d'Avenir Labex, Investissements d'Avenir Idex and ANR, France; DFG and AvH Foundation, Germany; Herakleitos, Thales and Aristeia programmes co-financed by EU-ESF and the Greek NSRF, Greece; BSF-NSF and MINERVA, Israel; Norwegian Financial Mechanism 2014-2021, Norway; NCN and NAWA, Poland; La Caixa Banking Foundation, CERCA Programme Generalitat de Catalunya and PROMETEO and GenT Programmes Generalitat Valenciana, Spain; Göran Gustafssons Stiftelse, Sweden; The Royal Society and Leverhulme Trust, United Kingdom. In addition, individual members wish to acknowledge support from CERN: European Organization for Nuclear Research (CERN PJAS); Chile: Agencia Nacional de Investigación y Desarrollo (FONDECYT 1190886, FONDECYT 1230812, FONDECYT 1230987); China: Chinese Ministry of Science and Technology (MOST-2023YFA1605700), National Natural Science Foundation of China (NSFC—12175119, NSFC 12275265, NSFC-12075060); Czech Republic: Czech Science Foundation (GACR—24-11373S), Ministry of Education Youth and Sports (FORTE CZ.02.01.01/00/22_008/0004632), PRIMUS Research Programme (PRIMUS/21/SCI/017); EU: H2020 European Research Council (ERC—101002463); European Union: European Research Council (ERC—948254, ERC 101089007), Horizon 2020 Framework Programme (MUCCA—CHIST-ERA-19-XAI-00), European Union, Future Artificial Intelligence Research (FAIR-NextGenerationEU PE00000013), Italian Center for High Performance Computing, Big Data and Quantum Computing (ICSC, NextGenerationEU); France: Agence Nationale de la Recherche (ANR-20-CE31-0013, ANR-21-CE31-0013, ANR-21-CE31-0022, ANR-22-EDIR-0002), Investissements d'Avenir Labex (ANR-11-LABX-0012); Germany: Baden-Württemberg Stiftung (BW Stiftung-Postdoc Eliteprogramme), Deutsche Forschungsgemeinschaft (DFG—469666862, DFG—CR 312/5-2); Italy: Istituto Nazionale di Fisica Nucleare (ICSC, NextGenerationEU), Ministero dell'Università e della Ricerca (PRIN—20223N7F8K—PNRR M4.C2.1.1); Japan: Japan Society for the Promotion of Science (JSPS KAKENHI JP21H05085, JSPS KAKENHI JP22H01227, JSPS KAKENHI JP22H04944, JSPS KAKENHI JP22KK0227); Netherlands: Netherlands Organisation for Scientific Research (NWO Veni 2020—VI.Veni.202.179); Norway: Research Council of Norway (RCN-314472); Poland: Ministry of Science and Higher Education (IDUB AGH, POB8, D4 no 9722), Polish National Agency for Academic Exchange (PPN/PPO/2020/1/00002/U/00001), Polish National Science Centre (NCN 2021/42/E/ST2/00350, NCN OPUS nr 2022/47/B/ST2/03059, NCN UMO-2019/34/E/ST2/00393, UMO-2020/37/B/ST2/01043, UMO-2021/40/C/ST2/00187, UMO-2022/47/O/ST2/00148, UMO-2023/49/B/ST2/04085); Slovenia: Slovenian Research Agency (ARIS grant J1-3010); Spain: Generalitat Valenciana (Artemisa, FEDER, IDIFEDER/2018/048), Ministry of Science and Innovation (MCIN & NextGenEU PCI2022-135018-2, MICIN & FEDER PID2021-125273NB, RYC2019-028510-I, RYC2020-030254-I, RYC2021-031273-I, RYC2022-038164-I), PROMETEO and GenT Programmes Generalitat Valenciana (CIDEGENT/2019/023, CIDEGENT/2019/027); Sweden: Swedish Research Council (Swedish Research Council 2023-04654, VR 2018-00482, VR 2022-03845, VR 2022-04683, VR 2023-03403, VR grant 2021-03651), Knut and Alice Wallenberg Foundation (KAW 2018.0157, KAW 2018.0458, KAW 2019.0447, KAW 2022.0358); Switzerland: Swiss National Science Foundation (SNSF—PCEFP2_194658); United Kingdom: Leverhulme Trust (Leverhulme Trust RPG-2020-004), Royal Society (NIF-R1-231091); United States of America: U.S. Department of Energy (ECA DE-AC02-76SF00515), Neubauer Family Foundation.

[1] G. Bellini, L. Ludhova, G. Ranucci, and F. L. Villante, Neutrino oscillations, Adv. High Energy Phys. **2014**, 191960 (2014).

[2] B. Pontecorvo, Inverse beta processes and nonconservation of lepton charge, Sov. Phys. JETP **7**, 172 (1958), http://jetp.ras.ru/cgi-bin/dn/e_007_01_0172.pdf.

[3] L. Wolfenstein, Neutrino oscillations in matter, Phys. Rev. D **17**, 2369 (1978).

[4] S. P. Mikheyev and A. Y. Smirnov, Resonant amplification of $\nu$ oscillations in matter and solar-neutrino spectroscopy, Il Nuovo Cimento C **9**, 17 (1986).

[5] T. Yanagida, Horizontal symmetry and masses of neutrinos, Prog. Theor. Phys. **64**, 1103 (1980).

[6] L. Evans and P. Bryant, LHC Machine, J. Instrum. **3**, S08001 (2008).

[7] DELPHI Collaboration, Search for neutral heavy leptons produced in Z decays, Z. Phys. C **74**, 57 (1997); **75**, 580(E) (1997).

[8] CMS Collaboration, Probing heavy majorana neutrinos and the weinberg operator through vector boson fusion processes in proton-proton collisions at $\sqrt{s} = 13$ TeV, Phys. Rev. Lett. **131**, 011803 (2023).

[9] CMS Collaboration, Search for long-lived heavy neutral leptons decaying in the CMS muon detectors in proton-proton collisions at $\sqrt{s} = 13$ TeV, Phys. Rev. D **110**, 012004 (2024).
[10] CMS Collaboration, Search for heavy neutral leptons in final states with electrons, muons, and hadronically decaying tau leptons in proton–proton collisions at $\sqrt{s} = 13$ TeV, J. High Energy Phys. 06 (2024) 123.
[11] ATLAS Collaboration, Search for heavy neutral leptons in decays of $W$ bosons produced in 13 TeV pp collisions using prompt and displaced signatures with the ATLAS detector, J. High Energy Phys. 10 (2019) 265.
[12] ATLAS Collaboration, Search for heavy neutral leptons in decays of $W$ bosons using a dilepton displaced vertex in $\sqrt{s} = 13$ TeV $pp$ collisions with the ATLAS detector, Phys. Rev. Lett. **131**, 061803 (2023).
[13] ATLAS Collaboration, Search for Majorana neutrinos in same-sign $WW$ scattering events from pp collisions at $\sqrt{s} = 13$ TeV, Eur. Phys. J. C **83**, 824 (2023).
[14] ATLAS Collaboration, Search for heavy Majorana neutrinos in $e^{\pm}e^{\pm}$ and $e^{\pm}\mu^{\pm}$ final states via $WW$ scattering in $pp$ collisions at $\sqrt{s} = 13$ TeV with the ATLAS detector, Phys. Lett. B **856**, 138865 (2024).
[15] N. Liu, Z.-g. Si, L. Wu, H. Zhou, and B. Zhu, Top quark as a probe of heavy Majorana neutrino at the LHC and future colliders, Phys. Rev. D **101**, 071701 (2020); **105**, 079901(E) (2022).
[16] ATLAS Collaboration, The ATLAS experiment at the CERN Large Hadron Collider, J. Instrum. **3**, S08003 (2008).
[17] ATLAS Collaboration, ATLAS insertable B-Layer: Technical design report, Reports No. ATLAS-TDR-19, No. CERN-LHCC-2010-013, 2010, https://cds.cern.ch/record/1291633; Addendum: Reports No. ATLAS-TDR-19-ADD-1, No. CERN-LHCC-2012-009, 2012, https://cds.cern.ch/record/1451888.
[18] B. Abbott *et al.*, Production and integration of the ATLAS insertable B-layer, J. Instrum. **13**, T05008 (2018).
[19] G. Avoni *et al.*, The new LUCID-2 detector for luminosity measurement and monitoring in ATLAS, J. Instrum. **13**, P07017 (2018).
[20] ATLAS Collaboration, Performance of the ATLAS trigger system in 2015, Eur. Phys. J. C **77**, 317 (2017).
[21] ATLAS Collaboration, Software and computing for Run 3 of the ATLAS experiment at the LHC, arXiv:2404.06335.
[22] ATLAS Collaboration, ATLAS data quality operations and performance for 2015–2018 data-taking, J. Instrum. **15**, P04003 (2020).
[23] ATLAS Collaboration, Luminosity determination in $pp$ collisions at $\sqrt{s} = 13$ TeV using the ATLAS detector at the LHC, Eur. Phys. J. C **83**, 982 (2023),
[24] ATLAS Collaboration, The ATLAS simulation infrastructure, Eur. Phys. J. C **70**, 823 (2010).
[25] S. Agostinelli *et al.*, GEANT4—a simulation toolkit, Nucl. Instrum. Methods Phys. Res., Sect. A **506**, 250 (2003).
[26] T. Sjstrand, S. Mrenna, and P. Skands, A brief introduction to PYTHIA8.1, Comput. Phys. Commun. **178**, 852 (2008).
[27] ATLAS Collaboration, The PYTHIA8 A3 tune description of ATLAS minimum bias and inelastic measurements incorporating the Donnachie–Landshoff diffractive model, Report No. ATL-PHYS-PUB-2016-017, 2016, https://cds.cern.ch/record/2206965.
[28] S. Frixione, G. Ridolfi, and P. Nason, A positive-weight next-to-leading-order Monte Carlo for heavy flavour hadroproduction, J. High Energy Phys. 09 (2007) 126.
[29] P. Nason, A new method for combining NLO QCD with shower Monte Carlo algorithms, J. High Energy Phys. 11 (2004) 040.
[30] S. Frixione, P. Nason, and C. Oleari, Matching NLO QCD computations with parton shower simulations: The POWHEG method, J. High Energy Phys. 11 (2007) 070.
[31] S. Alioli, P. Nason, C. Oleari, and E. Re, A general framework for implementing NLO calculations in shower Monte Carlo programs: The POWHEG BOX, J. High Energy Phys. 06 (2010) 043.
[32] J. Alwall *et al.*, The automated computation of tree-level and next-to-leading order differential cross sections, and their matching to parton shower simulations, J. High Energy Phys. 07 (2014) 079.
[33] ATLAS Collaboration, ATLAS PYTHIA8 tunes to 7 TeV data, Report No. ATL-PHYS-PUB-2014-021, 2014, https://cds.cern.ch/record/1966419.
[34] R. D. Ball *et al.* (NNPDF Collaboration), Parton distributions with LHC data, Nucl. Phys. **B867**, 244 (2013).
[35] M. Bähr *et al.*, HERWIG++ physics and manual, Eur. Phys. J. C **58**, 639 (2008).
[36] J. Bellm *et al.*, HERWIG7.0/HERWIG++3.0 release note, Eur. Phys. J. C **76**, 196 (2016).
[37] D. J. Lange, The EvtGen particle decay simulation package, Nucl. Instrum. Methods Phys. Res., Sect. A **462**, 152 (2001).
[38] T. Asaka, S. Blanchet, and M. Shaposhnikov, The $\nu$MSM, dark matter and neutrino masses, Phys. Lett. B **631**, 151 (2005).
[39] C. Degrande, O. Mattelaer, R. Ruiz, and J. Turner, Fully automated precision predictions for heavy neutrino production mechanisms at hadron colliders, Phys. Rev. D **94**, 053002 (2016).
[40] R. D. Ball *et al.* (NNPDF Collaboration), Parton distributions for the LHC run II, J. High Energy Phys. 04 (2015) 040.
[41] R. Frederix, D. Pagani, and M. Zaro, Large NLO corrections in $t\bar{t}W^{\pm}$ and $t\bar{t}t\bar{t}$ hadroproduction from supposedly subleading EW contributions, J. High Energy Phys. 02 (2018) 031.
[42] S. Frixione, E. Laenen, P. Motylinski, and B. R. Webber, Angular correlations of lepton pairs from vector boson and top quark decays in Monte Carlo simulations, J. High Energy Phys. 04 (2007) 081.
[43] P. Artoisenet, R. Frederix, O. Mattelaer, and R. Rietkerk, Automatic spin-entangled decays of heavy resonances in Monte Carlo simulations, J. High Energy Phys. 03 (2013) 015.
[44] ATLAS Collaboration, Studies on top-quark Monte Carlo modelling for Top2016, Report No. ATL-PHYS-PUB-2016-020, 2016, https://cds.cern.ch/record/2216168.
[45] S. Höche, S. Mrenna, S. Payne, C. T. Preuss, and P. Skands, A study of QCD radiation in VBF Higgs production with vincia and PYTHIA, SciPost Phys. **12**, 010 (2022).

[46] ATLAS Collaboration, Studies on the improvement of the matching uncertainty definition in top-quark processes simulated with POWHEG+PYTHIA8, Report No. ATL-PHYS-PUB-2023-029, 2023, https://cds.cern.ch/record/2872787.

[47] J. Bellm *et al.*, HERWIG7.1 release note, arXiv:1705.06919.

[48] L. A. Harland-Lang, A. D. Martin, P. Motylinski, and R. S. Thorne, Parton distributions in the LHC era: MMHT 2014 PDFs, Eur. Phys. J. C **75**, 204 (2015).

[49] M. Beneke, P. Falgari, S. Klein, and C. Schwinn, Hadronic top-quark pair production with NNLL threshold resummation, Nucl. Phys. **B855**, 695 (2012).

[50] M. Cacciari, M. Czakon, M. Mangano, A. Mitov, and P. Nason, Top-pair production at hadron colliders with next-to-next-to-leading logarithmic soft-gluon resummation, Phys. Lett. B **710**, 612 (2012).

[51] P. Bärnreuther, M. Czakon, and A. Mitov, Percent-level-precision physics at the tevatron: Next-to-next-to-leading order QCD corrections to $q\bar{q} \to t\bar{t} + X$, Phys. Rev. Lett. **109**, 132001 (2012).

[52] M. Czakon and A. Mitov, NNLO corrections to top-pair production at hadron colliders: The all-fermionic scattering channels, J. High Energy Phys. 12 (2012) 054.

[53] M. Czakon and A. Mitov, NNLO corrections to top pair production at hadron colliders: the quark-gluon reaction, J. High Energy Phys. 01 (**2013**) 080.

[54] M. Czakon, P. Fiedler, and A. Mitov, Total top-quark pair-production cross section at hadron colliders through $\mathcal{O}(\alpha_S^4)$, Phys. Rev. Lett. **110**, 252004 (2013).

[55] M. Czakon and A. Mitov, Top++: A program for the calculation of the top-pair cross-section at hadron colliders, Comput. Phys. Commun. **185**, 2930 (2014).

[56] D. de Florian *et al.*, Handbook of LHC Higgs cross sections: 4. Deciphering the nature of the Higgs sector, arXiv:1610.07922.

[57] E. Bothmann *et al.*, Event generation with SHERPA2.2, SciPost Phys. **7**, 034 (2019).

[58] S. Höche, F. Krauss, M. Schönherr, and F. Siegert, A critical appraisal of NLO + PS matching methods, J. High Energy Phys. 09 (2012) 049.

[59] S. Höche, F. Krauss, M. Schönherr, and F. Siegert, QCD matrix elements + parton showers. The NLO case, J. High Energy Phys. 04 (2013) 027.

[60] S. Catani, F. Krauss, B. R. Webber, and R. Kuhn, QCD matrix elements + parton showers, J. High Energy Phys. 11 (2001) 063.

[61] S. Höche, F. Krauss, S. Schumann, and F. Siegert, QCD matrix elements and truncated showers, J. High Energy Phys. 05 (2009) 053.

[62] R. Frederix and I. Tsinikos, On improving NLO merging for ttW production, J. High Energy Phys. 11 (2021) 029.

[63] ATLAS Collaboration, Measurement of the charge asymmetry in top-quark pair production in association with a photon with the ATLAS experiment, Phys. Lett. B **843**, 137848 (2023).

[64] T. Gleisberg and S. Höche, Comix, a new matrix element generator, J. High Energy Phys. 12 (2008) 039.

[65] F. Cascioli, P. Maierhöfer, and S. Pozzorini, Scattering amplitudes with open loops, Phys. Rev. Lett. **108**, 111601 (2012).

[66] A. Denner, S. Dittmaier, and L. Hofer, Collier: A fortran-based complex one-loop library in extended regularizations, Comput. Phys. Commun. **212**, 220 (2017).

[67] S. Schumann and F. Krauss, A parton shower algorithm based on Catani–Seymour dipole factorisation, J. High Energy Phys. 03 (2008) 038.

[68] C. Anastasiou, L. Dixon, K. Melnikov, and F. Petriello, High-precision QCD at hadron colliders: Electroweak gauge boson rapidity distributions at next-to-next-to leading order, Phys. Rev. D **69**, 094008 (2004).

[69] ATLAS Collaboration, Electron and photon performance measurements with the ATLAS detector using the 2015–2017 LHC proton–proton collision data, J. Instrum. **14**, P12006 (2019).

[70] ATLAS Collaboration, Evidence for the associated production of the Higgs boson and a top quark pair with the ATLAS detector, Phys. Rev. D **97**, 072003 (2018).

[71] ATLAS Collaboration, Muon reconstruction and identification efficiency in ATLAS using the full Run 2 $pp$ collision data set at $\sqrt{s} = 13$ TeV, Eur. Phys. J. C **81**, 578 (2021).

[72] ATLAS Collaboration, Jet reconstruction and performance using particle flow with the ATLAS Detector, Eur. Phys. J. C **77**, 466 (2017).

[73] M. Cacciari, G. P. Salam, and G. Soyez, The anti-$k_t$ jet clustering algorithm, J. High Energy Phys. 04 (2008) 063.

[74] M. Cacciari, G. P. Salam, and G. Soyez, FastJet user manual, Eur. Phys. J. C **72**, 1896 (2012).

[75] ATLAS Collaboration, Jet energy scale and resolution measured in proton–proton collisions at $\sqrt{s} = 13$ TeV with the ATLAS detector, Eur. Phys. J. C **81**, 689 (2021).

[76] ATLAS Collaboration, Performance of pile-up mitigation techniques for jets in $pp$ collisions at $\sqrt{s} = 8$ TeV using the ATLAS detector, Eur. Phys. J. C **76**, 581 (2016).

[77] ATLAS Collaboration, Forward jet vertex tagging using the particle flow algorithm, Report No. ATL-PHYS-PUB-2019-026, 2019, https://cds.cern.ch/record/2683100.

[78] ATLAS Collaboration, ATLAS flavour-tagging algorithms for the LHC Run 2 pp collision dataset, Eur. Phys. J. C **83**, 681 (2023).

[79] ATLAS Collaboration, The performance of missing transverse momentum reconstruction and its significance with the ATLAS detector using 140 fb$^{-1}$ of $\sqrt{s} = 13$ TeV $pp$ collisions, arXiv:2402.05858.

[80] ATLAS Collaboration, Performance of electron and photon triggers in ATLAS during LHC Run 2, Eur. Phys. J. C **80**, 47 (2020).

[81] ATLAS Collaboration, Performance of the ATLAS muon triggers in Run 2, J. Instrum. **15**, P09015 (2020).

[82] Particle Data Group, Review of particle physics, Prog. Theor. Exp. Phys. **2020**, 083C01 (2020).

[83] F. Pedregosa *et al.*, Scikit-learn: Machine learning in PYTHON, J. Mach. Learn. Res. **12**, 2825 (2011), https://dl.acm.org/doi/10.5555/1953048.2078195.

[84] ATLAS Collaboration, Electron and photon efficiencies in LHC Run 2 with the ATLAS experiment, J. High Energy Phys. 05 (2023) 162.

[85] ATLAS Collaboration, Muon reconstruction performance of the ATLAS detector in proton–proton collision data at $\sqrt{s} = 13$ TeV, Eur. Phys. J. C **76**, 292 (2016).

[86] ATLAS Collaboration, ATLAS $b$-jet identification performance and efficiency measurement with $t\bar{t}$ events in $pp$ collisions at $\sqrt{s} = 13$ TeV, Eur. Phys. J. C **79**, 970 (2019).
[87] ATLAS Collaboration, Calibration of the light-flavour jet mistagging efficiency of the $b$-tagging algorithms with $Z+$jets events using 139 fb$^{-1}$ of ATLAS proton–proton collision data at $\sqrt{s} = 13$ TeV, Eur. Phys. J. C **83**, 728 (2023).
[88] ATLAS Collaboration, Measurement of the $c$-jet mistagging efficiency in $t\bar{t}$ events using $pp$ collision data at $\sqrt{s} =$ 13 TeV collected with the ATLAS detector, Eur. Phys. J. C **82**, 95 (2022).
[89] ATLAS Collaboration, Measurements of the production cross section of a $Z$ boson in association with jets in pp collisions at $\sqrt{s} = 13$ TeV with the ATLAS detector, Eur. Phys. J. C **77**, 361 (2017).
[90] ATLAS Collaboration, Measurement of $W^{\pm}Z$ production cross sections and gauge boson polarisation in $pp$ collisions at $\sqrt{s} = 13$ TeV with the ATLAS detector, Eur. Phys. J. C **79**, 535 (2019).
[91] J. Butterworth *et al.*, PDF4LHC recommendations for LHC Run II, J. Phys. G **43**, 023001 (2016).
[92] A. D. Martin, W. J. Stirling, R. S. Thorne, and G. Watt, Parton distributions for the LHC, Eur. Phys. J. C **63**, 189 (2009).
[93] A. D. Martin, W. J. Stirling, R. S. Thorne, and G. Watt, Uncertainties on $\alpha_S$ in global PDF analyses and implications for predicted hadronic cross sections, Eur. Phys. J. C **64**, 653 (2009).
[94] H.-L. Lai *et al.*, New parton distributions for collider physics, Phys. Rev. D **82**, 074024 (2010).
[95] J. Gao *et al.*, CT10 next-to-next-to-leading order global analysis of QCD, Phys. Rev. D **89**, 033009 (2014).
[96] G. Cowan, K. Cranmer, E. Gross, and O. Vitells, Asymptotic formulae for likelihood-based tests of new physics, Eur. Phys. J. C **71**, 1554 (2011); **73**, 2501(E) (2013).
[97] K. Cranmer, G. Lewis, L. Moneta, A. Shibata, and W. Verkerke, HistFactory: A tool for creating statistical models for use with RooFit and RooStats, Report No. CERN-OPEN-2012-016, 2012, https://cds.cern.ch/record/1456844.
[98] L. Moneta, K. Cranmer, G. Schott, and W. Verkerke, The RooStats project, Proc. Sci., ACAT2010 (**2011**) 057 [arXiv:1009.1003].
[99] A. L. Read, Presentation of search results: The $CL_s$ technique, J. Phys. G **28**, 2693 (2002).
[100] L. Lehman, Extending the Standard Model effective field theory with the complete set of dimension-7 operators, Phys. Rev. D **90**, 125023 (2014).
[101] ATLAS Collaboration, ATLAS computing acknowledgements, Report No. ATL-SOFT-PUB-2023-001, 2023, https://cds.cern.ch/record/2869272.

G. Aad,[104] E. Aakvaag,[17] B. Abbott,[123] S. Abdelhameed,[119a] K. Abeling,[56] N. J. Abicht,[50] S. H. Abidi,[30] M. Aboelela,[45] A. Aboulhorma,[36e] H. Abramowicz,[154] H. Abreu,[153] Y. Abulaiti,[120] B. S. Acharya,[70a,70b,a] A. Ackermann,[64a] C. Adam Bourdarios,[4] L. Adamczyk,[87a] S. V. Addepalli,[27] M. J. Addison,[103] J. Adelman,[118] A. Adiguzel,[22c] T. Adye,[137] A. A. Affolder,[139] Y. Afik,[40] M. N. Agaras,[13] J. Agarwala,[74a,74b] A. Aggarwal,[102] C. Agheorghiesei,[28c] F. Ahmadov,[39,b] W. S. Ahmed,[106] S. Ahuja,[97] X. Ai,[63e] G. Aielli,[77a,77b] A. Aikot,[166] M. Ait Tamlihat,[36e] B. Aitbenchikh,[36a] M. Akbiyik,[102] T. P. A. Åkesson,[100] A. V. Akimov,[38] D. Akiyama,[171] N. N. Akolkar,[25] S. Aktas,[22a] K. Al Khoury,[42] G. L. Alberghi,[24b] J. Albert,[168] P. Albicocco,[54] G. L. Albouy,[61] S. Alderweireldt,[53] Z. L. Alegria,[124] M. Aleksa,[37] I. N. Aleksandrov,[39] C. Alexa,[28b] T. Alexopoulos,[10] F. Alfonsi,[24b] M. Algren,[57] M. Alhroob,[170] B. Ali,[135] H. M. J. Ali,[93] S. Ali,[32] S. W. Alibocus,[94] M. Aliev,[34c] G. Alimonti,[72a] W. Alkakhi,[56] C. Allaire,[67] B. M. M. Allbrooke,[149] J. F. Allen,[53] C. A. Allendes Flores,[140f] P. P. Allport,[21] A. Aloisio,[73a,73b] F. Alonso,[92] C. Alpigiani,[141] Z. M. K. Alsolami,[93] M. Alvarez Estevez,[101] A. Alvarez Fernandez,[102] M. Alves Cardoso,[57] M. G. Alviggi,[73a,73b] M. Aly,[103] Y. Amaral Coutinho,[84b] A. Ambler,[106] C. Amelung,[37] M. Amerl,[103] C. G. Ames,[111] D. Amidei,[108] K. J. Amirie,[158] S. P. Amor Dos Santos,[133a] K. R. Amos,[166] S. An,[85] V. Ananiev,[128] C. Anastopoulos,[142] T. Andeen,[11] J. K. Anders,[37] A. C. Anderson,[60] S. Y. Andrean,[48a,48b] A. Andreazza,[72a,72b] S. Angelidakis,[9] A. Angerami,[42] A. V. Anisenkov,[38] A. Annovi,[75a] C. Antel,[57] E. Antipov,[148] M. Antonelli,[54] F. Anulli,[76a] M. Aoki,[85] T. Aoki,[156] M. A. Aparo,[149] L. Aperio Bella,[49] C. Appelt,[19] A. Apyan,[27] S. J. Arbiol Val,[88] C. Arcangeletti,[54] A. T. H. Arce,[52] E. Arena,[94] J-F. Arguin,[110] S. Argyropoulos,[55] J.-H. Arling,[49] O. Arnaez,[4] H. Arnold,[148] G. Artoni,[76a,76b] H. Asada,[113] K. Asai,[121] S. Asai,[156] N. A. Asbah,[37] R. A. Ashby Pickering,[170] K. Assamagan,[30] R. Astalos,[29a] K. S. V. Astrand,[100] S. Atashi,[162] R. J. Atkin,[34a] M. Atkinson,[165] H. Atmani,[36f] P. A. Atmasiddha,[131] K. Augsten,[135] S. Auricchio,[73a,73b] A. D. Auriol,[21] V. A. Austrup,[103] G. Avolio,[37] K. Axiotis,[57] G. Azuelos,[110,c] D. Babal,[29b] H. Bachacou,[138] K. Bachas,[155,d] A. Bachiu,[35] F. Backman,[48a,48b] A. Badea,[40] T. M. Baer,[108] P. Bagnaia,[76a,76b] M. Bahmani,[19] D. Bahner,[55] K. Bai,[126] J. T. Baines,[137] L. Baines,[96] O. K. Baker,[175] E. Bakos,[16] D. Bakshi Gupta,[8] L. E. Balabram Filho,[84b] V. Balakrishnan,[123] R. Balasubramanian,[117]

E. M. Baldin,[38] P. Balek,[87a] E. Ballabene,[24b,24a] F. Balli,[138] L. M. Baltes,[64a] W. K. Balunas,[33] J. Balz,[102] I. Bamwidhi,[119b] E. Banas,[88] M. Bandieramonte,[132] A. Bandyopadhyay,[25] S. Bansal,[25] L. Barak,[154] M. Barakat,[49] E. L. Barberio,[107] D. Barberis,[58b,58a] M. Barbero,[104] M. Z. Barel,[117] K. N. Barends,[34a] T. Barillari,[112] M-S. Barisits,[37] T. Barklow,[146] P. Baron,[125] D. A. Baron Moreno,[103] A. Baroncelli,[63a] A. J. Barr,[129] J. D. Barr,[98] F. Barreiro,[101] J. Barreiro Guimarães da Costa,[14] U. Barron,[154] M. G. Barros Teixeira,[133a] S. Barsov,[38] F. Bartels,[64a] R. Bartoldus,[146] A. E. Barton,[93] P. Bartos,[29a] A. Basan,[102] M. Baselga,[50] A. Bassalat,[67,e] M. J. Basso,[159a] S. Bataju,[45] R. Bate,[167] R. L. Bates,[60] S. Batlamous,[101] B. Batool,[144] M. Battaglia,[139] D. Battulga,[19] M. Bauce,[76a,76b] M. Bauer,[80] P. Bauer,[25] L. T. Bazzano Hurrell,[31] J. B. Beacham,[52] T. Beau,[130] J. Y. Beaucamp,[92] P. H. Beauchemin,[161] P. Bechtle,[25] H. P. Beck,[20,f] K. Becker,[170] A. J. Beddall,[83] V. A. Bednyakov,[39] C. P. Bee,[148] L. J. Beemster,[16] T. A. Beermann,[37] M. Begalli,[84d] M. Begel,[30] A. Behera,[148] J. K. Behr,[49] J. F. Beirer,[37] F. Beisiegel,[25] M. Belfkir,[119b] G. Bella,[154] L. Bellagamba,[24b] A. Bellerive,[35] P. Bellos,[21] K. Beloborodov,[38] D. Benchekroun,[36a] F. Bendebba,[36a] Y. Benhammou,[154] K. C. Benkendorfer,[62] L. Beresford,[49] M. Beretta,[54] E. Bergeaas Kuutmann,[164] N. Berger,[4] B. Bergmann,[135] J. Beringer,[18a] G. Bernardi,[5] C. Bernius,[146] F. U. Bernlochner,[25] F. Bernon,[37,104] A. Berrocal Guardia,[13] T. Berry,[97] P. Berta,[136] A. Berthold,[51] S. Bethke,[112] A. Betti,[76a,76b] A. J. Bevan,[96] N. K. Bhalla,[55] S. Bhatta,[148] D. S. Bhattacharya,[169] P. Bhattarai,[146] K. D. Bhide,[55] V. S. Bhopatkar,[124] R. M. Bianchi,[132] G. Bianco,[24b,24a] O. Biebel,[111] R. Bielski,[126] M. Biglietti,[78a] C. S. Billingsley,[45] M. Bindi,[56] A. Bingul,[22b] C. Bini,[76a,76b] A. Biondini,[94] G. A. Bird,[33] M. Birman,[172] M. Biros,[136] S. Biryukov,[149] T. Bisanz,[50] E. Bisceglie,[44b,44a] J. P. Biswal,[137] D. Biswas,[144] I. Bloch,[49] A. Blue,[60] U. Blumenschein,[96] J. Blumenthal,[102] V. S. Bobrovnikov,[38] M. Boehler,[55] B. Boehm,[169] D. Bogavac,[37] A. G. Bogdanchikov,[38] C. Bohm,[48a] V. Boisvert,[97] P. Bokan,[37] T. Bold,[87a] M. Bomben,[5] M. Bona,[96] M. Boonekamp,[138] C. D. Booth,[97] A. G. Borbély,[60] I. S. Bordulev,[38] H. M. Borecka-Bielska,[110] G. Borissov,[93] D. Bortoletto,[129] D. Boscherini,[24b] M. Bosman,[13] J. D. Bossio Sola,[37] K. Bouaouda,[36a] N. Bouchhar,[166] L. Boudet,[4] J. Boudreau,[132] E. V. Bouhova-Thacker,[93] D. Boumediene,[41] R. Bouquet,[58b,58a] A. Boveia,[122] J. Boyd,[37] D. Boye,[30] I. R. Boyko,[39] L. Bozianu,[57] J. Bracinik,[21] N. Brahimi,[4] G. Brandt,[174] O. Brandt,[33] F. Braren,[49] B. Brau,[105] J. E. Brau,[126] R. Brener,[172] L. Brenner,[117] R. Brenner,[164] S. Bressler,[172] G. Brianti,[79a,79b] D. Britton,[60] D. Britzger,[112] I. Brock,[25] R. Brock,[109] G. Brooijmans,[42] E. M. Brooks,[159b] E. Brost,[30] L. M. Brown,[168] L. E. Bruce,[62] T. L. Bruckler,[129] P. A. Bruckman de Renstrom,[88] B. Brüers,[49] A. Bruni,[24b] G. Bruni,[24b] M. Bruschi,[24b] N. Bruscino,[76a,76b] T. Buanes,[17] Q. Buat,[141] D. Buchin,[112] A. G. Buckley,[60] O. Bulekov,[38] B. A. Bullard,[146] S. Burdin,[94] C. D. Burgard,[50] A. M. Burger,[37] B. Burghgrave,[8] O. Burlayenko,[55] J. Burleson,[165] J. T. P. Burr,[33] J. C. Burzynski,[145] E. L. Busch,[42] V. Büscher,[102] P. J. Bussey,[60] J. M. Butler,[26] C. M. Buttar,[60] J. M. Butterworth,[98] W. Buttinger,[137] C. J. Buxo Vazquez,[109] A. R. Buzykaev,[38] S. Cabrera Urbán,[166] L. Cadamuro,[67] D. Caforio,[59] H. Cai,[132] Y. Cai,[14,114c] Y. Cai,[114a] V. M. M. Cairo,[37] O. Cakir,[3a] N. Calace,[37] P. Calafiura,[18a] G. Calderini,[130] P. Calfayan,[69] G. Callea,[60] L. P. Caloba,[84b] D. Calvet,[41] S. Calvet,[41] M. Calvetti,[75a,75b] R. Camacho Toro,[130] S. Camarda,[37] D. Camarero Munoz,[27] P. Camarri,[77a,77b] M. T. Camerlingo,[73a,73b] D. Cameron,[37] C. Camincher,[168] M. Campanelli,[98] A. Camplani,[43] V. Canale,[73a,73b] A. C. Canbay,[3a] E. Canonero,[97] J. Cantero,[166] Y. Cao,[165] F. Capocasa,[27] M. Capua,[44b,44a] A. Carbone,[72a,72b] R. Cardarelli,[77a] J. C. J. Cardenas,[8] G. Carducci,[44b,44a] T. Carli,[37] G. Carlino,[73a] J. I. Carlotto,[13] B. T. Carlson,[132,g] E. M. Carlson,[168,159a] J. Carmignani,[94] L. Carminati,[72a,72b] A. Carnelli,[138] M. Carnesale,[76a,76b] S. Caron,[116] E. Carquin,[140f] S. Carrá,[72a] G. Carratta,[24b,24a] A. M. Carroll,[126] T. M. Carter,[53] M. P. Casado,[13,h] M. Caspar,[49] F. L. Castillo,[4] L. Castillo Garcia,[13] V. Castillo Gimenez,[166] N. F. Castro,[133a,133e] A. Catinaccio,[37] J. R. Catmore,[128] T. Cavaliere,[4] V. Cavaliere,[30] N. Cavalli,[24b,24a] L. J. Caviedes Betancourt,[23b] Y. C. Cekmecelioglu,[49] E. Celebi,[83] S. Cella,[37] F. Celli,[129] M. S. Centonze,[71a,71b] V. Cepaitis,[57] K. Cerny,[125] A. S. Cerqueira,[84a] A. Cerri,[149] L. Cerrito,[77a,77b] F. Cerutti,[18a] B. Cervato,[144] A. Cervelli,[24b] G. Cesarini,[54] S. A. Cetin,[83] D. Chakraborty,[118] J. Chan,[18a] W. Y. Chan,[156] J. D. Chapman,[33] E. Chapon,[138] B. Chargeishvili,[152b] D. G. Charlton,[21] M. Chatterjee,[20] C. Chauhan,[136] Y. Che,[114a] S. Chekanov,[6] S. V. Chekulaev,[159a] G. A. Chelkov,[39,i] A. Chen,[108] B. Chen,[154] B. Chen,[168] H. Chen,[114a] H. Chen,[30] J. Chen,[63c] J. Chen,[145] M. Chen,[129] S. Chen,[156] S. J. Chen,[114a] X. Chen,[63c,138] X. Chen,[15,j] Y. Chen,[63a] C. L. Cheng,[173] H. C. Cheng,[65a] S. Cheong,[146] A. Cheplakov,[39] E. Cheremushkina,[49] E. Cherepanova,[117] R. Cherkaoui El Moursli,[36e] E. Cheu,[7] K. Cheung,[66] L. Chevalier,[138]

V. Chiarella,[54] G. Chiarelli,[75a] N. Chiedde,[104] G. Chiodini,[71a] A. S. Chisholm,[21] A. Chitan,[28b] M. Chitishvili,[166] M. V. Chizhov,[39,k] K. Choi,[11] Y. Chou,[141] E. Y. S. Chow,[116] K. L. Chu,[172] M. C. Chu,[65a] X. Chu,[14,114c] Z. Chubinidze,[54] J. Chudoba,[134] J. J. Chwastowski,[88] D. Cieri,[112] K. M. Ciesla,[87a] V. Cindro,[95] A. Ciocio,[18a] F. Cirotto,[73a,73b] Z. H. Citron,[172] M. Citterio,[72a] D. A. Ciubotaru,[28b] A. Clark,[57] P. J. Clark,[53] N. Clarke Hall,[98] C. Clarry,[158] J. M. Clavijo Columbie,[49] S. E. Clawson,[49] C. Clement,[48a,48b] Y. Coadou,[104] M. Cobal,[70a,70c] A. Coccaro,[58b] R. F. Coelho Barrue,[133a] R. Coelho Lopes De Sa,[105] S. Coelli,[72a] B. Cole,[42] J. Collot,[61] P. Conde Muiño,[133a,133g] M. P. Connell,[34c] S. H. Connell,[34c] E. I. Conroy,[129] F. Conventi,[73a,l] H. G. Cooke,[21] A. M. Cooper-Sarkar,[129] F. A. Corchia,[24b,24a] A. Cordeiro Oudot Choi,[130] L. D. Corpe,[41] M. Corradi,[76a,76b] F. Corriveau,[106,m] A. Cortes-Gonzalez,[19] M. J. Costa,[166] F. Costanza,[4] D. Costanzo,[142] B. M. Cote,[122] J. Couthures,[4] G. Cowan,[97] K. Cranmer,[173] D. Cremonini,[24b,24a] S. Crépé-Renaudin,[61] F. Crescioli,[130] M. Cristinziani,[144] M. Cristoforetti,[79a,79b] V. Croft,[117] J. E. Crosby,[124] G. Crosetti,[44b,44a] A. Cueto,[101] H. Cui,[98] Z. Cui,[7] W. R. Cunningham,[60] F. Curcio,[166] J. R. Curran,[53] P. Czodrowski,[37] M. M. Czurylo,[37] M. J. Da Cunha Sargedas De Sousa,[58b,58a] J. V. Da Fonseca Pinto,[84b] C. Da Via,[103] W. Dabrowski,[87a] T. Dado,[50] S. Dahbi,[151] T. Dai,[108] D. Dal Santo,[20] C. Dallapiccola,[105] M. Dam,[43] G. D'amen,[30] V. D'Amico,[111] J. Damp,[102] J. R. Dandoy,[35] D. Dannheim,[37] M. Danninger,[145] V. Dao,[148] G. Darbo,[58b] S. J. Das,[30,n] F. Dattola,[49] S. D'Auria,[72a,72b] A. D'Avanzo,[73a,73b] C. David,[34a] T. Davidek,[136] I. Dawson,[96] H. A. Day-hall,[135] K. De,[8] R. De Asmundis,[73a] N. De Biase,[49] S. De Castro,[24b,24a] N. De Groot,[116] P. de Jong,[117] H. De la Torre,[118] A. De Maria,[114a] A. De Salvo,[76a] U. De Sanctis,[77a,77b] F. De Santis,[71a,71b] A. De Santo,[149] J. B. De Vivie De Regie,[61] D. V. Dedovich,[39] J. Degens,[94] A. M. Deiana,[45] F. Del Corso,[24b,24a] J. Del Peso,[101] F. Del Rio,[64a] L. Delagrange,[130] F. Deliot,[138] C. M. Delitzsch,[50] M. Della Pietra,[73a,73b] D. Della Volpe,[57] A. Dell'Acqua,[37] L. Dell'Asta,[72a,72b] M. Delmastro,[4] P. A. Delsart,[61] S. Demers,[175] M. Demichev,[39] S. P. Denisov,[38] L. D'Eramo,[41] D. Derendarz,[88] F. Derue,[130] P. Dervan,[94] K. Desch,[25] C. Deutsch,[25] F. A. Di Bello,[58b,58a] A. Di Ciaccio,[77a,77b] L. Di Ciaccio,[4] A. Di Domenico,[76a,76b] C. Di Donato,[73a,73b] A. Di Girolamo,[37] G. Di Gregorio,[37] A. Di Luca,[79a,79b] B. Di Micco,[78a,78b] R. Di Nardo,[78a,78b] K. F. Di Petrillo,[40] M. Diamantopoulou,[35] F. A. Dias,[117] T. Dias Do Vale,[145] M. A. Diaz,[140a,140b] F. G. Diaz Capriles,[25] A. R. Didenko,[39] M. Didenko,[166] E. B. Diehl,[108] S. Díez Cornell,[49] C. Diez Pardos,[144] C. Dimitriadi,[164] A. Dimitrievska,[21] J. Dingfelder,[25] T. Dingley,[129] I-M. Dinu,[28b] S. J. Dittmeier,[64b] F. Dittus,[37] M. Divisek,[136] F. Djama,[104] T. Djobava,[152b] C. Doglioni,[103,100] A. Dohnalova,[29a] J. Dolejsi,[136] Z. Dolezal,[136] K. Domijan,[87a] K. M. Dona,[40] M. Donadelli,[84d] B. Dong,[109] J. Donini,[41] A. D'Onofrio,[73a,73b] M. D'Onofrio,[94] J. Dopke,[137] A. Doria,[73a] N. Dos Santos Fernandes,[133a] P. Dougan,[103] M. T. Dova,[92] A. T. Doyle,[60] M. A. Draguet,[129] E. Dreyer,[172] I. Drivas-koulouris,[10] M. Drnevich,[120] M. Drozdova,[57] D. Du,[63a] T. A. du Pree,[117] F. Dubinin,[38] M. Dubovsky,[29a] E. Duchovni,[172] G. Duckeck,[111] O. A. Ducu,[28b] D. Duda,[53] A. Dudarev,[37] E. R. Duden,[27] M. D'uffizi,[103] L. Duflot,[67] M. Dührssen,[37] I. Duminica,[28g] A. E. Dumitriu,[28b] M. Dunford,[64a] S. Dungs,[50] K. Dunne,[48a,48b] A. Duperrin,[104] H. Duran Yildiz,[3a] M. Düren,[59] A. Durglishvili,[152b] B. L. Dwyer,[118] G. I. Dyckes,[18a] M. Dyndal,[87a] B. S. Dziedzic,[37] Z. O. Earnshaw,[149] G. H. Eberwein,[129] B. Eckerova,[29a] S. Eggebrecht,[56] E. Egidio Purcino De Souza,[130] L. F. Ehrke,[57] G. Eigen,[17] K. Einsweiler,[18a] T. Ekelof,[164] P. A. Ekman,[100] S. El Farkh,[36b] Y. El Ghazali,[63a] H. El Jarrari,[37] A. El Moussaouy,[36a] V. Ellajosyula,[164] M. Ellert,[164] F. Ellinghaus,[174] N. Ellis,[37] J. Elmsheuser,[30] M. Elsawy,[119a] M. Elsing,[37] D. Emeliyanov,[137] Y. Enari,[156] I. Ene,[18a] S. Epari,[13] P. A. Erland,[88] D. Ernani Martins Neto,[88] M. Errenst,[174] M. Escalier,[67] C. Escobar,[166] E. Etzion,[154] G. Evans,[133a] H. Evans,[69] L. S. Evans,[97] A. Ezhilov,[38] S. Ezzarqtouni,[36a] F. Fabbri,[24b,24a] L. Fabbri,[24b,24a] G. Facini,[98] V. Fadeyev,[139] R. M. Fakhrutdinov,[38] D. Fakoudis,[102] S. Falciano,[76a] L. F. Falda Ulhoa Coelho,[37] F. Fallavollita,[112] G. Falsetti,[44b,44a] J. Faltova,[136] C. Fan,[165] Y. Fan,[14] Y. Fang,[14,114c] M. Fanti,[72a,72b] M. Faraj,[70a,70b] Z. Farazpay,[99] A. Farbin,[8] A. Farilla,[78a] T. Farooque,[109] S. M. Farrington,[53] F. Fassi,[36e] D. Fassouliotis,[9] M. Faucci Giannelli,[77a,77b] W. J. Fawcett,[33] L. Fayard,[67] P. Federic,[136] P. Federicova,[134] O. L. Fedin,[38,i] M. Feickert,[173] L. Feligioni,[104] D. E. Fellers,[126] C. Feng,[63b] M. Feng,[15] Z. Feng,[117] M. J. Fenton,[162] L. Ferencz,[49] R. A. M. Ferguson,[93] S. I. Fernandez Luengo,[140f] P. Fernandez Martinez,[13] M. J. V. Fernoux,[104] J. Ferrando,[93] A. Ferrari,[164] P. Ferrari,[117,116] R. Ferrari,[74a] D. Ferrere,[57] C. Ferretti,[108] D. Fiacco,[76a,76b] F. Fiedler,[102] P. Fiedler,[135] A. Filipčič,[95] E. K. Filmer,[1] F. Filthaut,[116] M. C. N. Fiolhais,[133a,133c,o] L. Fiorini,[166] W. C. Fisher,[109] T. Fitschen,[103] P. M. Fitzhugh,[138]

I. Fleck,[144] P. Fleischmann,[108] T. Flick,[174] M. Flores,[34d,p] L. R. Flores Castillo,[65a] L. Flores Sanz De Acedo,[37] F. M. Follega,[79a,79b] N. Fomin,[33] J. H. Foo,[158] A. Formica,[138] A. C. Forti,[103] E. Fortin,[37] A. W. Fortman,[18a] M. G. Foti,[18a] L. Fountas,[9,q] D. Fournier,[67] H. Fox,[93] P. Francavilla,[75a,75b] S. Francescato,[62] S. Franchellucci,[57] M. Franchini,[24b,24a] S. Franchino,[64a] D. Francis,[37] L. Franco,[116] V. Franco Lima,[37] L. Franconi,[49] M. Franklin,[62] G. Frattari,[27] Y. Y. Frid,[154] J. Friend,[60] N. Fritzsche,[51] A. Froch,[55] D. Froidevaux,[37] J. A. Frost,[129] Y. Fu,[63a] S. Fuenzalida Garrido,[140f] M. Fujimoto,[104] K. Y. Fung,[65a] E. Furtado De Simas Filho,[84e] M. Furukawa,[156] J. Fuster,[166] A. Gaa,[56] A. Gabrielli,[24b,24a] A. Gabrielli,[158] P. Gadow,[37] G. Gagliardi,[58b,58a] L. G. Gagnon,[18a] S. Gaid,[163] S. Galantzan,[154] E. J. Gallas,[129] B. J. Gallop,[137] K. K. Gan,[122] S. Ganguly,[156] Y. Gao,[53] F. M. Garay Walls,[140a,140b] B. Garcia,[30] C. García,[166] A. Garcia Alonso,[117] A. G. Garcia Caffaro,[175] J. E. García Navarro,[166] M. Garcia-Sciveres,[18a] G. L. Gardner,[131] R. W. Gardner,[40] N. Garelli,[161] D. Garg,[81] R. B. Garg,[146] J. M. Gargan,[53] C. A. Garner,[158] C. M. Garvey,[34a] V. K. Gassmann,[161] G. Gaudio,[74a] V. Gautam,[13] P. Gauzzi,[76a,76b] J. Gavranovic,[95] I. L. Gavrilenko,[38] A. Gavrilyuk,[38] C. Gay,[167] G. Gaycken,[126] E. N. Gazis,[10] A. A. Geanta,[28b] C. M. Gee,[139] A. Gekow,[122] C. Gemme,[58b] M. H. Genest,[61] A. D. Gentry,[115] S. George,[97] W. F. George,[21] T. Geralis,[47] P. Gessinger-Befurt,[37] M. E. Geyik,[174] M. Ghani,[170] K. Ghorbanian,[96] A. Ghosal,[144] A. Ghosh,[162] A. Ghosh,[7] B. Giacobbe,[24b] S. Giagu,[76a,76b] T. Giani,[117] A. Giannini,[63a] S. M. Gibson,[97] M. Gignac,[139] D. T. Gil,[87b] A. K. Gilbert,[87a] B. J. Gilbert,[42] D. Gillberg,[35] G. Gilles,[117] L. Ginabat,[130] D. M. Gingrich,[2,c] M. P. Giordani,[70a,70c] P. F. Giraud,[138] G. Giugliarelli,[70a,70c] D. Giugni,[72a] F. Giuli,[37] I. Gkialas,[9,q] L. K. Gladilin,[38] C. Glasman,[101] G. R. Gledhill,[126] G. Glemža,[49] M. Glisic,[126] I. Gnesi,[44b,r] Y. Go,[30] M. Goblirsch-Kolb,[37] B. Gocke,[50] D. Godin,[110] B. Gokturk,[22a] S. Goldfarb,[107] T. Golling,[57] M. G. D. Gololo,[34g] D. Golubkov,[38] J. P. Gombas,[109] A. Gomes,[133a,133b] G. Gomes Da Silva,[144] A. J. Gomez Delegido,[166] R. Gonçalo,[133a] L. Gonella,[21] A. Gongadze,[152c] F. Gonnella,[21] J. L. Gonski,[146] R. Y. González Andana,[53] S. González de la Hoz,[166] R. Gonzalez Lopez,[94] C. Gonzalez Renteria,[18a] M. V. Gonzalez Rodrigues,[49] R. Gonzalez Suarez,[164] S. Gonzalez-Sevilla,[57] L. Goossens,[37] B. Gorini,[37] E. Gorini,[71a,71b] A. Gorišek,[95] T. C. Gosart,[131] A. T. Goshaw,[52] M. I. Gostkin,[39] S. Goswami,[124] C. A. Gottardo,[37] S. A. Gotz,[111] M. Gouighri,[36b] V. Goumarre,[49] A. G. Goussiou,[141] N. Govender,[34c] R. P. Grabarczyk,[129] I. Grabowska-Bold,[87a] K. Graham,[35] E. Gramstad,[128] S. Grancagnolo,[71a,71b] C. M. Grant,[1,138] P. M. Gravila,[28f] F. G. Gravili,[71a,71b] H. M. Gray,[18a] M. Greco,[71a,71b] M. J. Green,[1] C. Grefe,[25] A. S. Grefsrud,[17] I. M. Gregor,[49] K. T. Greif,[162] P. Grenier,[146] S. G. Grewe,[112] A. A. Grillo,[139] K. Grimm,[32] S. Grinstein,[13,s] J.-F. Grivaz,[67] E. Gross,[172] J. Grosse-Knetter,[56] J. C. Grundy,[129] L. Guan,[108] J. G. R. Guerrero Rojas,[166] G. Guerrieri,[70a,70c] R. Gugel,[102] J. A. M. Guhit,[108] A. Guida,[19] E. Guilloton,[170] S. Guindon,[37] F. Guo,[14,114c] J. Guo,[63c] L. Guo,[49] Y. Guo,[108] R. Gupta,[132] S. Gurbuz,[25] S. S. Gurdasani,[55] G. Gustavino,[76a,76b] P. Gutierrez,[123] L. F. Gutierrez Zagazeta,[131] M. Gutsche,[51] C. Gutschow,[98] C. Gwenlan,[129] C. B. Gwilliam,[94] E. S. Haaland,[128] A. Haas,[120] M. Habedank,[49] C. Haber,[18a] H. K. Hadavand,[8] A. Hadef,[51] S. Hadzic,[112] A. I. Hagan,[93] J. J. Hahn,[144] E. H. Haines,[98] M. Haleem,[169] J. Haley,[124] J. J. Hall,[142] G. D. Hallewell,[104] L. Halser,[20] K. Hamano,[168] M. Hamer,[25] G. N. Hamity,[53] E. J. Hampshire,[97] J. Han,[63b] K. Han,[63a] L. Han,[114a] L. Han,[63a] S. Han,[18a] Y. F. Han,[158] K. Hanagaki,[85] M. Hance,[139] D. A. Hangal,[42] H. Hanif,[145] M. D. Hank,[131] J. B. Hansen,[43] P. H. Hansen,[43] K. Hara,[160] D. Harada,[57] T. Harenberg,[174] S. Harkusha,[38] M. L. Harris,[105] Y. T. Harris,[129] J. Harrison,[13] N. M. Harrison,[122] P. F. Harrison,[170] N. M. Hartman,[112] N. M. Hartmann,[111] R. Z. Hasan,[97,137] Y. Hasegawa,[143] S. Hassan,[17] R. Hauser,[109] C. M. Hawkes,[21] R. J. Hawkings,[37] Y. Hayashi,[156] S. Hayashida,[113] D. Hayden,[109] C. Hayes,[108] R. L. Hayes,[117] C. P. Hays,[129] J. M. Hays,[96] H. S. Hayward,[94] F. He,[63a] M. He,[14,114c] Y. He,[157] Y. He,[49] Y. He,[98] N. B. Heatley,[96] V. Hedberg,[100] A. L. Heggelund,[128] N. D. Hehir,[96] C. Heidegger,[55] K. K. Heidegger,[55] J. Heilman,[35] S. Heim,[49] T. Heim,[18a] J. G. Heinlein,[131] J. J. Heinrich,[126] L. Heinrich,[112,t] J. Hejbal,[134] A. Held,[173] S. Hellesund,[17] C. M. Helling,[167] S. Hellman,[48a,48b] R. C. W. Henderson,[93] L. Henkelmann,[33] A. M. Henriques Correia,[37] H. Herde,[100] Y. Hernández Jiménez,[148] L. M. Herrmann,[25] T. Herrmann,[51] G. Herten,[55] R. Hertenberger,[111] L. Hervas,[37] M. E. Hesping,[102] N. P. Hessey,[159a] M. Hidaoui,[36b] N. Hidic,[136] E. Hill,[158] S. J. Hillier,[21] J. R. Hinds,[109] F. Hinterkeuser,[25] M. Hirose,[127] S. Hirose,[160] D. Hirschbuehl,[174] T. G. Hitchings,[103] B. Hiti,[95] J. Hobbs,[148] R. Hobincu,[28e] N. Hod,[172] M. C. Hodgkinson,[142] B. H. Hodkinson,[129] A. Hoecker,[37] D. D. Hofer,[108] J. Hofer,[49] T. Holm,[25] M. Holzbock,[112] L. B. A. H. Hommels,[33] B. P. Honan,[103] J. J. Hong,[69] J. Hong,[63c] T. M. Hong,[132]

B. H. Hooberman,[165] W. H. Hopkins,[6] M. C. Hoppesch,[165] Y. Horii,[113] S. Hou,[151] A. S. Howard,[95] J. Howarth,[60] J. Hoya,[6] M. Hrabovsky,[125] A. Hrynevich,[49] T. Hryn'ova,[4] P. J. Hsu,[66] S.-C. Hsu,[141] T. Hsu,[67] M. Hu,[18a] Q. Hu,[63a] S. Huang,[65b] X. Huang,[14,114c] Y. Huang,[142] Y. Huang,[102] Y. Huang,[14] Z. Huang,[103] Z. Hubacek,[135] M. Huebner,[25] F. Huegging,[25] T. B. Huffman,[129] C. A. Hugli,[49] M. Huhtinen,[37] S. K. Huiberts,[17] R. Hulsken,[106] N. Huseynov,[12,u] J. Huston,[109] J. Huth,[62] R. Hyneman,[146] G. Iacobucci,[57] G. Iakovidis,[30] L. Iconomidou-Fayard,[67] J. P. Iddon,[37] P. Iengo,[73a,73b] R. Iguchi,[156] Y. Iiyama,[156] T. Iizawa,[129] Y. Ikegami,[85] N. Ilic,[158] H. Imam,[84c] M. Ince Lezki,[57] T. Ingebretsen Carlson,[48a,48b] J. M. Inglis,[96] G. Introzzi,[74a,74b] M. Iodice,[78a] V. Ippolito,[76a,76b] R. K. Irwin,[94] M. Ishino,[156] W. Islam,[173] C. Issever,[19,49] S. Istin,[22a,v] H. Ito,[171] R. Iuppa,[79a,79b] A. Ivina,[172] J. M. Izen,[46] V. Izzo,[73a] P. Jacka,[134] P. Jackson,[1] C. S. Jagfeld,[111] G. Jain,[159a] P. Jain,[49] K. Jakobs,[55] T. Jakoubek,[172] J. Jamieson,[60] W. Jang,[156] M. Javurkova,[105] P. Jawahar,[103] L. Jeanty,[126] J. Jejelava,[152a,w] P. Jenni,[55,x] C. E. Jessiman,[35] C. Jia,[63b] J. Jia,[148] X. Jia,[62] X. Jia,[14,114c] Z. Jia,[114a] C. Jiang,[53] S. Jiggins,[49] J. Jimenez Pena,[13] S. Jin,[114a] A. Jinaru,[28b] O. Jinnouchi,[157] P. Johansson,[142] K. A. Johns,[7] J. W. Johnson,[139] D. M. Jones,[149] E. Jones,[49] K. S. Jones,[8] P. Jones,[33] R. W. L. Jones,[93] T. J. Jones,[94] H. L. Joos,[56,37] R. Joshi,[122] J. Jovicevic,[16] X. Ju,[18a] J. J. Junggeburth,[105] T. Junkermann,[64a] A. Juste Rozas,[13,s] M. K. Juzek,[88] S. Kabana,[140e] A. Kaczmarska,[88] M. Kado,[112] H. Kagan,[122] M. Kagan,[146] A. Kahn,[131] C. Kahra,[102] T. Kaji,[156] E. Kajomovitz,[153] N. Kakati,[172] I. Kalaitzidou,[55] C. W. Kalderon,[30] N. J. Kang,[139] D. Kar,[34g] K. Karava,[129] M. J. Kareem,[159b] E. Karentzos,[55] O. Karkout,[117] S. N. Karpov,[39] Z. M. Karpova,[39] V. Kartvelishvili,[93] A. N. Karyukhin,[38] E. Kasimi,[155] J. Katzy,[49] S. Kaur,[35] K. Kawade,[143] M. P. Kawale,[123] C. Kawamoto,[89] T. Kawamoto,[63a] E. F. Kay,[37] F. I. Kaya,[161] S. Kazakos,[109] V. F. Kazanin,[38] Y. Ke,[148] J. M. Keaveney,[34a] R. Keeler,[168] G. V. Kehris,[62] J. S. Keller,[35] A. S. Kelly,[98] J. J. Kempster,[149] P. D. Kennedy,[102] O. Kepka,[134] B. P. Kerridge,[137] S. Kersten,[174] B. P. Kerševan,[95] L. Keszeghova,[29a] S. Ketabchi Haghighat,[158] R. A. Khan,[132] A. Khanov,[124] A. G. Kharlamov,[38] T. Kharlamova,[38] E. E. Khoda,[141] M. Kholodenko,[38] T. J. Khoo,[19] G. Khoriauli,[169] J. Khubua,[152b] Y. A. R. Khwaira,[130] B. Kibirige,[34g] D. Kim,[6] D. W. Kim,[48a,48b] Y. K. Kim,[40] N. Kimura,[98] M. K. Kingston,[56] A. Kirchhoff,[56] C. Kirfel,[25] F. Kirfel,[25] J. Kirk,[137] A. E. Kiryunin,[112] C. Kitsaki,[10] O. Kivernyk,[25] M. Klassen,[161] C. Klein,[35] L. Klein,[169] M. H. Klein,[45] S. B. Klein,[57] U. Klein,[94] P. Klimek,[37] A. Klimentov,[30] T. Klioutchnikova,[37] P. Kluit,[117] S. Kluth,[112] E. Kneringer,[80] T. M. Knight,[158] A. Knue,[50] R. Kobayashi,[89] D. Kobylianskii,[172] S. F. Koch,[129] M. Kocian,[146] P. Kodyš,[136] D. M. Koeck,[126] P. T. Koenig,[25] T. Koffas,[35] O. Kolay,[51] I. Koletsou,[4] T. Komarek,[88] K. Köneke,[55] A. X. Y. Kong,[1] T. Kono,[121] N. Konstantinidis,[98] P. Kontaxakis,[57] B. Konya,[100] R. Kopeliansky,[42] S. Koperny,[87a] K. Korcyl,[88] K. Kordas,[155,y] A. Korn,[98] S. Korn,[56] I. Korolkov,[13] N. Korotkova,[38] B. Kortman,[117] O. Kortner,[112] S. Kortner,[112] W. H. Kostecka,[118] V. V. Kostyukhin,[144] A. Kotsokechagia,[138] A. Kotwal,[52] A. Koulouris,[37] A. Kourkoumeli-Charalampidi,[74a,74b] C. Kourkoumelis,[9] E. Kourlitis,[112,t] O. Kovanda,[126] R. Kowalewski,[168] W. Kozanecki,[138] A. S. Kozhin,[38] V. A. Kramarenko,[38] G. Kramberger,[95] P. Kramer,[102] M. W. Krasny,[130] A. Krasznahorkay,[37] A. C. Kraus,[118] J. W. Kraus,[174] J. A. Kremer,[49] T. Kresse,[51] L. Kretschmann,[174] J. Kretzschmar,[94] K. Kreul,[19] P. Krieger,[158] S. Krishnamurthy,[105] M. Krivos,[136] K. Krizka,[21] K. Kroeninger,[50] H. Kroha,[112] J. Kroll,[134] J. Kroll,[131] K. S. Krowpman,[109] U. Kruchonak,[39] H. Krüger,[25] N. Krumnack,[82] M. C. Kruse,[52] O. Kuchinskaia,[38] S. Kuday,[3a] S. Kuehn,[37] R. Kuesters,[55] T. Kuhl,[49] V. Kukhtin,[39] Y. Kulchitsky,[38,i] S. Kuleshov,[140d,140b] M. Kumar,[34g] N. Kumari,[49] P. Kumari,[159b] A. Kupco,[134] T. Kupfer,[50] A. Kupich,[38] O. Kuprash,[55] H. Kurashige,[86] L. L. Kurchaninov,[159a] O. Kurdysh,[67] Y. A. Kurochkin,[38] A. Kurova,[38] M. Kuze,[157] A. K. Kvam,[105] J. Kvita,[125] T. Kwan,[106] N. G. Kyriacou,[108] L. A. O. Laatu,[104] C. Lacasta,[166] F. Lacava,[76a,76b] H. Lacker,[19] D. Lacour,[130] N. N. Lad,[98] E. Ladygin,[39] A. Lafarge,[41] B. Laforge,[130] T. Lagouri,[175] F. Z. Lahbabi,[36a] S. Lai,[56] J. E. Lambert,[168] S. Lammers,[69] W. Lampl,[7] C. Lampoudis,[155,y] G. Lamprinoudis,[102] A. N. Lancaster,[118] E. Lançon,[30] U. Landgraf,[55] M. P. J. Landon,[96] V. S. Lang,[55] O. K. B. Langrekken,[128] A. J. Lankford,[162] F. Lanni,[37] K. Lantzsch,[25] A. Lanza,[74a] J. F. Laporte,[138] T. Lari,[72a] F. Lasagni Manghi,[24b] M. Lassnig,[37] V. Latonova,[134] A. Laurier,[153] S. D. Lawlor,[142] Z. Lawrence,[103] R. Lazaridou,[170] M. Lazzaroni,[72a,72b] B. Le,[103] E. M. Le Boulicaut,[52] L. T. Le Pottier,[18a] B. Leban,[24b,24a] A. Lebedev,[82] M. LeBlanc,[103] F. Ledroit-Guillon,[61] S. C. Lee,[151] S. Lee,[48a,48b] T. F. Lee,[94] L. L. Leeuw,[34c] H. P. Lefebvre,[97] M. Lefebvre,[168] C. Leggett,[18a] G. Lehmann Miotto,[37] M. Leigh,[57] W. A. Leight,[105] W. Leinonen,[116] A. Leisos,[155,z] M. A. L. Leite,[84c] C. E. Leitgeb,[19] R. Leitner,[136]

K. J. C. Leney,[45] T. Lenz,[25] S. Leone,[75a] C. Leonidopoulos,[53] A. Leopold,[147] R. Les,[109] C. G. Lester,[33] M. Levchenko,[38] J. Levêque,[4] L. J. Levinson,[172] G. Levrini,[24b,24a] M. P. Lewicki,[88] C. Lewis,[141] D. J. Lewis,[4] A. Li,[5] B. Li,[63b] C. Li,[63a] C-Q. Li,[112] H. Li,[63a] H. Li,[63b] H. Li,[114a] H. Li,[15] H. Li,[63b] J. Li,[63c] K. Li,[141] L. Li,[63c] M. Li,[14,114c] S. Li,[14,114c] S. Li,[63d,63c] T. Li,[5] X. Li,[106] Z. Li,[129] Z. Li,[156] Z. Li,[14,114c] Z. Li,[63a] S. Liang,[14,114c] Z. Liang,[14] M. Liberatore,[138] B. Liberti,[77a] K. Lie,[65c] J. Lieber Marin,[84e] H. Lien,[69] H. Lin,[108] K. Lin,[109] R. E. Lindley,[7] J. H. Lindon,[2] J. Ling,[62] E. Lipeles,[131] A. Lipniacka,[17] A. Lister,[167] J. D. Little,[69] B. Liu,[14] B. X. Liu,[114b] D. Liu,[63d,63c] E. H. L. Liu,[21] J. B. Liu,[63a] J. K. K. Liu,[33] K. Liu,[63d] K. Liu,[63d,63c] M. Liu,[63a] M. Y. Liu,[63a] P. Liu,[14] Q. Liu,[63d,141,63c] X. Liu,[63a] X. Liu,[63b] Y. Liu,[114b,114c] Y. L. Liu,[63b] Y. W. Liu,[63a] J. Llorente Merino,[145] S. L. Lloyd,[96] E. M. Lobodzinska,[49] P. Loch,[7] T. Lohse,[19] K. Lohwasser,[142] E. Loiacono,[49] M. Lokajicek,[134] J. D. Lomas,[21] J. D. Long,[165] I. Longarini,[162] R. Longo,[165] I. Lopez Paz,[68] A. Lopez Solis,[49] N. A. Lopez-canelas,[7] N. Lorenzo Martinez,[4] A. M. Lory,[111] M. Losada,[119a] G. Löschcke Centeno,[149] O. Loseva,[38] X. Lou,[48a,48b] X. Lou,[14,114c] A. Lounis,[67] P. A. Love,[93] G. Lu,[14,114c] M. Lu,[67] S. Lu,[131] Y. J. Lu,[66] H. J. Lubatti,[141] C. Luci,[76a,76b] F. L. Lucio Alves,[114a] F. Luehring,[69] I. Luise,[148] O. Lukianchuk,[67] O. Lundberg,[147] B. Lund-Jensen,[147] N. A. Luongo,[6] M. S. Lutz,[37] A. B. Lux,[26] D. Lynn,[30] R. Lysak,[134] E. Lytken,[100] V. Lyubushkin,[39] T. Lyubushkina,[39] M. M. Lyukova,[148] M. Firdaus M. Soberi,[53] H. Ma,[30] K. Ma,[63a] L. L. Ma,[63b] W. Ma,[63a] Y. Ma,[124] J. C. MacDonald,[102] P. C. Machado De Abreu Farias,[84e] R. Madar,[41] T. Madula,[98] J. Maeda,[86] T. Maeno,[30] H. Maguire,[142] V. Maiboroda,[138] A. Maio,[133a,133b,133d] K. Maj,[87a] O. Majersky,[49] S. Majewski,[126] N. Makovec,[67] V. Maksimovic,[16] B. Malaescu,[130] Pa. Malecki,[88] V. P. Maleev,[38] F. Malek,[61,aa] M. Mali,[95] D. Malito,[97] U. Mallik,[81] S. Maltezos,[10] S. Malyukov,[39] J. Mamuzic,[13] G. Mancini,[54] M. N. Mancini,[27] G. Manco,[74a,74b] J. P. Mandalia,[96] S. S. Mandarry,[149] I. Mandić,[95] L. Manhaes de Andrade Filho,[84a] I. M. Maniatis,[172] J. Manjarres Ramos,[91] D. C. Mankad,[172] A. Mann,[111] S. Manzoni,[37] L. Mao,[63c] X. Mapekula,[34c] A. Marantis,[155,z] G. Marchiori,[5] M. Marcisovsky,[134] C. Marcon,[72a] M. Marinescu,[21] S. Marium,[49] M. Marjanovic,[123] A. Markhoos,[55] M. Markovitch,[67] E. J. Marshall,[93] Z. Marshall,[18a] S. Marti-Garcia,[166] J. Martin,[98] T. A. Martin,[137] V. J. Martin,[53] B. Martin dit Latour,[17] L. Martinelli,[76a,76b] M. Martinez,[13,s] P. Martinez Agullo,[166] V. I. Martinez Outschoorn,[105] P. Martinez Suarez,[13] S. Martin-Haugh,[137] G. Martinovicova,[136] V. S. Martoiu,[28b] A. C. Martyniuk,[98] A. Marzin,[37] D. Mascione,[79a,79b] L. Masetti,[102] T. Mashimo,[156] J. Masik,[103] A. L. Maslennikov,[38] P. Massarotti,[73a,73b] P. Mastrandrea,[75a,75b] A. Mastroberardino,[44b,44a] T. Masubuchi,[156] T. Mathisen,[164] J. Matousek,[136] N. Matsuzawa,[156] J. Maurer,[28b] A. J. Maury,[67] B. Maček,[95] D. A. Maximov,[38] A. E. May,[103] R. Mazini,[151] I. Maznas,[118] M. Mazza,[109] S. M. Mazza,[139] E. Mazzeo,[72a,72b] C. Mc Ginn,[30] J. P. Mc Gowan,[168] S. P. Mc Kee,[108] C. C. McCracken,[167] E. F. McDonald,[107] A. E. McDougall,[117] J. A. Mcfayden,[149] R. P. McGovern,[131] R. P. Mckenzie,[34g] T. C. Mclachlan,[49] D. J. Mclaughlin,[98] S. J. McMahon,[137] C. M. Mcpartland,[94] R. A. McPherson,[168,m] S. Mehlhase,[111] A. Mehta,[94] D. Melini,[166] B. R. Mellado Garcia,[34g] A. H. Melo,[56] F. Meloni,[49] A. M. Mendes Jacques Da Costa,[103] H. Y. Meng,[158] L. Meng,[93] S. Menke,[112] M. Mentink,[37] E. Meoni,[44b,44a] G. Mercado,[118] S. Merianos,[155] C. Merlassino,[70a,70c] L. Merola,[73a,73b] C. Meroni,[72a,72b] J. Metcalfe,[6] A. S. Mete,[6] E. Meuser,[102] C. Meyer,[69] J-P. Meyer,[138] R. P. Middleton,[137] L. Mijović,[53] G. Mikenberg,[172] M. Mikestikova,[134] M. Mikuž,[95] H. Mildner,[102] A. Milic,[37] D. W. Miller,[40] E. H. Miller,[146] L. S. Miller,[35] A. Milov,[172] D. A. Milstead,[48a,48b] T. Min,[114a] A. A. Minaenko,[38] I. A. Minashvili,[152b] L. Mince,[60] A. I. Mincer,[120] B. Mindur,[87a] M. Mineev,[39] Y. Mino,[89] L. M. Mir,[13] M. Miralles Lopez,[60] M. Mironova,[18a] A. Mishima,[156] M. C. Missio,[116] A. Mitra,[170] V. A. Mitsou,[166] Y. Mitsumori,[113] O. Miu,[158] P. S. Miyagawa,[96] T. Mkrtchyan,[64a] M. Mlinarevic,[98] T. Mlinarevic,[98] M. Mlynarikova,[37] S. Mobius,[20] P. Mogg,[111] M. H. Mohamed Farook,[115] A. F. Mohammed,[14,114c] S. Mohapatra,[42] G. Mokgatitswane,[34g] L. Moleri,[172] B. Mondal,[144] S. Mondal,[135] K. Mönig,[49] E. Monnier,[104] L. Monsonis Romero,[166] J. Montejo Berlingen,[13] A. Montella,[48a,48b] M. Montella,[122] F. Montereali,[78a,78b] F. Monticelli,[92] S. Monzani,[70a,70c] A. Morancho Tarda,[43] N. Morange,[67] A. L. Moreira De Carvalho,[49] M. Moreno Llácer,[166] C. Moreno Martinez,[57] P. Morettini,[58b] S. Morgenstern,[37] M. Morii,[62] M. Morinaga,[156] F. Morodei,[76a,76b] L. Morvaj,[37] P. Moschovakos,[37] B. Moser,[37] M. Mosidze,[152b] T. Moskalets,[45] P. Moskvitina,[116] J. Moss,[32,bb] P. Moszkowicz,[87a] A. Moussa,[36d] E. J. W. Moyse,[105] O. Mtintsilana,[34g] S. Muanza,[104] J. Mueller,[132] D. Muenstermann,[93] R. Müller,[37] G. A. Mullier,[164] A. J. Mullin,[33] J. J. Mullin,[131] D. P. Mungo,[158] D. Munoz Perez,[166] F. J. Munoz Sanchez,[103] M. Murin,[103] W. J. Murray,[170,137]

M. Muškinja,[95] C. Mwewa,[30] A. G. Myagkov,[38,i] A. J. Myers,[8] G. Myers,[108] M. Myska,[135] B. P. Nachman,[18a] O. Nackenhorst,[50] K. Nagai,[129] K. Nagano,[85] J. L. Nagle,[30,n] E. Nagy,[104] A. M. Nairz,[37] Y. Nakahama,[85] K. Nakamura,[85] K. Nakkalil,[5] H. Nanjo,[127] E. A. Narayanan,[115] I. Naryshkin,[38] L. Nasella,[72a,72b] M. Naseri,[35] S. Nasri,[119b] C. Nass,[25] G. Navarro,[23a] J. Navarro-Gonzalez,[166] R. Nayak,[154] A. Nayaz,[19] P. Y. Nechaeva,[38] S. Nechaeva,[24b,24a] F. Nechansky,[49] L. Nedic,[129] T. J. Neep,[21] A. Negri,[74a,74b] M. Negrini,[24b] C. Nellist,[117] C. Nelson,[106] K. Nelson,[108] S. Nemecek,[134] M. Nessi,[37,cc] M. S. Neubauer,[165] F. Neuhaus,[102] J. Neundorf,[49] P. R. Newman,[21] C. W. Ng,[132] Y. W. Y. Ng,[49] B. Ngair,[119a] H. D. N. Nguyen,[110] R. B. Nickerson,[129] R. Nicolaidou,[138] J. Nielsen,[139] M. Niemeyer,[56] J. Niermann,[56] N. Nikiforou,[37] V. Nikolaenko,[38,i] I. Nikolic-Audit,[130] K. Nikolopoulos,[21] P. Nilsson,[30] I. Ninca,[49] G. Ninio,[154] A. Nisati,[76a] N. Nishu,[2] R. Nisius,[112] J-E. Nitschke,[51] E. K. Nkadimeng,[34g] T. Nobe,[156] T. Nommensen,[150] M. B. Norfolk,[142] B. J. Norman,[35] M. Noury,[36a] J. Novak,[95] T. Novak,[95] L. Novotny,[135] R. Novotny,[115] L. Nozka,[125] K. Ntekas,[162] N. M. J. Nunes De Moura Junior,[84b] J. Ocariz,[130] A. Ochi,[86] I. Ochoa,[133a] S. Oerdek,[49,dd] J. T. Offermann,[40] A. Ogrodnik,[136] A. Oh,[103] C. C. Ohm,[147] H. Oide,[85] R. Oishi,[156] M. L. Ojeda,[49] Y. Okumura,[156] L. F. Oleiro Seabra,[133a] I. Oleksiyuk,[57] S. A. Olivares Pino,[140d] G. Oliveira Correa,[13] D. Oliveira Damazio,[30] D. Oliveira Goncalves,[84a] J. L. Oliver,[162] Ö. O. Öncel,[55] A. P. O'Neill,[20] A. Onofre,[133a,133e] P. U. E. Onyisi,[11] M. J. Oreglia,[40] G. E. Orellana,[92] D. Orestano,[78a,78b] N. Orlando,[13] R. S. Orr,[158] L. M. Osojnak,[131] R. Ospanov,[63a] G. Otero y Garzon,[31] H. Otono,[90] P. S. Ott,[64a] G. J. Ottino,[18a] M. Ouchrif,[36d] F. Ould-Saada,[128] T. Ovsiannikova,[141] M. Owen,[60] R. E. Owen,[137] V. E. Ozcan,[22a] F. Ozturk,[88] N. Ozturk,[8] S. Ozturk,[83] H. A. Pacey,[129] A. Pacheco Pages,[13] C. Padilla Aranda,[13] G. Padovano,[76a,76b] S. Pagan Griso,[18a] G. Palacino,[69] A. Palazzo,[71a,71b] J. Pampel,[25] J. Pan,[175] T. Pan,[65a] D. K. Panchal,[11] C. E. Pandini,[117] J. G. Panduro Vazquez,[137] H. D. Pandya,[1] H. Pang,[15] P. Pani,[49] G. Panizzo,[70a,70c] L. Panwar,[130] L. Paolozzi,[57] S. Parajuli,[165] A. Paramonov,[6] C. Paraskevopoulos,[54] D. Paredes Hernandez,[65b] A. Pareti,[74a,74b] K. R. Park,[42] T. H. Park,[158] M. A. Parker,[33] F. Parodi,[58b,58a] E. W. Parrish,[118] V. A. Parrish,[53] J. A. Parsons,[42] U. Parzefall,[55] B. Pascual Dias,[110] L. Pascual Dominguez,[101] E. Pasqualucci,[76a] S. Passaggio,[58b] F. Pastore,[97] P. Patel,[88] U. M. Patel,[52] J. R. Pater,[103] T. Pauly,[37] C. I. Pazos,[161] J. Pearkes,[146] M. Pedersen,[128] R. Pedro,[133a] S. V. Peleganchuk,[38] O. Penc,[37] E. A. Pender,[53] S. Peng,[15] G. D. Penn,[175] K. E. Penski,[111] M. Penzin,[38] B. S. Peralva,[84d] A. P. Pereira Peixoto,[141] L. Pereira Sanchez,[146] D. V. Perepelitsa,[30,n] G. Perera,[105] E. Perez Codina,[159a] M. Perganti,[10] H. Pernegger,[37] S. Perrella,[76a,76b] O. Perrin,[41] K. Peters,[49] R. F. Y. Peters,[103] B. A. Petersen,[37] T. C. Petersen,[43] E. Petit,[104] V. Petousis,[135] C. Petridou,[155,y] T. Petru,[136] A. Petrukhin,[144] M. Pettee,[18a] A. Petukhov,[38] K. Petukhova,[37] R. Pezoa,[140f] L. Pezzotti,[37] G. Pezzullo,[175] T. M. Pham,[173] T. Pham,[107] P. W. Phillips,[137] G. Piacquadio,[148] E. Pianori,[18a] F. Piazza,[126] R. Piegaia,[31] D. Pietreanu,[28b] A. D. Pilkington,[103] M. Pinamonti,[70a,70c] J. L. Pinfold,[2] B. C. Pinheiro Pereira,[133a] A. E. Pinto Pinoargote,[138] L. Pintucci,[70a,70c] K. M. Piper,[149] A. Pirttikoski,[57] D. A. Pizzi,[35] L. Pizzimento,[65b] A. Pizzini,[117] M.-A. Pleier,[30] V. Pleskot,[136] E. Plotnikova,[39] G. Poddar,[96] R. Poettgen,[100] L. Poggioli,[130] I. Pokharel,[56] S. Polacek,[136] G. Polesello,[74a] A. Poley,[145,159a] A. Polini,[24b] C. S. Pollard,[170] Z. B. Pollock,[122] E. Pompa Pacchi,[76a,76b] N. I. Pond,[98] D. Ponomarenko,[116] L. Pontecorvo,[37] S. Popa,[28a] G. A. Popeneciu,[28d] A. Poreba,[37] D. M. Portillo Quintero,[159a] S. Pospisil,[135] M. A. Postill,[142] P. Postolache,[28c] K. Potamianos,[170] P. A. Potepa,[87a] I. N. Potrap,[39] C. J. Potter,[33] H. Potti,[150] J. Poveda,[166] M. E. Pozo Astigarraga,[37] A. Prades Ibanez,[166] J. Pretel,[168] D. Price,[103] M. Primavera,[71a] L. Primomo,[70a,70c] M. A. Principe Martin,[101] R. Privara,[125] T. Procter,[60] M. L. Proffitt,[141] N. Proklova,[131] K. Prokofiev,[65c] G. Proto,[112] J. Proudfoot,[6] M. Przybycien,[87a] W. W. Przygoda,[87b] A. Psallidas,[47] J. E. Puddefoot,[142] D. Pudzha,[55] D. Pyatiizbyantseva,[38] J. Qian,[108] D. Qichen,[103] Y. Qin,[13] T. Qiu,[53] A. Quadt,[56] M. Queitsch-Maitland,[103] G. Quetant,[57] R. P. Quinn,[167] G. Rabanal Bolanos,[62] D. Rafanoharana,[55] F. Raffaeli,[77a,77b] F. Ragusa,[72a,72b] J. L. Rainbolt,[40] J. A. Raine,[57] S. Rajagopalan,[30] E. Ramakoti,[38] I. A. Ramirez-Berend,[35] K. Ran,[49,114c] D. S. Rankin,[131] N. P. Rapheeha,[34g] H. Rasheed,[28b] V. Raskina,[130] D. F. Rassloff,[64a] A. Rastogi,[18a] S. Rave,[102] S. Ravera,[58b,58a] B. Ravina,[56] I. Ravinovich,[172] M. Raymond,[37] A. L. Read,[128] N. P. Readioff,[142] D. M. Rebuzzi,[74a,74b] G. Redlinger,[30] A. S. Reed,[112] K. Reeves,[27] J. A. Reidelsturz,[174] D. Reikher,[154] A. Rej,[50] C. Rembser,[37] M. Renda,[28b] F. Renner,[49] A. G. Rennie,[162] A. L. Rescia,[49] S. Resconi,[72a] M. Ressegotti,[58b,58a] S. Rettie,[37] J. G. Reyes Rivera,[109] E. Reynolds,[18a] O. L. Rezanova,[38] P. Reznicek,[136] H. Riani,[36d] N. Ribaric,[93]

E. Ricci,[79a,79b] R. Richter,[112] S. Richter,[48a,48b] E. Richter-Was,[87b] M. Ridel,[130] S. Ridouani,[36d] P. Rieck,[120] P. Riedler,[37] E. M. Riefel,[48a,48b] J. O. Rieger,[117] M. Rijssenbeek,[148] M. Rimoldi,[37] L. Rinaldi,[24b,24a] P. Rincke,[56,164] T. T. Rinn,[30] M. P. Rinnagel,[111] G. Ripellino,[164] I. Riu,[13] J. C. Rivera Vergara,[168] F. Rizatdinova,[124] E. Rizvi,[96] B. R. Roberts,[18a] S. S. Roberts,[139] S. H. Robertson,[106,m] D. Robinson,[33] C. M. Robles Gajardo,[140f] M. Robles Manzano,[102] A. Robson,[60] A. Rocchi,[77a,77b] C. Roda,[75a,75b] S. Rodriguez Bosca,[37] Y. Rodriguez Garcia,[23a] A. Rodriguez Rodriguez,[55] A. M. Rodríguez Vera,[118] S. Roe,[37] J. T. Roemer,[37] A. R. Roepe-Gier,[139] O. Røhne,[128] R. A. Rojas,[105] C. P. A. Roland,[130] J. Roloff,[30] A. Romaniouk,[38] E. Romano,[74a,74b] M. Romano,[24b] A. C. Romero Hernandez,[165] N. Rompotis,[94] L. Roos,[130] S. Rosati,[76a] B. J. Rosser,[40] E. Rossi,[129] E. Rossi,[73a,73b] L. P. Rossi,[62] L. Rossini,[55] R. Rosten,[122] M. Rotaru,[28b] B. Rottler,[55] C. Rougier,[91] D. Rousseau,[67] D. Rousso,[49] A. Roy,[165] S. Roy-Garand,[158] A. Rozanov,[104] Z. M. A. Rozario,[60] Y. Rozen,[153] A. Rubio Jimenez,[166] A. J. Ruby,[94] V. H. Ruelas Rivera,[19] T. A. Ruggeri,[1] A. Ruggiero,[129] A. Ruiz-Martinez,[166] A. Rummler,[37] Z. Rurikova,[55] N. A. Rusakovich,[39] H. L. Russell,[168] G. Russo,[76a,76b] J. P. Rutherfoord,[7] S. Rutherford Colmenares,[33] M. Rybar,[136] E. B. Rye,[128] A. Ryzhov,[45] J. A. Sabater Iglesias,[57] P. Sabatini,[166] H. F-W. Sadrozinski,[139] F. Safai Tehrani,[76a] B. Safarzadeh Samani,[137] S. Saha,[1] M. Sahinsoy,[112] A. Saibel,[166] M. Saimpert,[138] M. Saito,[156] T. Saito,[156] A. Sala,[72a,72b] D. Salamani,[37] A. Salnikov,[146] J. Salt,[166] A. Salvador Salas,[154] D. Salvatore,[44b,44a] F. Salvatore,[149] A. Salzburger,[37] D. Sammel,[55] E. Sampson,[93] D. Sampsonidis,[155,y] D. Sampsonidou,[126] J. Sánchez,[166] V. Sanchez Sebastian,[166] H. Sandaker,[128] C. O. Sander,[49] J. A. Sandesara,[105] M. Sandhoff,[174] C. Sandoval,[23b] L. Sanfilippo,[64a] D. P. C. Sankey,[137] T. Sano,[89] A. Sansoni,[54] L. Santi,[37,76b] C. Santoni,[41] H. Santos,[133a,133b] A. Santra,[172] E. Sanzani,[24b,24a] K. A. Saoucha,[163] J. G. Saraiva,[133a,133d] J. Sardain,[7] O. Sasaki,[85] K. Sato,[160] C. Sauer,[64b] E. Sauvan,[4] P. Savard,[158,c] R. Sawada,[156] C. Sawyer,[137] L. Sawyer,[99] C. Sbarra,[24b] A. Sbrizzi,[24b,24a] T. Scanlon,[98] J. Schaarschmidt,[141] U. Schäfer,[102] A. C. Schaffer,[67,45] D. Schaile,[111] R. D. Schamberger,[148] C. Scharf,[19] M. M. Schefer,[20] V. A. Schegelsky,[38] D. Scheirich,[136] M. Schernau,[162] C. Scheulen,[56] C. Schiavi,[58b,58a] M. Schioppa,[44b,44a] B. Schlag,[146,ee] K. E. Schleicher,[55] S. Schlenker,[37] J. Schmeing,[174] M. A. Schmidt,[174] K. Schmieden,[102] C. Schmitt,[102] N. Schmitt,[102] S. Schmitt,[49] L. Schoeffel,[138] A. Schoening,[64b] P. G. Scholer,[35] E. Schopf,[129] M. Schott,[25] J. Schovancova,[37] S. Schramm,[57] T. Schroer,[57] H-C. Schultz-Coulon,[64a] M. Schumacher,[55] B. A. Schumm,[139] Ph. Schune,[138] A. J. Schuy,[141] H. R. Schwartz,[139] A. Schwartzman,[146] T. A. Schwarz,[108] Ph. Schwemling,[138] R. Schwienhorst,[109] F. G. Sciacca,[20] A. Sciandra,[30] G. Sciolla,[27] F. Scuri,[75a] C. D. Sebastiani,[94] K. Sedlaczek,[118] S. C. Seidel,[115] A. Seiden,[139] B. D. Seidlitz,[42] C. Seitz,[49] J. M. Seixas,[84b] G. Sekhniaidze,[73a] L. Selem,[61] N. Semprini-Cesari,[24b,24a] D. Sengupta,[57] V. Senthilkumar,[166] L. Serin,[67] M. Sessa,[77a,77b] H. Severini,[123] F. Sforza,[58b,58a] A. Sfyrla,[57] Q. Sha,[14] E. Shabalina,[56] A. H. Shah,[33] R. Shaheen,[147] J. D. Shahinian,[131] D. Shaked Renous,[172] L. Y. Shan,[14] M. Shapiro,[18a] A. Sharma,[37] A. S. Sharma,[167] P. Sharma,[81] P. B. Shatalov,[38] K. Shaw,[149] S. M. Shaw,[103] Q. Shen,[63c] D. J. Sheppard,[145] P. Sherwood,[98] L. Shi,[98] X. Shi,[14] S. Shimizu,[85] C. O. Shimmin,[175] J. D. Shinner,[97] I. P. J. Shipsey,[129] S. Shirabe,[90] M. Shiyakova,[39,ff] M. J. Shochet,[40] D. R. Shope,[128] B. Shrestha,[123] S. Shrestha,[122,gg] M. J. Shroff,[168] P. Sicho,[134] A. M. Sickles,[165] E. Sideras Haddad,[34g] A. C. Sidley,[117] A. Sidoti,[24b] F. Siegert,[51] Dj. Sijacki,[16] F. Sili,[92] J. M. Silva,[53] I. Silva Ferreira,[84b] M. V. Silva Oliveira,[30] S. B. Silverstein,[48a] S. Simion,[67] R. Simoniello,[37] E. L. Simpson,[103] H. Simpson,[149] L. R. Simpson,[108] N. D. Simpson,[100] S. Simsek,[83] S. Sindhu,[56] P. Sinervo,[158] S. Singh,[158] S. Sinha,[49] S. Sinha,[103] M. Sioli,[24b,24a] I. Siral,[37] E. Sitnikova,[49] J. Sjölin,[48a,48b] A. Skaf,[56] E. Skorda,[21] P. Skubic,[123] M. Slawinska,[88] V. Smakhtin,[172] B. H. Smart,[137] S. Yu. Smirnov,[38] Y. Smirnov,[38] L. N. Smirnova,[38,i] O. Smirnova,[100] A. C. Smith,[42] D. R. Smith,[162] E. A. Smith,[40] H. A. Smith,[129] J. L. Smith,[103] R. Smith,[146] M. Smizanska,[93] K. Smolek,[135] A. A. Snesarev,[38] S. R. Snider,[158] H. L. Snoek,[117] S. Snyder,[30] R. Sobie,[168,m] A. Soffer,[154] C. A. Solans Sanchez,[37] E. Yu. Soldatov,[38] U. Soldevila,[166] A. A. Solodkov,[38] S. Solomon,[27] A. Soloshenko,[39] K. Solovieva,[55] O. V. Solovyanov,[41] P. Sommer,[37] A. Sonay,[13] W. Y. Song,[159b] A. Sopczak,[135] A. L. Sopio,[98] F. Sopkova,[29b] J. D. Sorenson,[115] I. R. Sotarriva Alvarez,[157] V. Sothilingam,[64a] O. J. Soto Sandoval,[140c,140b] S. Sottocornola,[69] R. Soualah,[163] Z. Soumaimi,[36e] D. South,[49] N. Soybelman,[172] S. Spagnolo,[71a,71b] M. Spalla,[112] D. Sperlich,[55] G. Spigo,[37] S. Spinali,[93] B. Spisso,[73a,73b] D. P. Spiteri,[60] M. Spousta,[136] E. J. Staats,[35] R. Stamen,[64a] A. Stampekis,[21] M. Standke,[25] E. Stanecka,[88]

W. Stanek-Maslouska,[49] M. V. Stange,[51] B. Stanislaus,[18a] M. M. Stanitzki,[49] B. Stapf,[49] E. A. Starchenko,[38] G. H. Stark,[139] J. Stark,[91] P. Staroba,[134] P. Starovoitov,[64a] S. Stärz,[106] R. Staszewski,[88] G. Stavropoulos,[47] A. Stefl,[37] P. Steinberg,[30] B. Stelzer,[145,159a] H. J. Stelzer,[132] O. Stelzer-Chilton,[159a] H. Stenzel,[59] T. J. Stevenson,[149] G. A. Stewart,[37] J. R. Stewart,[124] M. C. Stockton,[37] G. Stoicea,[28b] M. Stolarski,[133a] S. Stonjek,[112] A. Straessner,[51] J. Strandberg,[147] S. Strandberg,[48a,48b] M. Stratmann,[174] M. Strauss,[123] T. Strebler,[104] P. Strizenec,[29b] R. Ströhmer,[169] D. M. Strom,[126] R. Stroynowski,[45] A. Strubig,[48a,48b] S. A. Stucci,[30] B. Stugu,[17] J. Stupak,[123] N. A. Styles,[49] D. Su,[146] S. Su,[63a] W. Su,[63d] X. Su,[63a] D. Suchy,[29a] K. Sugizaki,[156] V. V. Sulin,[38] M. J. Sullivan,[94] D. M. S. Sultan,[129] L. Sultanaliyeva,[38] S. Sultansoy,[3b] T. Sumida,[89] S. Sun,[173] O. Sunneborn Gudnadottir,[164] N. Sur,[104] M. R. Sutton,[149] H. Suzuki,[160] M. Svatos,[134] M. Swiatlowski,[159a] T. Swirski,[169] I. Sykora,[29a] M. Sykora,[136] T. Sykora,[136] D. Ta,[102] K. Tackmann,[49,dd] A. Taffard,[162] R. Tafirout,[159a] J. S. Tafoya Vargas,[67] Y. Takubo,[85] M. Talby,[104] A. A. Talyshev,[38] K. C. Tam,[65b] N. M. Tamir,[154] A. Tanaka,[156] J. Tanaka,[156] R. Tanaka,[67] M. Tanasini,[148] Z. Tao,[167] S. Tapia Araya,[140f] S. Tapprogge,[102] A. Tarek Abouelfadl Mohamed,[109] S. Tarem,[153] K. Tariq,[14] G. Tarna,[28b] G. F. Tartarelli,[72a] M. J. Tartarin,[91] P. Tas,[136] M. Tasevsky,[134] E. Tassi,[44b,44a] A. C. Tate,[165] G. Tateno,[156] Y. Tayalati,[36e,hh] G. N. Taylor,[107] W. Taylor,[159b] R. Teixeira De Lima,[146] P. Teixeira-Dias,[97] J. J. Teoh,[158] K. Terashi,[156] J. Terron,[101] S. Terzo,[13] M. Testa,[54] R. J. Teuscher,[158,m] A. Thaler,[80] O. Theiner,[57] N. Themistokleous,[53] T. Theveneaux-Pelzer,[104] O. Thielmann,[174] D. W. Thomas,[97] J. P. Thomas,[21] E. A. Thompson,[18a] P. D. Thompson,[21] E. Thomson,[131] R. E. Thornberry,[45] C. Tian,[63a] Y. Tian,[56] V. Tikhomirov,[38,i] Yu. A. Tikhonov,[38] S. Timoshenko,[38] D. Timoshyn,[136] E. X. L. Ting,[1] P. Tipton,[175] A. Tishelman-Charny,[30] S. H. Tlou,[34g] K. Todome,[157] S. Todorova-Nova,[136] S. Todt,[51] L. Toffolin,[70a,70c] M. Togawa,[85] J. Tojo,[90] S. Tokár,[29a] K. Tokushuku,[85] O. Toldaiev,[69] R. Tombs,[33] M. Tomoto,[85,113] L. Tompkins,[146,ee] K. W. Topolnicki,[87b] E. Torrence,[126] H. Torres,[91] E. Torró Pastor,[166] M. Toscani,[31] C. Tosciri,[40] M. Tost,[11] D. R. Tovey,[142] I. S. Trandafir,[28b] T. Trefzger,[169] A. Tricoli,[30] I. M. Trigger,[159a] S. Trincaz-Duvoid,[130] D. A. Trischuk,[27] B. Trocmé,[61] A. Tropina,[39] L. Truong,[34c] M. Trzebinski,[88] A. Trzupek,[88] F. Tsai,[148] M. Tsai,[108] A. Tsiamis,[155,y] P. V. Tsiareshka,[38] S. Tsigaridas,[159a] A. Tsirigotis,[155,z] V. Tsiskaridze,[158] E. G. Tskhadadze,[152a] M. Tsopoulou,[155] Y. Tsujikawa,[89] I. I. Tsukerman,[38] V. Tsulaia,[18a] S. Tsuno,[85] K. Tsuri,[121] D. Tsybychev,[148] Y. Tu,[65b] A. Tudorache,[28b] V. Tudorache,[28b] A. N. Tuna,[62] S. Turchikhin,[58b,58a] I. Turk Cakir,[3a] R. Turra,[72a] T. Turtuvshin,[39,ii] P. M. Tuts,[42] S. Tzamarias,[155,y] E. Tzovara,[102] F. Ukegawa,[160] P. A. Ulloa Poblete,[140c,140b] E. N. Umaka,[30] G. Unal,[37] A. Undrus,[30] G. Unel,[162] J. Urban,[29b] P. Urrejola,[140a] G. Usai,[8] R. Ushioda,[157] M. Usman,[110] Z. Uysal,[83] V. Vacek,[135] B. Vachon,[106] T. Vafeiadis,[37] A. Vaitkus,[98] C. Valderanis,[111] E. Valdes Santurio,[48a,48b] M. Valente,[159a] S. Valentinetti,[24b,24a] A. Valero,[166] E. Valiente Moreno,[166] A. Vallier,[91] J. A. Valls Ferrer,[166] D. R. Van Arneman,[117] T. R. Van Daalen,[141] A. Van Der Graaf,[50] P. Van Gemmeren,[6] M. Van Rijnbach,[37] S. Van Stroud,[98] I. Van Vulpen,[117] P. Vana,[136] M. Vanadia,[77a,77b] W. Vandelli,[37] E. R. Vandewall,[124] D. Vannicola,[154] L. Vannoli,[54] R. Vari,[76a] E. W. Varnes,[7] C. Varni,[18b] T. Varol,[151] D. Varouchas,[67] L. Varriale,[166] K. E. Varvell,[150] M. E. Vasile,[28b] L. Vaslin,[85] G. A. Vasquez,[168] A. Vasyukov,[39] L. M. Vaughan,[124] R. Vavricka,[102] T. Vazquez Schroeder,[37] J. Veatch,[32] V. Vecchio,[103] M. J. Veen,[105] I. Veliscek,[30] L. M. Veloce,[158] F. Veloso,[133a,133c] S. Veneziano,[76a] A. Ventura,[71a,71b] S. Ventura Gonzalez,[138] A. Verbytskyi,[112] M. Verducci,[75a,75b] C. Vergis,[96] M. Verissimo De Araujo,[84b] W. Verkerke,[117] J. C. Vermeulen,[117] C. Vernieri,[146] M. Vessella,[105] M. C. Vetterli,[145,c] A. Vgenopoulos,[102] N. Viaux Maira,[140f] T. Vickey,[142] O. E. Vickey Boeriu,[142] G. H. A. Viehhauser,[129] L. Vigani,[64b] M. Vigl,[112] M. Villa,[24b,24a] M. Villaplana Perez,[166] E. M. Villhauer,[53] E. Vilucchi,[54] M. G. Vincter,[35] A. Visibile,[117] C. Vittori,[37] I. Vivarelli,[24b,24a] E. Voevodina,[112] F. Vogel,[111] J. C. Voigt,[51] P. Vokac,[135] Yu. Volkotrub,[87b] J. Von Ahnen,[49] E. Von Toerne,[25] B. Vormwald,[37] V. Vorobel,[136] K. Vorobev,[38] M. Vos,[166] K. Voss,[144] M. Vozak,[117] L. Vozdecky,[123] N. Vranjes,[16] M. Vranjes Milosavljevic,[16] M. Vreeswijk,[117] N. K. Vu,[63d,63c] R. Vuillermet,[37] O. Vujinovic,[102] I. Vukotic,[40] S. Wada,[160] C. Wagner,[105] J. M. Wagner,[18a] W. Wagner,[174] S. Wahdan,[174] H. Wahlberg,[92] M. Wakida,[113] J. Walder,[137] R. Walker,[111] W. Walkowiak,[144] A. Wall,[131] E. J. Wallin,[100] T. Wamorkar,[6] A. Z. Wang,[139] C. Wang,[102] C. Wang,[11] H. Wang,[18a] J. Wang,[65c] P. Wang,[98] R. Wang,[62] R. Wang,[6] S. M. Wang,[151] S. Wang,[63b] S. Wang,[14] T. Wang,[63a] W. T. Wang,[81] W. Wang,[14] X. Wang,[114a] X. Wang,[165] X. Wang,[63c] Y. Wang,[63d] Y. Wang,[114a] Y. Wang,[63a] Z. Wang,[108] Z. Wang,[63d,52,63c] Z. Wang,[108]

A. Warburton,[106] R. J. Ward,[21] N. Warrack,[60] S. Waterhouse,[97] A. T. Watson,[21] H. Watson,[60] M. F. Watson,[21] E. Watton,[60,137] G. Watts,[141] B. M. Waugh,[98] J. M. Webb,[55] C. Weber,[30] H. A. Weber,[19] M. S. Weber,[20] S. M. Weber,[64a] C. Wei,[63a] Y. Wei,[55] A. R. Weidberg,[129] E. J. Weik,[120] J. Weingarten,[50] C. Weiser,[55] C. J. Wells,[49] T. Wenaus,[30] B. Wendland,[50] T. Wengler,[37] N. S. Wenke,[112] N. Wermes,[25] M. Wessels,[64a] A. M. Wharton,[93] A. S. White,[62] A. White,[8] M. J. White,[1] D. Whiteson,[162] L. Wickremasinghe,[127] W. Wiedenmann,[173] M. Wielers,[137] C. Wiglesworth,[43] D. J. Wilbern,[123] H. G. Wilkens,[37] J. J. H. Wilkinson,[33] D. M. Williams,[42] H. H. Williams,[131] S. Williams,[33] S. Willocq,[105] B. J. Wilson,[103] P. J. Windischhofer,[40] F. I. Winkel,[31] F. Winklmeier,[126] B. T. Winter,[55] J. K. Winter,[103] M. Wittgen,[146] M. Wobisch,[99] T. Wojtkowski,[61] Z. Wolffs,[117] J. Wollrath,[162] M. W. Wolter,[88] H. Wolters,[133a,133c] M. C. Wong,[139] E. L. Woodward,[42] S. D. Worm,[49] B. K. Wosiek,[88] K. W. Woźniak,[88] S. Wozniewski,[56] K. Wraight,[60] C. Wu,[21] M. Wu,[114b] M. Wu,[116] S. L. Wu,[173] X. Wu,[57] Y. Wu,[63a] Z. Wu,[4] J. Wuerzinger,[112,t] T. R. Wyatt,[103] B. M. Wynne,[53] S. Xella,[43] L. Xia,[114a] M. Xia,[15] M. Xie,[63a] S. Xin,[14,114c] A. Xiong,[126] J. Xiong,[18a] D. Xu,[14] H. Xu,[63a] L. Xu,[63a] R. Xu,[131] T. Xu,[108] Y. Xu,[15] Z. Xu,[53] Z. Xu,[114a] B. Yabsley,[150] S. Yacoob,[34a] Y. Yamaguchi,[157] E. Yamashita,[156] H. Yamauchi,[160] T. Yamazaki,[18a] Y. Yamazaki,[86] J. Yan,[63c] S. Yan,[60] Z. Yan,[105] H. J. Yang,[63c,63d] H. T. Yang,[63a] S. Yang,[63a] T. Yang,[65c] X. Yang,[37] X. Yang,[14] Y. Yang,[45] Y. Yang,[63a] Z. Yang,[63a] W-M. Yao,[18a] H. Ye,[114a] H. Ye,[56] J. Ye,[14] S. Ye,[30] X. Ye,[63a] Y. Yeh,[98] I. Yeletskikh,[39] B. Yeo,[18b] M. R. Yexley,[98] T. P. Yildirim,[129] P. Yin,[42] K. Yorita,[171] S. Younas,[28b] C. J. S. Young,[37] C. Young,[146] C. Yu,[14,114c] Y. Yu,[63a] J. Yuan,[14,114c] M. Yuan,[108] R. Yuan,[63d,63c] L. Yue,[98] M. Zaazoua,[63a] B. Zabinski,[88] E. Zaid,[53] Z. K. Zak,[88] T. Zakareishvili,[166] S. Zambito,[57] J. A. Zamora Saa,[140d,140b] J. Zang,[156] D. Zanzi,[55] O. Zaplatilek,[135] C. Zeitnitz,[174] H. Zeng,[14] J. C. Zeng,[165] D. T. Zenger Jr.,[27] O. Zenin,[38] T. Ženiš,[29a] S. Zenz,[96] S. Zerradi,[36a] D. Zerwas,[67] M. Zhai,[14,114c] D. F. Zhang,[142] J. Zhang,[63b] J. Zhang,[6] K. Zhang,[14,114c] L. Zhang,[63a] L. Zhang,[114a] P. Zhang,[14,114c] R. Zhang,[173] S. Zhang,[108] S. Zhang,[91] T. Zhang,[156] X. Zhang,[63c] X. Zhang,[63b] Y. Zhang,[63c] Y. Zhang,[98] Y. Zhang,[114a] Z. Zhang,[18a] Z. Zhang,[63b] Z. Zhang,[67] H. Zhao,[141] T. Zhao,[63b] Y. Zhao,[139] Z. Zhao,[63a] Z. Zhao,[63a] A. Zhemchugov,[39] J. Zheng,[114a] K. Zheng,[165] X. Zheng,[63a] Z. Zheng,[146] D. Zhong,[165] B. Zhou,[108] H. Zhou,[7] N. Zhou,[63c] Y. Zhou,[15] Y. Zhou,[114a] Y. Zhou,[7] C. G. Zhu,[63b] J. Zhu,[108] X. Zhu,[63d] Y. Zhu,[63c] Y. Zhu,[63a] X. Zhuang,[14] K. Zhukov,[38] N. I. Zimine,[39] J. Zinsser,[64b] M. Ziolkowski,[144] L. Živković,[16] A. Zoccoli,[24b,24a] K. Zoch,[62] T. G. Zorbas,[142] O. Zormpa,[47] W. Zou,[42] and L. Zwalinski[37]

(ATLAS Collaboration)

[1]*Department of Physics, University of Adelaide, Adelaide, Australia*
[2]*Department of Physics, University of Alberta, Edmonton, Alberta, Canada*
[3a]*Department of Physics, Ankara University, Ankara, Türkiye*
[3b]*Division of Physics, TOBB University of Economics and Technology, Ankara, Türkiye*
[4]*LAPP, Université Savoie Mont Blanc, CNRS/IN2P3, Annecy, France*
[5]*APC, Université Paris Cité, CNRS/IN2P3, Paris, France*
[6]*High Energy Physics Division, Argonne National Laboratory, Argonne, Illinois, USA*
[7]*Department of Physics, University of Arizona, Tucson, Arizona, USA*
[8]*Department of Physics, University of Texas at Arlington, Arlington, Texas, USA*
[9]*Physics Department, National and Kapodistrian University of Athens, Athens, Greece*
[10]*Physics Department, National Technical University of Athens, Zografou, Greece*
[11]*Department of Physics, University of Texas at Austin, Austin, Texas, USA*
[12]*Institute of Physics, Azerbaijan Academy of Sciences, Baku, Azerbaijan*
[13]*Institut de Física d'Altes Energies (IFAE), Barcelona Institute of Science and Technology, Barcelona, Spain*
[14]*Institute of High Energy Physics, Chinese Academy of Sciences, Beijing, China*
[15]*Physics Department, Tsinghua University, Beijing, China*
[16]*Institute of Physics, University of Belgrade, Belgrade, Serbia*
[17]*Department for Physics and Technology, University of Bergen, Bergen, Norway*
[18a]*Physics Division, Lawrence Berkeley National Laboratory, Berkeley, California, USA*
[18b]*University of California, Berkeley, California, USA*
[19]*Institut für Physik, Humboldt Universität zu Berlin, Berlin, Germany*

[20]Albert Einstein Center for Fundamental Physics and Laboratory for High Energy Physics, University of Bern, Bern, Switzerland
[21]School of Physics and Astronomy, University of Birmingham, Birmingham, United Kingdom
[22a]Department of Physics, Bogazici University, Istanbul, Türkiye
[22b]Department of Physics Engineering, Gaziantep University, Gaziantep, Türkiye
[22c]Department of Physics, Istanbul University, Istanbul, Türkiye
[23a]Facultad de Ciencias y Centro de Investigaciónes, Universidad Antonio Nariño, Bogotá, Colombia
[23b]Departamento de Física, Universidad Nacional de Colombia, Bogotá, Colombia
[24a]Dipartimento di Fisica e Astronomia A. Righi, Università di Bologna, Bologna, Italy
[24b]INFN Sezione di Bologna, Italy
[25]Physikalisches Institut, Universität Bonn, Bonn, Germany
[26]Department of Physics, Boston University, Boston, Massachusetts, USA
[27]Department of Physics, Brandeis University, Waltham, Massachusetts, USA
[28a]Transilvania University of Brasov, Brasov, Romania
[28b]Horia Hulubei National Institute of Physics and Nuclear Engineering, Bucharest, Romania
[28c]Department of Physics, Alexandru Ioan Cuza University of Iasi, Iasi, Romania
[28d]National Institute for Research and Development of Isotopic and Molecular Technologies, Physics Department, Cluj-Napoca, Romania
[28e]National University of Science and Technology Politechnica, Bucharest, Romania
[28f]West University in Timisoara, Timisoara, Romania
[28g]Faculty of Physics, University of Bucharest, Bucharest, Romania
[29a]Faculty of Mathematics, Physics and Informatics, Comenius University, Bratislava, Slovak Republic
[29b]Department of Subnuclear Physics, Institute of Experimental Physics of the Slovak Academy of Sciences, Kosice, Slovak Republic
[30]Physics Department, Brookhaven National Laboratory, Upton, New York, USA
[31]Universidad de Buenos Aires, Facultad de Ciencias Exactas y Naturales, Departamento de Física, y CONICET, Instituto de Física de Buenos Aires (IFIBA), Buenos Aires, Argentina
[32]California State University, California, USA
[33]Cavendish Laboratory, University of Cambridge, Cambridge, United Kingdom
[34a]Department of Physics, University of Cape Town, Cape Town, South Africa
[34b]iThemba Labs, Western Cape, South Africa
[34c]Department of Mechanical Engineering Science, University of Johannesburg, Johannesburg, South Africa
[34d]National Institute of Physics, University of the Philippines Diliman (Philippines), Philippines
[34e]University of South Africa, Department of Physics, Pretoria, South Africa
[34f]University of Zululand, KwaDlangezwa, South Africa
[34g]School of Physics, University of the Witwatersrand, Johannesburg, South Africa
[35]Department of Physics, Carleton University, Ottawa, Ontario, Canada
[36a]Faculté des Sciences Ain Chock, Université Hassan II de Casablanca, Morocco
[36b]Faculté des Sciences, Université Ibn-Tofail, Kénitra, Morocco
[36c]Faculté des Sciences Semlalia, Université Cadi Ayyad, LPHEA-Marrakech, Morocco
[36d]LPMR, Faculté des Sciences, Université Mohamed Premier, Oujda, Morocco
[36e]Faculté des sciences, Université Mohammed V, Rabat, Morocco
[36f]Institute of Applied Physics, Mohammed VI Polytechnic University, Ben Guerir, Morocco
[37]CERN, Geneva, Switzerland
[38]Affiliated with an institute covered by a cooperation agreement with CERN
[39]Affiliated with an international laboratory covered by a cooperation agreement with CERN
[40]Enrico Fermi Institute, University of Chicago, Chicago, Illinois, USA
[41]LPC, Université Clermont Auvergne, CNRS/IN2P3, Clermont-Ferrand, France
[42]Nevis Laboratory, Columbia University, Irvington, New York, USA
[43]Niels Bohr Institute, University of Copenhagen, Copenhagen, Denmark
[44a]Dipartimento di Fisica, Università della Calabria, Rende, Italy
[44b]INFN Gruppo Collegato di Cosenza, Laboratori Nazionali di Frascati, Italy
[45]Physics Department, Southern Methodist University, Dallas, Texas, USA
[46]Physics Department, University of Texas at Dallas, Richardson, Texas, USA
[47]National Centre for Scientific Research "Demokritos", Agia Paraskevi, Greece
[48a]Department of Physics, Stockholm University, Sweden
[48b]Oskar Klein Centre, Stockholm, Sweden
[49]Deutsches Elektronen-Synchrotron DESY, Hamburg and Zeuthen, Germany
[50]Fakultät Physik, Technische Universität Dortmund, Dortmund, Germany

[51]*Institut für Kern- und Teilchenphysik, Technische Universität Dresden, Dresden, Germany*
[52]*Department of Physics, Duke University, Durham, North Carolina, USA*
[53]*SUPA—School of Physics and Astronomy, University of Edinburgh, Edinburgh, United Kingdom*
[54]*INFN e Laboratori Nazionali di Frascati, Frascati, Italy*
[55]*Physikalisches Institut, Albert-Ludwigs-Universität Freiburg, Freiburg, Germany*
[56]*II. Physikalisches Institut, Georg-August-Universität Göttingen, Göttingen, Germany*
[57]*Département de Physique Nucléaire et Corpusculaire, Université de Genève, Genève, Switzerland*
[58a]*Dipartimento di Fisica, Università di Genova, Genova, Italy*
[58b]*INFN Sezione di Genova, Italy*
[59]*II. Physikalisches Institut, Justus-Liebig-Universität Giessen, Giessen, Germany*
[60]*SUPA—School of Physics and Astronomy, University of Glasgow, Glasgow, United Kingdom*
[61]*LPSC, Université Grenoble Alpes, CNRS/IN2P3, Grenoble INP, Grenoble, France*
[62]*Laboratory for Particle Physics and Cosmology, Harvard University, Cambridge, Massachusetts, USA*
[63a]*Department of Modern Physics and State Key Laboratory of Particle Detection and Electronics, University of Science and Technology of China, Hefei, China*
[63b]*Institute of Frontier and Interdisciplinary Science and Key Laboratory of Particle Physics and Particle Irradiation (MOE), Shandong University, Qingdao, China*
[63c]*School of Physics and Astronomy, Shanghai Jiao Tong University, Key Laboratory for Particle Astrophysics and Cosmology (MOE), SKLPPC, Shanghai, China*
[63d]*Tsung-Dao Lee Institute, Shanghai, China*
[63e]*School of Physics and Microelectronics, Zhengzhou University, China*
[64a]*Kirchhoff-Institut für Physik, Ruprecht-Karls-Universität Heidelberg, Heidelberg, Germany*
[64b]*Physikalisches Institut, Ruprecht-Karls-Universität Heidelberg, Heidelberg, Germany*
[65a]*Department of Physics, Chinese University of Hong Kong, Shatin, N.T., Hong Kong, China*
[65b]*Department of Physics, University of Hong Kong, Hong Kong, China*
[65c]*Department of Physics and Institute for Advanced Study, Hong Kong University of Science and Technology, Clear Water Bay, Kowloon, Hong Kong, China*
[66]*Department of Physics, National Tsing Hua University, Hsinchu, Taiwan*
[67]*IJCLab, Université Paris-Saclay, CNRS/IN2P3, 91405, Orsay, France*
[68]*Centro Nacional de Microelectrónica (IMB-CNM-CSIC), Barcelona, Spain*
[69]*Department of Physics, Indiana University, Bloomington, Indiana, USA*
[70a]*INFN Gruppo Collegato di Udine, Sezione di Trieste, Udine, Italy*
[70b]*ICTP, Trieste, Italy*
[70c]*Dipartimento Politecnico di Ingegneria e Architettura, Università di Udine, Udine, Italy*
[71a]*INFN Sezione di Lecce, Italy*
[71b]*Dipartimento di Matematica e Fisica, Università del Salento, Lecce, Italy*
[72a]*INFN Sezione di Milano, Italy*
[72b]*Dipartimento di Fisica, Università di Milano, Milano, Italy*
[73a]*INFN Sezione di Napoli, Italy*
[73b]*Dipartimento di Fisica, Università di Napoli, Napoli, Italy*
[74a]*INFN Sezione di Pavia, Italy*
[74b]*Dipartimento di Fisica, Università di Pavia, Pavia, Italy*
[75a]*INFN Sezione di Pisa, Italy*
[75b]*Dipartimento di Fisica E. Fermi, Università di Pisa, Pisa, Italy*
[76a]*INFN Sezione di Roma, Italy*
[76b]*Dipartimento di Fisica, Sapienza Università di Roma, Roma, Italy*
[77a]*INFN Sezione di Roma Tor Vergata, Italy*
[77b]*Dipartimento di Fisica, Università di Roma Tor Vergata, Roma, Italy*
[78a]*INFN Sezione di Roma Tre, Italy*
[78b]*Dipartimento di Matematica e Fisica, Università Roma Tre, Roma, Italy*
[79a]*INFN-TIFPA, Italy*
[79b]*Università degli Studi di Trento, Trento, Italy*
[80]*Universität Innsbruck, Department of Astro and Particle Physics, Innsbruck, Austria*
[81]*University of Iowa, Iowa City, Iowa, USA*
[82]*Department of Physics and Astronomy, Iowa State University, Ames, Iowa, USA*
[83]*Istinye University, Sariyer, Istanbul, Türkiye*
[84a]*Departamento de Engenharia Elétrica, Universidade Federal de Juiz de Fora (UFJF), Juiz de Fora, Brazil*
[84b]*Universidade Federal do Rio De Janeiro COPPE/EE/IF, Rio de Janeiro, Brazil*
[84c]*Instituto de Física, Universidade de São Paulo, São Paulo, Brazil*

[84d]Rio de Janeiro State University, Rio de Janeiro, Brazil
[84e]Federal University of Bahia, Bahia, Brazil
[85]KEK, High Energy Accelerator Research Organization, Tsukuba, Japan
[86]Graduate School of Science, Kobe University, Kobe, Japan
[87a]AGH University of Krakow, Faculty of Physics and Applied Computer Science, Krakow, Poland
[87b]Marian Smoluchowski Institute of Physics, Jagiellonian University, Krakow, Poland
[88]Institute of Nuclear Physics Polish Academy of Sciences, Krakow, Poland
[89]Faculty of Science, Kyoto University, Kyoto, Japan
[90]Research Center for Advanced Particle Physics and Department of Physics, Kyushu University, Fukuoka, Japan
[91]L2IT, Université de Toulouse, CNRS/IN2P3, UPS, Toulouse, France
[92]Instituto de Física La Plata, Universidad Nacional de La Plata and CONICET, La Plata, Argentina
[93]Physics Department, Lancaster University, Lancaster, United Kingdom
[94]Oliver Lodge Laboratory, University of Liverpool, Liverpool, United Kingdom
[95]Department of Experimental Particle Physics, Jožef Stefan Institute and Department of Physics, University of Ljubljana, Ljubljana, Slovenia
[96]School of Physics and Astronomy, Queen Mary University of London, London, United Kingdom
[97]Department of Physics, Royal Holloway University of London, Egham, United Kingdom
[98]Department of Physics and Astronomy, University College London, London, United Kingdom
[99]Louisiana Tech University, Ruston, Los Angeles, USA
[100]Fysiska institutionen, Lunds universitet, Lund, Sweden
[101]Departamento de Física Teorica C-15 and CIAFF, Universidad Autónoma de Madrid, Madrid, Spain
[102]Institut für Physik, Universität Mainz, Mainz, Germany
[103]School of Physics and Astronomy, University of Manchester, Manchester, United Kingdom
[104]CPPM, Aix-Marseille Université, CNRS/IN2P3, Marseille, France
[105]Department of Physics, University of Massachusetts, Amherst, Massachusetts, USA
[106]Department of Physics, McGill University, Montreal, Quebec, Canada
[107]School of Physics, University of Melbourne, Victoria, Australia
[108]Department of Physics, University of Michigan, Ann Arbor, Michigan, USA
[109]Department of Physics and Astronomy, Michigan State University, East Lansing, Michigan, USA
[110]Group of Particle Physics, University of Montreal, Montreal, Quebec, Canada
[111]Fakultät für Physik, Ludwig-Maximilians-Universität München, München, Germany
[112]Max-Planck-Institut für Physik (Werner-Heisenberg-Institut), München, Germany
[113]Graduate School of Science and Kobayashi-Maskawa Institute, Nagoya University, Nagoya, Japan
[114a]Department of Physics, Nanjing University, Nanjing, China
[114b]School of Science, Shenzhen Campus of Sun Yat-sen University, China
[114c]University of Chinese Academy of Science (UCAS), Beijing, China
[115]Department of Physics and Astronomy, University of New Mexico, Albuquerque, New Mexico, USA
[116]Institute for Mathematics, Astrophysics and Particle Physics, Radboud University/Nikhef, Nijmegen, Netherlands
[117]Nikhef National Institute for Subatomic Physics and University of Amsterdam, Amsterdam, Netherlands
[118]Department of Physics, Northern Illinois University, DeKalb, Illinois, USA
[119a]New York University Abu Dhabi, Abu Dhabi, United Arab Emirates
[119b]United Arab Emirates University, Al Ain, United Arab Emirates
[120]Department of Physics, New York University, New York, New York, USA
[121]Ochanomizu University, Otsuka, Bunkyo-ku, Tokyo, Japan
[122]Ohio State University, Columbus, Ohio, USA
[123]Homer L. Dodge Department of Physics and Astronomy, University of Oklahoma, Norman, Oklahoma, USA
[124]Department of Physics, Oklahoma State University, Stillwater, Oklahoma, USA
[125]Palacký University, Joint Laboratory of Optics, Olomouc, Czech Republic
[126]Institute for Fundamental Science, University of Oregon, Eugene, Oregon, USA
[127]Graduate School of Science, Osaka University, Osaka, Japan
[128]Department of Physics, University of Oslo, Oslo, Norway
[129]Department of Physics, Oxford University, Oxford, United Kingdom
[130]LPNHE, Sorbonne Université, Université Paris Cité, CNRS/IN2P3, Paris, France
[131]Department of Physics, University of Pennsylvania, Philadelphia, Pennsylvania, USA
[132]Department of Physics and Astronomy, University of Pittsburgh, Pittsburgh, Pennsylvania, USA
[133a]Laboratório de Instrumentação e Física Experimental de Partículas—LIP, Lisboa, Portugal
[133b]Departamento de Física, Faculdade de Ciências, Universidade de Lisboa, Lisboa, Portugal

[133c]*Departamento de Física, Universidade de Coimbra, Coimbra, Portugal*
[133d]*Centro de Física Nuclear da Universidade de Lisboa, Lisboa, Portugal*
[133e]*Departamento de Física, Universidade do Minho, Braga, Portugal*
[133f]*Departamento de Física Teórica y del Cosmos, Universidad de Granada, Granada (Spain), Spain*
[133g]*Departamento de Física, Instituto Superior Técnico, Universidade de Lisboa, Lisboa, Portugal*
[134]*Institute of Physics of the Czech Academy of Sciences, Prague, Czech Republic*
[135]*Czech Technical University in Prague, Prague, Czech Republic*
[136]*Charles University, Faculty of Mathematics and Physics, Prague, Czech Republic*
[137]*Particle Physics Department, Rutherford Appleton Laboratory, Didcot, United Kingdom*
[138]*IRFU, CEA, Université Paris-Saclay, Gif-sur-Yvette, France*
[139]*Santa Cruz Institute for Particle Physics, University of California Santa Cruz, Santa Cruz, California, USA*
[140a]*Departamento de Física, Pontificia Universidad Católica de Chile, Santiago, Chile*
[140b]*Millennium Institute for Subatomic physics at high energy frontier (SAPHIR), Santiago, Chile*
[140c]*Instituto de Investigación Multidisciplinario en Ciencia y Tecnología, y Departamento de Física, Universidad de La Serena, Chile*
[140d]*Universidad Andres Bello, Department of Physics, Santiago, Chile*
[140e]*Instituto de Alta Investigación, Universidad de Tarapacá, Arica, Chile*
[140f]*Departamento de Física, Universidad Técnica Federico Santa María, Valparaíso, Chile*
[141]*Department of Physics, University of Washington, Seattle, Washington, USA*
[142]*Department of Physics and Astronomy, University of Sheffield, Sheffield, United Kingdom*
[143]*Department of Physics, Shinshu University, Nagano, Japan*
[144]*Department Physik, Universität Siegen, Siegen, Germany*
[145]*Department of Physics, Simon Fraser University, Burnaby, British Columbia, Canada*
[146]*SLAC National Accelerator Laboratory, Stanford, California, USA*
[147]*Department of Physics, Royal Institute of Technology, Stockholm, Sweden*
[148]*Departments of Physics and Astronomy, Stony Brook University, Stony Brook, New York, USA*
[149]*Department of Physics and Astronomy, University of Sussex, Brighton, United Kingdom*
[150]*School of Physics, University of Sydney, Sydney, Australia*
[151]*Institute of Physics, Academia Sinica, Taipei, Taiwan*
[152a]*E. Andronikashvili Institute of Physics, Iv. Javakhishvili Tbilisi State University, Tbilisi, Georgia*
[152b]*High Energy Physics Institute, Tbilisi State University, Tbilisi, Georgia*
[152c]*University of Georgia, Tbilisi, Georgia*
[153]*Department of Physics, Technion, Israel Institute of Technology, Haifa, Israel*
[154]*Raymond and Beverly Sackler School of Physics and Astronomy, Tel Aviv University, Tel Aviv, Israel*
[155]*Department of Physics, Aristotle University of Thessaloniki, Thessaloniki, Greece*
[156]*International Center for Elementary Particle Physics and Department of Physics, University of Tokyo, Tokyo, Japan*
[157]*Department of Physics, Tokyo Institute of Technology, Tokyo, Japan*
[158]*Department of Physics, University of Toronto, Toronto, Ontario, Canada*
[159a]*TRIUMF, Vancouver, British Columbia, Canada*
[159b]*Department of Physics and Astronomy, York University, Toronto, Ontario, Canada*
[160]*Division of Physics and Tomonaga Center for the History of the Universe, Faculty of Pure and Applied Sciences, University of Tsukuba, Tsukuba, Japan*
[161]*Department of Physics and Astronomy, Tufts University, Medford, Massachusetts, USA*
[162]*Department of Physics and Astronomy, University of California Irvine, Irvine, California, USA*
[163]*University of Sharjah, Sharjah, United Arab Emirates*
[164]*Department of Physics and Astronomy, University of Uppsala, Uppsala, Sweden*
[165]*Department of Physics, University of Illinois, Urbana, Illinois, USA*
[166]*Instituto de Física Corpuscular (IFIC), Centro Mixto Universidad de Valencia—CSIC, Valencia, Spain*
[167]*Department of Physics, University of British Columbia, Vancouver, British Columbia, Canada*
[168]*Department of Physics and Astronomy, University of Victoria, Victoria, British Columbia, Canada*
[169]*Fakultät für Physik und Astronomie, Julius-Maximilians-Universität Würzburg, Würzburg, Germany*
[170]*Department of Physics, University of Warwick, Coventry, United Kingdom*
[171]*Waseda University, Tokyo, Japan*
[172]*Department of Particle Physics and Astrophysics, Weizmann Institute of Science, Rehovot, Israel*
[173]*Department of Physics, University of Wisconsin, Madison, Wisconsin, USA*
[174]*Fakultät für Mathematik und Naturwissenschaften, Fachgruppe Physik, Bergische Universität Wuppertal, Wuppertal, Germany*
[175]*Department of Physics, Yale University, New Haven, Connecticut, USA*

[a]Also at Department of Physics, King's College London, London, United Kingdom.
[b]Also at Institute of Physics, Azerbaijan Academy of Sciences, Baku, Azerbaijan.
[c]Also at TRIUMF, Vancouver, British Columbia, Canada.
[d]Also at Department of Physics, University of Thessaly, Greece.
[e]Also at An-Najah National University, Nablus, Palestine.
[f]Also at Department of Physics, University of Fribourg, Fribourg, Switzerland.
[g]Also at Department of Physics, Westmont College, Santa Barbara, USA.
[h]Also at Departament de Fisica de la Universitat Autonoma de Barcelona, Barcelona, Spain.
[i]Also at Affiliated with an institute covered by a cooperation agreement with CERN.
[j]Also at The Collaborative Innovation Center of Quantum Matter (CICQM), Beijing, China.
[k]Also at Faculty of Physics, Sofia University, 'St. Kliment Ohridski', Sofia, Bulgaria.
[l]Also at Università di Napoli Parthenope, Napoli, Italy.
[m]Also at Institute of Particle Physics (IPP), Canada.
[n]Also at University of Colorado Boulder, Department of Physics, Colorado, USA.
[o]Also at Borough of Manhattan Community College, City University of New York, New York, New York, USA.
[p]Also at National Institute of Physics, University of the Philippines Diliman (Philippines), Philippines.
[q]Also at Department of Financial and Management Engineering, University of the Aegean, Chios, Greece.
[r]Also at Centro Studi e Ricerche Enrico Fermi, Italy.
[s]Also at Institucio Catalana de Recerca i Estudis Avancats, ICREA, Barcelona, Spain.
[t]Also at Technical University of Munich, Munich, Germany.
[u]Also at CMD-AC UNEC Research Center, Azerbaijan State University of Economics (UNEC), Azerbaijan.
[v]Also at Yeditepe University, Physics Department, Istanbul, Türkiye.
[w]Also at Institute of Theoretical Physics, Ilia State University, Tbilisi, Georgia.
[x]Also at CERN, Geneva, Switzerland.
[y]Also at Center for Interdisciplinary Research and Innovation (CIRI-AUTH), Thessaloniki, Greece.
[z]Also at Hellenic Open University, Patras, Greece.
[aa]Also at Department of Physics, Stellenbosch University, South Africa.
[bb]Also at Department of Physics, California State University, Sacramento, USA.
[cc]Also at Département de Physique Nucléaire et Corpusculaire, Université de Genève, Genève, Switzerland.
[dd]Also at Institut für Experimentalphysik, Universität Hamburg, Hamburg, Germany.
[ee]Also at Department of Physics, Stanford University, Stanford, California, USA.
[ff]Also at Institute for Nuclear Research and Nuclear Energy (INRNE) of the Bulgarian Academy of Sciences, Sofia, Bulgaria.
[gg]Also at Washington College, Chestertown, Maryland, USA.
[hh]Also at Institute of Applied Physics, Mohammed VI Polytechnic University, Ben Guerir, Morocco.
[ii]Also at Institute of Physics and Technology, Mongolian Academy of Sciences, Ulaanbaatar, Mongolia.